



## AN ABSTRACT OF THE THESIS OF

Pranathi Bhattacharji for the degree of Master of Science in Electrical and Computer Engineering presented on September 11, 2014.

Title: Simplified WECC Modeling for Frequency Response, Wind Integration, and Energy Storage

Abstract approved:

---

Ted K. A. Brekken

The primary objective of a grid is to maintain a balance between generation and load. If these quantities are not in balance with each other, severe damages such as voltage fluctuations, low power quality, power outages or even cascaded blackouts may occur. Hence one of the primary factors that holds the grid together and makes it operative is the frequency. Thus maintaining the frequency within certain limits is the basic operational requirement. Lately, the power system's dependency on wind power has increased, suggesting that wind power generation is expected to contribute its services which are normally delivered by conventional power plants. However a system that has high wind penetration results in reduced system inertia due to the wind turbine's lack of droop characteristics that may lead to frequency control issues. Thus a backup system is needed such as an energy storage system that can be controlled to supply energy when demand is high i.e., during demand response operations, energy can be stored by increasing load and temperature, and energy can be effectively returned by reducing load and temperature. This thesis presents the

modelling of such an energy storage system which consists of several generators responding at different time scales and several water heaters that can be controlled based on the frequency deviation from its nominal value. The ultimate goal of this paper is to perform transient analysis on a simplified Western Electricity Coordinating Council (WECC) system for frequency response, wind integration and energy storage using primary frequency control and secondary frequency control. Simulation results will showcase the frequency excursions of the WECC system with and without energy storage under normal loss of generation event and under wind penetration.

©Copyright by Pranathi Bhattacharji

September 11, 2014

All Rights Reserved

Simplified WECC Modeling for Frequency Response, Wind Integration, and Energy  
Storage

by

Pranathi Bhattacharji

A THESIS

submitted to

Oregon State University

in partial fulfillment of  
the requirements for the  
degree of

Master of Science

Presented September 11, 2014

Commencement June 2015

Master of Science thesis of Pranathi Bhattacharji presented on September 11, 2014

APPROVED:

---

Major Professor, representing Electrical and Computer Engineering

---

Director of the School of Electrical Engineering and Computer Science

---

Dean of the Graduate School

I understand that my thesis will become part of the permanent collection of Oregon State University libraries. My signature below authorizes release of my thesis to any reader upon request.

---

Pranathi Bhattacharji, Author

## ACKNOWLEDGEMENTS

*“The mediocre teacher tells. The good teacher explains. The superior teacher demonstrates. The great teacher inspires” - William A. Ward.*

This quote made me think of one teacher who I honestly idealize: Dr. Ted Brekken, my advisor for the time I spent at Oregon State University. I couldn't have been more grateful to be under the guidance of Dr. Brekken who showcases so much curiosity and enthusiasm as a teacher. Thank You for working with me through the smallest details and making this research a success.

I would specially like to thank Dr. Eduardo Cotilla Sanchez for helping me with PSS/E in the initial stages of my research. I also extend my gratitude towards my committee members: Dr. Ted Brekken, Dr. Eduardo Cotilla Sanchez, Dr. Annette von Jouanne and Dr. Kathy K. Mullet.

Thank You National Science Foundation (NSF) for making this research possible. I would also like to thank my fellow graduate students for always keeping my spirits high. I thank Anirban Roy who offered to help me when I needed. I would like to extend my special thanks to Kaushal Biligri for always instilling confidence in me, during the course of this research. I would specially like to thank Kelcey Feeney for her encouragement. Also, thanks to my roommates who have always taken care of me at home.

Most of all, thanks to my parents, who always believed in me and supported me in all my endeavors. I wouldn't have been where I am today without their moral support. I would like to thank my sister who has been my pillar of strength throughout and my brother-in-law who always inspired me to do better.

## TABLE OF CONTENTS

1	INTRODUCTION .....	1
1.1	GENERAL SCENARIO OF RENEWABLE ENERGY .....	1
1.2	COMPONENTS OF FREQUENCY CONTROL FOR CONVENTIONAL AND WIND GENERATION .....	6
1.2.1	Frequency Response and Frequency Control .....	6
1.3	BACKDROP ON GRID-SCALE ENERGY STORAGE AND DEMAND RESPONSE.....	12
1.3.1	Grid Scale Energy Storage .....	12
1.3.2	Demand Response .....	14
1.4	MOTIVATION FOR THE THESIS.....	15
2	WECC'S PRIMARY FREQUENCY RESPONSE TO GENERATOR OUTAGE 16	
2.1	WINTER LOW LOAD-HIGH CAISO WIND BASE CASE FOR WECC .....	16
2.1.1	Response to Palo Verde Disturbance.....	18
2.2	WESTERN ELECTRICITY COORDINATING COUNCIL (WECC) SYSTEM MODEL .....	20
2.2.1	Concept of Speed Governing Control .....	20
2.2.2	Load Response to Frequency Deviation .....	27
2.2.3	Governors with Speed-Droop Characteristic.....	28
2.2.4	One Area Primary Frequency Control.....	30
2.2.5	Aggregated Performance of All Generators in a Power System .....	32
2.3	SIMULATION SETUP AND SIMULATION RESULTS OF THE WECC MODEL .....	33
2.4	RESULT CONCLUSION.....	47
3	ENERGY STORAGE MODELING .....	49
3.1	CASE I: SINGLE WATER HEATER MODELING.....	49
3.2	CASE II: MULTIPLE WATER HEATER MODELING.....	54



4	ENERGY STORAGE FOR TRANSIENT STABILITY OF BASE CASE - LOSS OF GENERATION.....	63
4.1.	SIMULATION SETUP OF BASE CASE SYSTEM WITHOUT ENERGY STORAGE.....	63
4.2.	SIMULATION SETUP OF BASE CASE SYSTEM WITH ENERGY STORAGE .....	63
4.3	SIMULATION RESULTS.....	64
4.3.1	Case A: Frequency Response of Base Case without Energy Storage System .....	64
4.3.2	Case B: Response of All Water Heaters per 3 Hz .....	66
4.3.3	Case C: Response of All Water Heaters per 0.23 Hz .....	69
4.4	RESULT CONCLUSION.....	73
5	ENERGY STORAGE FOR WIND INTEGRATION.....	77
5.1	CASE D: WIND PENETRATION TO THE WECC SYSTEM WITHOUT ENERGY STORAGE.....	78
5.2	CASE E: WIND PENETRATION TO THE WECC SYSTEM WITH ENERGY STORAGE, AND WATER HEATERS RESPONDING PER 3HZ.....	81
5.3	CASE F: WIND PENETRATION TO THE WECC SYSTEM WITH ENERGY STORAGE, AND WATER HEATERS RESPONDING PER 0.23HZ .....	88
5.4	CASE G: WIND PENETRATION TO THE WECC SYSTEM WITH ENERGY STORAGE, AND WATER HEATERS RESPONDING PER 0.02HZ .....	92
5.5	CASE H: ENERGY STORAGE FOR WIND INTEGRATION WITH SECONDARY CONTROL .....	95
5.6	RESULTS CONCLUSION .....	98
6	CONCLUSION .....	104
6.1	DISCUSSION.....	104
6.2	FUTURE WORK.....	106
7	REFERENCES .....	107

## LIST OF FIGURES

<u>Figure</u>	<u>Page</u>
Figure 1.1. U.S energy consumption by source, 2011 [4].....	2
Figure 1.2. Wind energy records by RTO/ISO [6].....	3
Figure 1.3. BPA balancing authority forecast and actual wind power generation (BPA Balancing Authority Total Wind Generation, 2014).....	5
Figure 1.4. Frequency response control continuum [13] .....	7
Figure 1.5. Inertial frequency response for loss of generation [11].....	9
Figure 1.6. Illustration of primary and secondary frequency response [13]....	11
Figure 1.7. Rated power of US grid storage projects [20].....	13
Figure 2.1. Frequency response to Palo Verde generation trip event [28].....	18
Figure 2.2. Governor response to Palo Verde generation trip event [28].....	19
Figure 2.3. Generator supplying isolated load [29].....	21
Figure 2.4. Transfer function relating speed and torque [29].....	24
Figure 2.5. Transfer function relating speed and torque [29].....	26
Figure 2.6. System block diagram to show the effect of load damping [29].....	28
Figure 2.7. Reduced system block diagram to show the effect of load damping [29].....	28

## LIST OF FIGURES (Continued)

<u>Figure</u>	<u>Page</u>
Figure 2.8. Ideal steady state characteristics of a governor with speed droop control [29].	29
Figure 2.9. Standard generator mechanism in a power system.	30
Figure 2.10. Commanded power and actual power characteristic.	31
Figure 2.11. Single area system with only primary speed control [29].	31
Figure 2.12. Aggregated generator system equivalent [29].	32
Figure 2.13. One-area system with primary speed control in Simulink.	34
Figure 2.14. WECC base case frequency response and WECC simulated frequency response with loss of generation.	35
Figure 2.15. Timing of governor response for the winter low load- high CAISO wind base case.	35
Figure 2.16. WECC model for one kind of generator having one response time.	38
Figure 2.17. WECC's frequency response with all the generators having one response time.	40
Figure 2.18. WECC model for fast and slow generator case.	41
Figure 2.19. Simulated and base case frequency responses for Fast and Slow generators in the WECC system.	42

## LIST OF FIGURES (Continued)

<u>Figure</u>	<u>Page</u>
Figure 2.20 WECC system model for fast, medium and slow responsive generator case.....	44
Figure 2.21. Simulated and base case frequency responses for Fast, Medium and Slow generators in the WECC system.....	44
Figure 2.22. Electric power responses of generators in the WECC system for fast, medium and slow responsive generators.....	46
Figure 2.23. Frequency response of the WECC system including fast, medium and slow generators and the contribution of electrical power by each generator and load for the loss of 2.69 GW.....	48
Figure 3.1. Basic energy storage modeling for a single energy storage system.....	49
Figure 3.2. One water heater unit as the energy storage.....	51
Figure 3.3. Operative region for a single water heater unit.....	52
Figure 3.4. Energy storage modeling for a single water heater unit.....	53
Figure 3.5. Three water heaters with half state of charge.....	54
Figure 3.6. Multiple water heaters.....	55
Figure 3.7. Straight line approximation.....	56
Figure 3.8 Operative regions of all the water heater units.....	57

## LIST OF FIGURES (Continued)

<u>Figure</u>	<u>Page</u>
Figure 3.9. Energy storage modeling for several thousand water heaters.....	59
Figure 4.1. Base case with energy storage system.....	64
Figure 4.2. Frequency response of Case A with a frequency nadir of 59.6659 Hz and settling frequency of 59.768 Hz.....	65
Figure 4.3. Frequency responses for Case A and Case B.....	66
Figure 4.4. Power response of the water heaters for Case B and its corresponding frequency response.....	67
Figure 4.5 Region of operation and SOC of all the water heaters for Case B..	68
Figure 4.6 Frequency response for Case A, B and C.....	70
Figure 4.7. Power response of the water heaters for Case C and its corresponding frequency response.....	71
Figure 4.8. Region of operation and SOC of all the water heaters for Case C.	72
Figure 4.9. Frequency responses for Case I, II and III.....	74
Figure 4.10. Actual water heater power for cases B and C.....	76
Figure 5 WECC system with wind penetration.....	79
Figure 5.1 Wind power (obtained from BPA) and the frequency response of the system.....	80

## LIST OF FIGURES(Continued)

<u>Figure</u>	<u>Page</u>
Figure 5.2 WECC system with wind penetration and energy storage system for Case E.....	82
Figure 5.3 Region of operation of the water heaters and the frequency response for Case E.....	83
Figure 5.4 Magnified plot of commanded power and actual water heater power for Case E.....	84
Figure 5.5 Commanded water heater power response, actual water heater power response, frequency and SOC for case E.....	85
Figure 5.6 Magnified plots of upper saturation limit and SOC for case E.....	86
Figure 5.7 Deployment of water heaters for every 1MW of wind power and the SOC of the energy storage system for Case E.....	87
Figure 5.8 Region of operation of the water heaters and the frequency response for Case F.....	89
Figure 5.9 Commanded water heater power response, actual water heater power response, frequency and SOC for case F.....	90
Figure 5.10 Deployment of water heaters for every 1MW of wind power and the SOC of the energy storage system for Case F.....	91
Figure 5.11 Region of operation of the water heaters and the frequency response for Case G.....	93
Figure 5.12 Deployment of water heaters for every 1MW of wind power and the SOC of the energy storage system for Case G.....	94

Figure 5.13. WECC model with secondary control for Case H.....	96
Figure 5.14. Frequency response, water heater power response and SOC with secondary control.....	97
Figure 5.15 Frequency responses of Case D, E,F,G and H.....	100
Figure 5.16 Power responses for all Cases D, E, F, G and H.....	102
Figure 5.17 State of Charge for Case E, F, G and H.....	103

## LIST OF TABLES

<u>Table</u>	<u>Page</u>
Table 2.1 WECC's Base Cases [20].....	17
Table 2.2 WECC's Base Cases [20].....	17
Table 2.3 Parameters that helped achieve the WECC frequency response....	45
Table 3.1 Control Law for overcharge and undercharge conditions.....	51
Table 4.1 Summary of frequency responses for Case A, B and C.....	73
Table 5.1 BPA Wind data.....	78
Table 5.2 Comparing the frequency response, water heater power response and state of charge for 5 different cases.....	99





# **Simplified WECC Modeling for Frequency Response, Wind Integration, and Energy Storage**

## **1 Introduction**

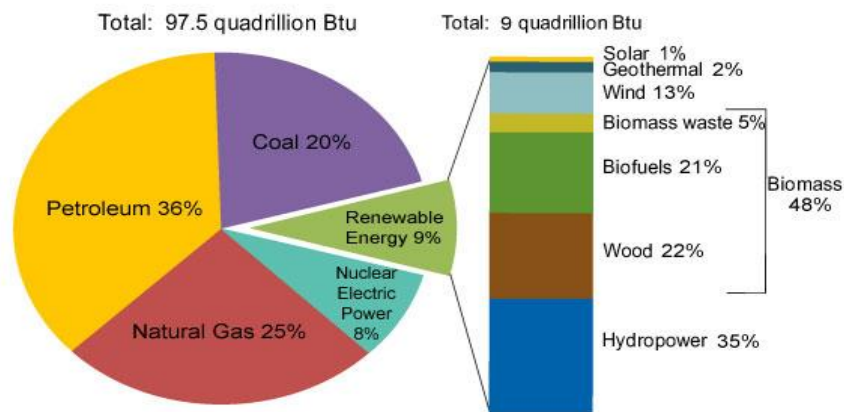
### **1.1 General Scenario of Renewable Energy**

In 2013, the United States generated about 4,058 billion kWh of electricity, of which 67% was generated from fossil fuels such as coal, natural gas and petroleum, with 39% attributed to coal and 27% to natural gas [1]. These figures give a sense that the United States massively relies on coal and natural gas for its energy. Fossil fuels are non-renewable and it is being burned much faster than the earth can generate them. This implies that fossil-based resources will slowly become too expensive and mankind has to shift its reliance onto other sources of energy. These other sources of energy are coined as renewable energy.

Renewable energy sources are those that are continually replenished. These include energy from wind, water, the sun, geothermal sources and biomass sources. Renewable sources of energy vary widely in their cost-effectiveness and in their availability in the United States. Although these renewables may appear free, their cost comes in collecting, harnessing and transporting energy so that it can do some useful work [2]. Renewable energy is accounted for about 13.2 % of the nation's net electric power generation in 2013 [3]. Figure 1.1 shows the total renewable energy consumption by source (hydro power, wind, solar etc.,) and sector (residential,

commercial, industrial, transportation and electric power) from 1949-2013 [4]. It also gives a comparison of renewable energy production with other resources that produce energy. It also shows that hydroelectric power accounts for a major contribution of the renewable energy production today in the United States.

## U.S. Energy Consumption by Energy Source, 2011



Source: U.S. Energy Information Administration, *Monthly Energy Review*, Table 10.1 (March 2012), preliminary 2011 data.

Figure 1.1. U.S energy consumption by source, 2011 [4]

Wind Energy continues to make inroads as a major contributor to the United States power mix. In fact, the growth was 30% on average for the past five years, helping the United States serve as a major market for wind energy globally [5]. According to [6], the total installed wind capacity in the U.S through the first quarter is about 61,327 MW, able to power the equivalent of roughly 15.5 million American homes which is about 4.13% of the nation's electricity. Figure 1.2 illustrates the wind energy records

as per the independent system operators and regional transmission organization. The figure shows that the Electric Reliability Council of Texas (ERCOT) had recorded the maximum wind output of about 10,300 MW. From the figure, according to BPA, wind produced on February 22, 2013 hit an average of about 4,464 MW for an hour; accounting for 39 percent of the generation in BPA's balancing area. These numbers tell us that the Pacific Northwest is not lagging far behind in the wind industry.

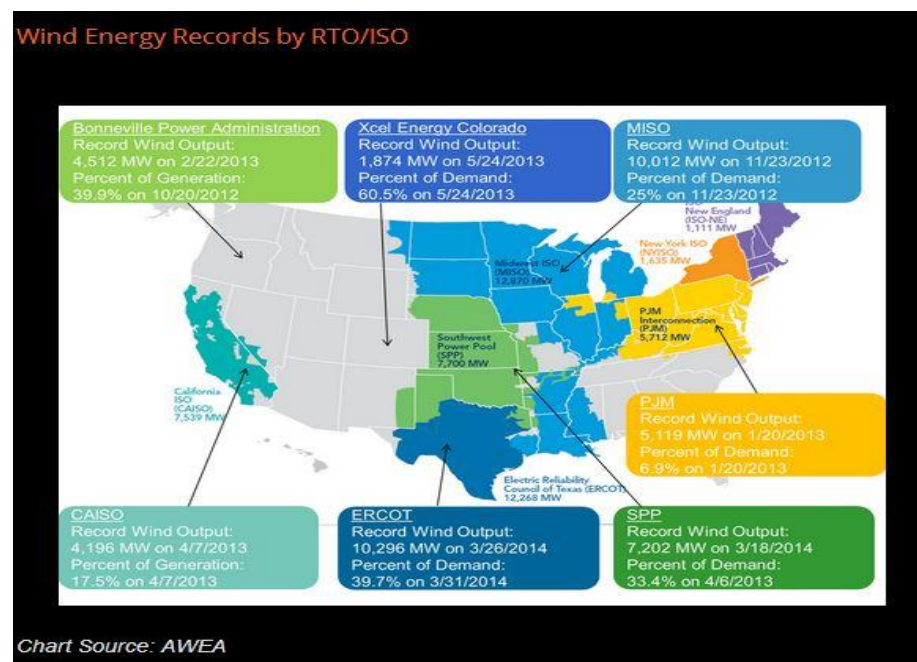


Figure 1.2. Wind energy records by RT and ISO [6]

Pacific Northwest is an early leader in the wind industry and has made some significant contributions to increase the penetration of renewables making it more clean and green. Since generating wind power creates no emissions and uses virtually no water, the water consumption savings from wind projects in the Pacific Northwest has accounted for more than 3.4 billion gallons of water per year. The installed wind

capacity in the Pacific Northwest is approximately 5900 MW, which accounts for 16.2 percent of electricity produced in 2013 [7]. Bonneville Power Administration expects to bring in 2,500 MW of additional wind energy to its existing system by 2015 [8].

Though renewables have several advantages in terms of it being environmentally friendly, sustainable, reduced cost of operation as their fuel is derived from natural and available resources, it also has several disadvantages such as dependence on weather forecast, for example hydro generators need rain to fill dams to continue the flow of water, wind turbines need wind to turn their blades, solar panels require sunlight to make electricity. When these resources are unavailable or not available enough to generate the electricity needed, reserve generation must be supplied from elsewhere [9]. In other words they are very unpredictable and inconsistent. To illustrate the above statement, Figure 1.3 shows BPA's balancing authority total wind generation and forecast for a period of 7 days in the month of July [10].

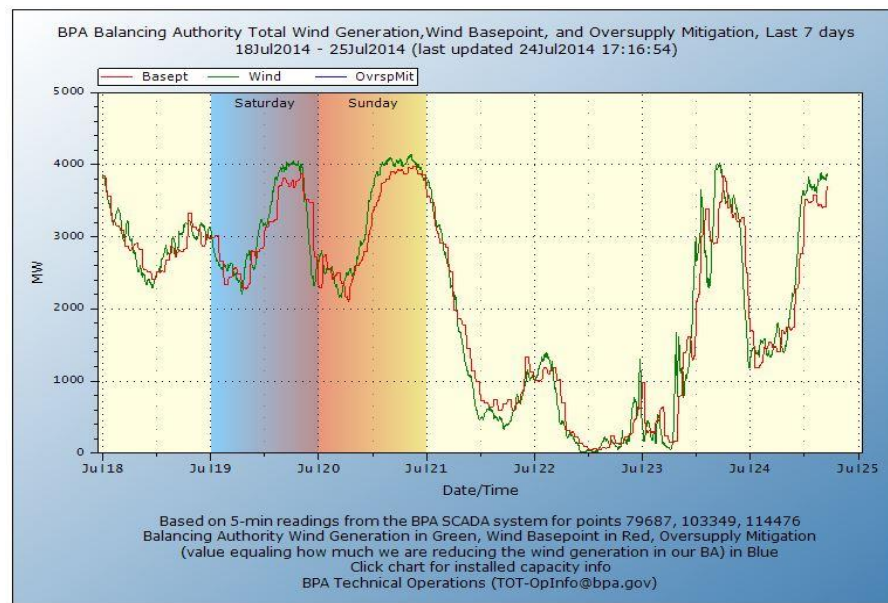


Figure 1.3. BPA balancing authority forecast and actual wind power generation (BPA Balancing Authority Total Wind Generation, 2014)

As we can see that both the forecasted wind generation (red) and the actual wind generation (green) are not in unison with each other and this could be a matter of concern because when wind generation is lower than predicted, some other type of generation has to kick in to fill in the void and if this is not achieved transients occur within a system which accounts for an imbalance in generation and load which will ultimately lead to grid collapse. Thus there is a need to study these frequency excursions and implement the concept of energy storage that would supply the energy needed when generation is not equal to load.

## **1.2 Components of Frequency Control for Conventional and Wind Generation**

### **1.2.1 Frequency Response and Frequency Control**

Frequency response can be defined as the automatic corrective response provided towards balancing demand and supply [11]. In a large complex interconnected power system, it is essential that there exists a balance between generation and load. To achieve this, it is very important that the grid is operated within a safe frequency range, by ensuring adequate resources that are available to respond to expected and unexpected imbalances. Hence, for an event occurring in the system, the frequency has to be controlled and driven back to its scheduled value (60 Hz) in order to provide uninterrupted electric service to customers [12]. Frequency can therefore be thought of as the pulse of the grid and an indispensable indicator of the health of the power system [13]. Frequency control can occur over a continuum of time using different resources, represented in Figure 1.4. This makes us visit to the concepts of inertial frequency response, primary frequency response, secondary frequency response and tertiary frequency response.

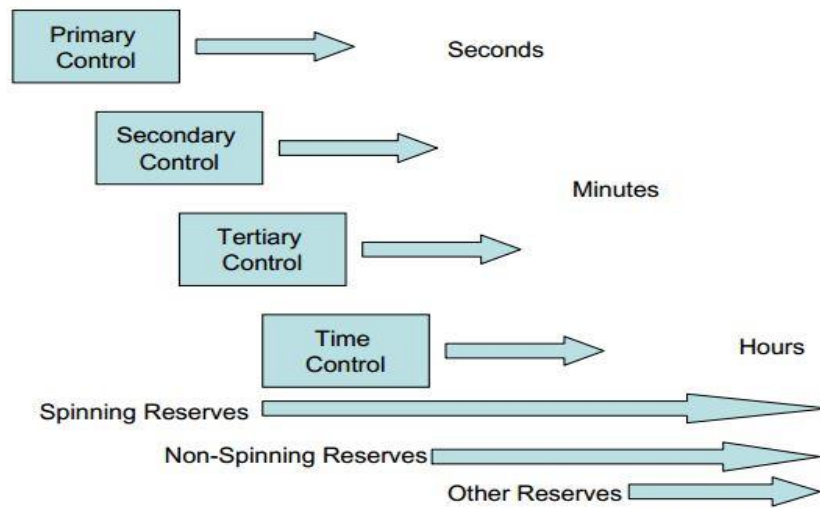


Figure 1.4. Frequency response control continuum [13]

### Inertial Frequency Response

Inertia is the resistance of any physical object to any change in its state of motion, including changes to its speed and direction [14]. In terms of power systems, inertial frequency response is the immediate response to a power disturbance that causes a frequency change, such as the loss of a large generator or a large loss of load. It is inherent in the system due to the rotating characteristic of typical load (motor, pumps) and conventional generation and it responds in seconds to arrest the frequency deviation. It is considered to be very important as it reduces the rate of change of frequency after a disturbance, which can avoid under frequency load shedding (UFLS) or worse issues, including blackouts. Conventional synchronous generators provide inertial response naturally from the stored energy in the rotating mass of their turbines [15].



To illustrate the concept of inertial frequency control and the impact of renewables into the power system, see Figure 1.5. The general equation for calculating rate of change of frequency using system inertia constant H is shown below [11].

$$\frac{df}{dt} = \frac{\Delta P}{2H} * f_o + \frac{D}{2H} * \Delta f$$

Assuming load dampening D=0, we get

$$\frac{df}{dt} = \frac{\Delta P}{2H} * f_o$$

Where;

H= System inertia constant on system base (seconds)

D= Load dampening constant in PU/Hz

$f_o$ = Frequency at the time of disturbance (Hz)

$\frac{df}{dt}$ = Rate of change of frequency (Hz/Sec)

$\Delta P$ = (PL-PG)/PG, Power change (per unit in system load base)

PL= Load prior to generation loss in MW

PG= System generation after loss in MW

$\Delta f$ =Change in frequency

Figure 1.5 illustrates the concept of inertial frequency response. The solid red line (case 1) represents the frequency response for a loss of an 890 MW generating unit. The total system load was approximately 50,000 MW, with about 700 MW of wind

generation in service. The dash line (case 2) in the plot represents the frequency response for a loss of 837 MW generating unit with a system load of approximately 24,000 MW with 4,300 MW of wind generation in service [10].

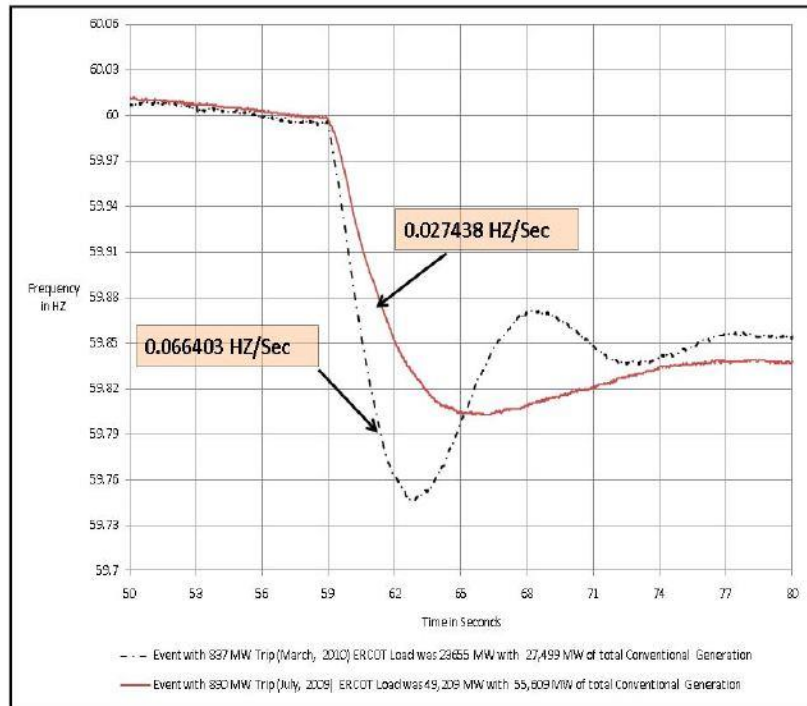


Figure 1.5. Inertial frequency response for loss of generation [11]

It can be seen that  $\frac{df}{dt}$  is higher for case 2 when compared to case 1. The two attributing reasons are:

- There was less number of generators online to supply the off-peak load.
- Higher wind generation displaced the conventional units and resulted in even less system inertia in the system [11].

Thus one conclusion that can be drawn from the above example is that, wind energy does not contribute or contributes very little towards inertial frequency response. Even though energy is stored in their rotating blades, they cannot contribute to inertial control as it is decoupled from the grid due to the presence of power electronics present in between them. Currently, several studies are being conducted to introduce synthetic inertia in to the system and to capture more energy from converters by providing some controls [16] [17] [18].

### **Primary Frequency Control**

This is also called as frequency responsive service or governor droop service and it follows inertial response. It occurs within the first few seconds following a disturbance in order to stabilize the grid. Frequency response is provided by governor action and load. The turbine governor controls senses the change in speed and adjusts the energy input into the generators' prime mover to stabilize the frequency. It is important to understand that, primary control does not return the frequency to normal, but it only stabilizes it [13].

All the frequency dependent loads change their speed in direct proportion to frequency. When there is a drop in frequency, the motors turn slower as load is higher than generation and thus draws less energy. In case the frequency exceeds the permissible limits (UFLS), load shedding are required and carried out in order to maintain interconnected operation [13].

## Secondary Frequency Control

Balancing services deployed in the “minutes” time frame typically includes secondary control. This control is accomplished using the balancing authorities’ manual actions taken by the dispatcher to provide additional adjustments. Basically, secondary control restores the system back to 60 Hz after a disturbance. It is provided by spinning and non- spinning reserves. Implementing Automatic Generation Control (AGC) is the most common method to adopt secondary control. Consider Figure 1.6, it highlights the concept of primary and secondary control [13].

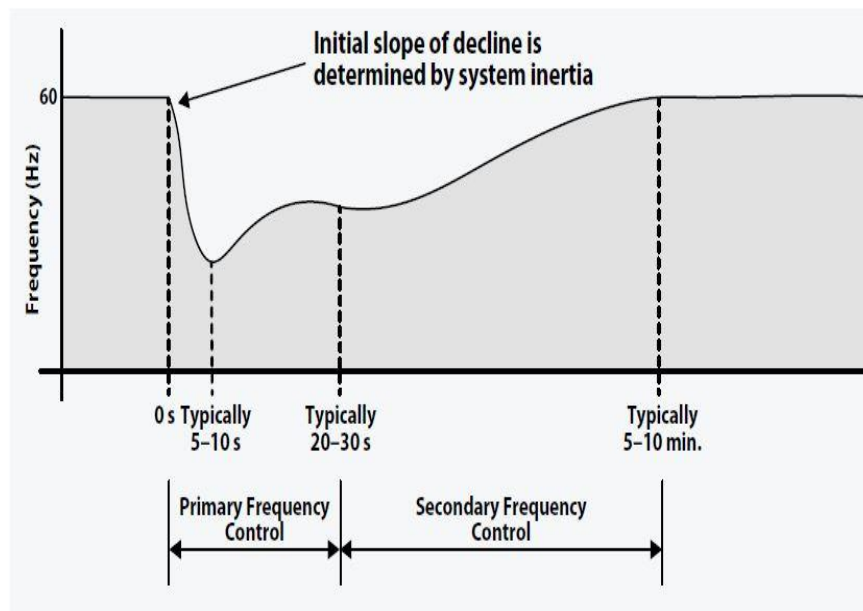


Figure 1.6. Illustration of primary and secondary frequency response [15]

The figure clearly exhibits the concept of inertial, primary and secondary control as discussed above.

### **Tertiary Frequency Control**

Tertiary control is activated when deviation in the control area last for longer than 15 minutes. It is used to relieve secondary control [19]. It gets resources in place to handle current and future contingencies. Reserve deployment and reserve restoration are common types of tertiary control [13].

## **1.3 Backdrop on Grid-Scale Energy Storage and Demand Response**

### **1.3.1 Grid Scale Energy Storage**

Currently the U.S. has about 25 GW of grid storage. The Department of Energy (DOE) provides a snapshot of the scope and range of energy storage systems deployed in United States [20]. From Figure 1.7, pumped hydro is the largest contributor as an energy storage system (95%), due to its enormous unit sizes and long history as the most suitable technology of choice by the electric utility sectors. Pumped hydro is currently used in several locations all around U.S. to employ off-peak electricity. Thermal storage, batteries, flywheel, compressed air etc., contributes for the remaining 5% of storage capability [20]. Each energy storage technology has its own characteristics that makes it suitable for certain grid services but not for others.

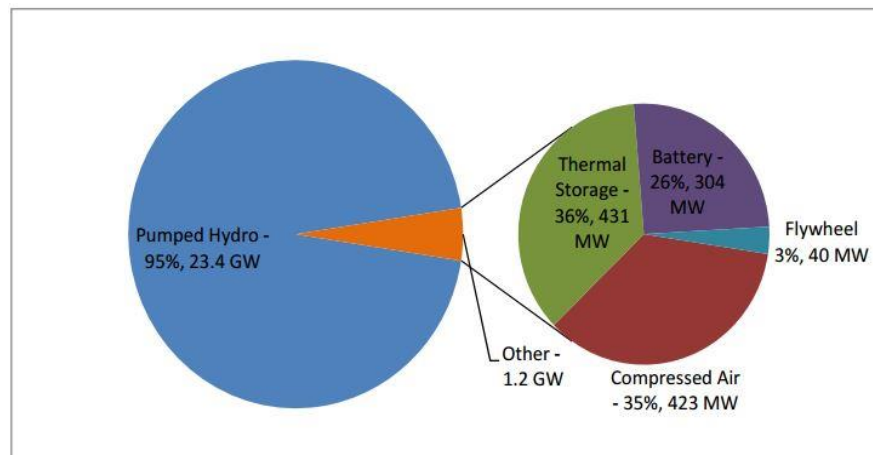


Figure 1.7. Rated power of US grid storage projects [20]

Energy storage technologies such as the ones mentioned above, provide energy management, load leveling, frequency regulation, grid stabilization, backup power etc.

Due to the high cost of energy storage, energy storage is not deployed widely today. For the energy storage system to provide flexibility, several cents per kWh are invested for capital costs alone, due to the increasingly limited availability of suitable plant sites. The value that energy storage provides for integrating wind energy is possible via wind integration studies. By modeling a 10% wind penetration on the Colorado power grid with and without the presence of a pumped hydro storage plant, a wind integration study found that the pumped hydro reduce the wind integration costs by \$0.00134 per kWh of wind energy. This would correspond to an annual saving of approximately \$2.5 million under the 10% wind scenario. Assuming that a new pumped hydro plant would typically cost \$1 million/MW of installed capacity, the time it would roughly take to pay back the initial cost of the plant would be more than a 100 years. Thus energy storage has a high cost hindrance to overcome [21].

Several new projects are being chalked out and implemented to improve the role of energy storage to provide balancing resource for wind integration in the Pacific Northwest. This includes the development of vanadium flow batteries which store energy in the form of two liquids in separate tanks. The three utilities in the Washington state that are implementing this technology for energy storage are Avista utilities, Puget Sound Energy and Snohomish County [22].

### **1.3.2 Demand Response**

According to Federal Energy Regulatory Commission (FERC), Demand Response (DR) is defined as: “Changes in electric usage by end-use customers from their normal consumption patterns in response to changes in the price of electricity over time, or to incentive payments designed to induce lower electricity use at times of high wholesale market prices or when system reliability is jeopardized” [23]. Consumers can play an important role in the operation of the electric grid by shifting or reducing their electricity usage during peak periods. Demand response programs are another way to balance the supply and demand since implementing energy storage technologies are very expensive.

In the Pacific Northwest, PacifiCorp has expected to have over 500 MW of demand response which includes direct load control of air conditioning and irrigation, dispatchable standby generation etc. PacifiCorp has more than 5% of peak load in firm demand response, and another 1-2 percent in non-firm demand response. Domestic water heating is an example of a load that could provide regulation to the power system in the Pacific Northwest [24]. A new study showed that electric

household water heaters could shave 5.3 GW off the nation's peak power demand and help store extra wind power [25]. They can store energy in the form of hot water. During demand response operations, energy can be stored by increasing load and temperature, and energy can be effectively returned by reducing load and temperature.

## **1.4 Motivation for the Thesis**

Electricity production from renewable energy has ramped in the past few years to meet renewable portfolio standards. Due to this increase, it is necessary to store this energy during low demands and supply when the demand is high. Thus energy storage seems to be an enabling technology for integrating variable renewable power into the electric grid for increasing grid reliability [26].

This research focuses to investigate the feasibility of using water heater load for renewable integration. The idea is to control residential water heaters in the presence of high wind penetration to study various frequency excursions and implement a control law to improve the frequency profile.



## **2 WECC's Primary Frequency Response to Generator Outage**

For the reliable operation of a power system it is very important that a balance is maintained between load and generation when load is constantly changing. The best indicator of this balance, or unbalance, is the grid frequency that has to be maintained within its predetermined limits around the nominal operating point of 60 Hz which can be achieved by controlling the output of the generators. This balancing and controlling of frequency occurs over a continuum of time using various resources that fall under the category of inertial, primary, secondary and tertiary controls as already discussed earlier [27].

WECC's response to primary control, immediately following a large disturbance (loss of generation) is addressed in this chapter of the thesis. To carry out transient analysis, a base case has been chosen to recreate the disturbance and study the frequency behavior and governor response.

### **2.1 Winter Low Load-High CAISO Wind Base Case for WECC**

The base cases selected by CAISO were intended to represent a spectrum of operating points with high levels of renewables in California, and conditions which could be challenging from a frequency response perspective. CAISO developed these cases starting from well-established planning data bases (WECC base case database). The base case that has been chosen to perform the transient analysis in response to the generator outage is the winter low load-high CAISO wind, which has been established

from WECC 2012 Light Winter base case. Table 2.1 gives a brief synopsis of the four base cases [27].

Table 2.1 WECC's Base Cases [27]

	<b>WECC Load (MW)</b>
<b>Winter Low Load- High CAISO Wind</b>	<b>91,300</b>
Weekend Morning-High CAISO Wind and Solar	1,10,798
Winter Off Peak- High Wind	97,447
Spring Peak- High Hydro and Wind	1,40,167

There were two important generation trip events that were considered in CAISO's study to perform transient analysis which is described Table 2.2.

Table 2.2 WECC's Base Cases [27]

Loss of two Palo Verde units: (2690 MW )	Outside California
Loss of two Diablo Canyon units (2400 MW)	Inside California

This research has considered the generation trip event outside California: Loss of two Palo Verde units accounting for 2690 MW of generation outage [27].

### 2.1.1 Response to Palo Verde Disturbance

The most crucial, front-line control of frequency in a power system is the action of generator governors. Hence, in a power system when load exceeds generation or generation exceeds load, the grid frequency either falls below a certain limit of adequacy, or rises above a certain limit of adequacy. When the frequency is below its nominal level, it indicates that the dominance of load is higher in the system than generation and therefore there is an urgent need to pump up the generation. Figure 2.1 shows the frequency response of the Western Interconnection to the Palo Verde generation tripping event imposed at 1 second [27].

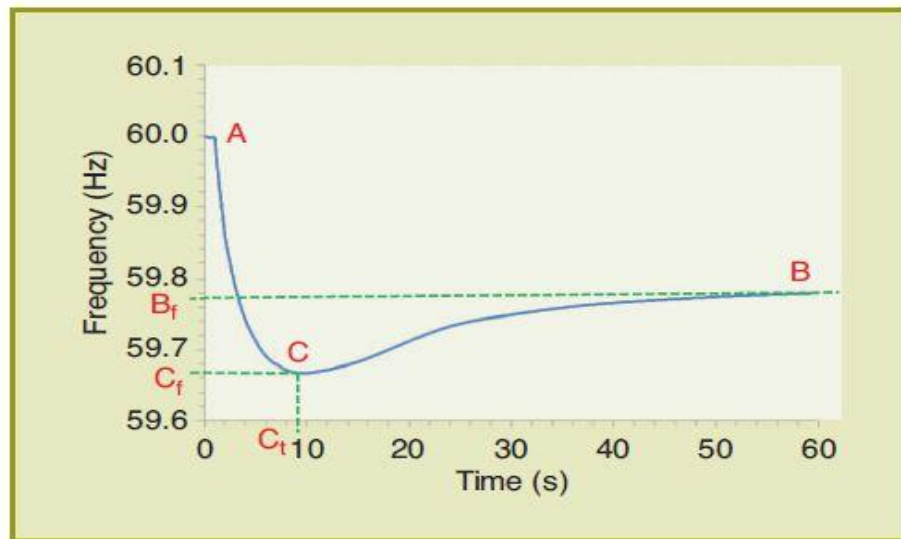


Figure 2.1. Frequency Response to Palo Verde Generation Trip Event [28]

The generation trip event, accounted for a sudden drop in the frequency (point A), also called as starting frequency. This is the system frequency before a disturbance; it is close to 60 Hz. Right after 1 second the frequency drops and the nadir of the frequency

(point C) occurs at about 9.8 seconds at a frequency of approximately 59.67 Hz. The settling frequency is around 59.78 Hz (point B), which is usually observed after the big swings are over and the primary frequency controls have acted but before the secondary frequency control becomes significant. The frequency nadir gives a margin of 170 mHz above the first stage of under frequency load shedding (UFLS) at 59.5 Hz [27].

As the frequency drops, the generator governors alter their output in response to the frequency change. Figure 2.2 shows the electrical and mechanical power output of the machines with enabled governors.

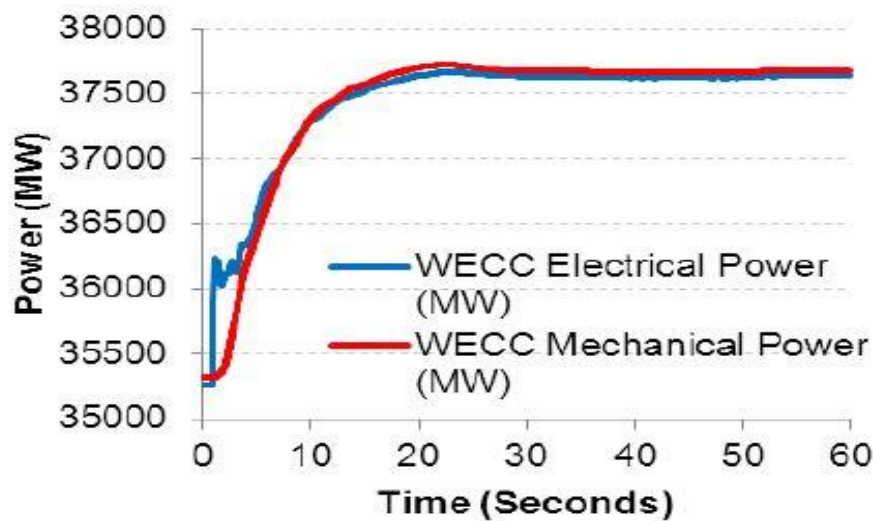


Figure 2.2. Governor Response to Palo Verde Generation Trip Event [28]

As the frequency droops and reaches its frequency nadir, the governor units deliver about an extra 2,350 MW and by the time the frequency settles out by 60 seconds, the electrical and mechanical power are substantially equal. The increase in generation

(WECC electrical power) of approximately 2350 MW by governor responsive units represents the majority of system response and almost equal to the lost generation (2,650 MW) after 60 seconds [28].

## **2.2 Western Electricity Coordinating Council (WECC) System Model**

This section of chapter 2 will demonstrate the theory behind speed governing, generator response to load change, governors with speed droop characteristics, aggregated performance of all generators in a power system and single area primary speed control. It will then showcase the implementation of the above concepts and theories to build a WECC model in Matlab Simulink with a scenario of sudden drop in generation (Palo Verde event). The simulation set up will be shown below accompanied with a detailed explanation of the model. The simulation results will present the process of recreating the responses and fine tuning several parameters of the model to achieve the responses as seen in Figure 2.1 and Figure 2.2.

### **2.2.1 Concept of Speed Governing Control**

The frequency of a system is dependent on active power balance. Frequency being one of the primary important and common factors in a power system, any small change in active power demand is reflected throughout the system by a change in frequency. As there are as so many generators that provide power into the power system, some kind of control mechanism must be provided to allocate change in demand to the generators. A speed governor on each generating unit provides that control mechanism

which varies the prime mover output automatically for changes in system speed (frequency) [29]. Figure 2.3 shows the basic speed governing mechanism.

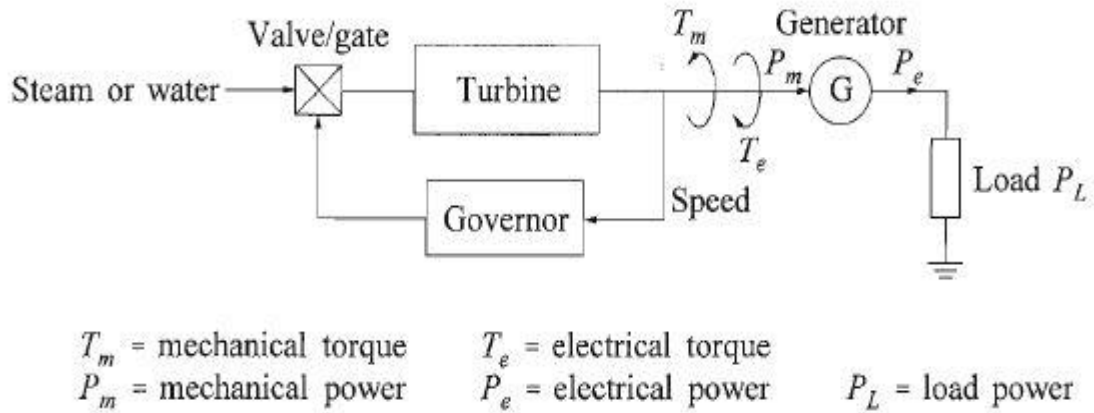


Figure 2.3. Generator supplying isolated load [29]

When there is a change in load, it is instantaneously reflected in  $T_e$  (electric torque) of the generator and as  $T_e$  and  $T_m$  (mechanical torque) are linked to each other, a mismatch occurs between the two quantities which results in speed variations and this is determined by the equations of motion (derived below). When there is a mismatch between the torques acting on the rotor of the machine, the net torque causes an acceleration or deceleration  $T_a$  as shown in (1)

$$T_a = T_m - T_e \quad (1)$$

Where,

$$T_a = \text{accelerating torque in } N - m$$

$$T_m = \text{mechanical torque in } N - m$$

$T_e = \text{electromagnetic torque in } N - m$

The combined inertia of the generator and prime mover is accelerated by the unbalance in the applied torques. Hence, the equation of motion is shown in (2)

$$J \frac{d\omega_m}{dt} = T_a = T_m - T_e \quad (2)$$

Where,

$J$  = combined moment of inertia of generator and turbine, kg.m<sup>2</sup>

$\omega_m$  = angular velocity of the rotor, rad/s

$t$  = time, s

Equation (2) can be normalized in terms of per unit inertia constant  $H$ , defined as the kinetic energy in watt-seconds at rated speed divided by the VA base. Using  $\omega_{0m}$  to denote rated angular velocity in mechanical radians per second, the inertia constant is shown in (3)

$$H = \frac{1}{2} \frac{J \omega_{0m}^2}{VA_{base}}$$

(3)

Where  $H$  is the inertia constant and can be defined as,

$$H = \frac{\text{stored energy at rated speed in MW's}}{\text{MVA rating}}$$

The moment of inertia  $J$  in terms of  $H$  is seen below in (4)

$$J = \frac{2H}{\omega_{0m}^2} V A_{base} \quad (4)$$

Substituting the above equation in (2) gives (5)

$$\frac{2H}{\omega_{0m}^2} V A_{base} \frac{d\omega_m}{dt} = T_m - T_e \quad (5)$$

Rearranging the above equation yields (6)

$$2H \frac{d}{dt} \left( \frac{\omega_m}{\omega_{0m}} \right) = \frac{T_m - T_e}{V A_{base} / \omega_{0m}} \quad (6)$$

Noting that  $T_{base} = V A_{base} / \omega_{0m}$ , the equation of motion in per unit form is given in (7)

$$2H \frac{d\omega_r}{dt} = \bar{T}_m - \bar{T}_e \quad (7)$$

In equation (7),

$$\bar{\omega}_r = \frac{\omega_m}{\omega_{0m}} = \frac{\omega_r / p_f}{\omega_0 / p_f} = \frac{\omega_r}{\omega_0} \quad (8)$$

where,  $\omega_r$  is the angular velocity of the rotor in electrical rad/s,  $\omega_0$  is its rated value, and  $p_f$  is the number of field poles. If  $\delta$  is the angular position of the rotor in electrical radians with respect to a synchronously rotating reference and  $\delta_0$  is its value at  $t=0$ ,

$$\delta = \omega_r t - \omega_0 t + \delta_0 \quad (9)$$



Taking the time derivative of (9), we get

$$\frac{d\delta}{dt} = \omega_r - \omega_0 = \Delta\omega_r \quad (10)$$

And performing a second derivative of (10) again we get,

$$\begin{aligned} \frac{d^2\delta}{dt^2} &= \frac{d\omega_r}{dt} = d \frac{(\Delta\omega_r)}{dt} \\ &= \omega_0 \frac{d\omega_r}{dt} = \omega_0 \frac{d(\Delta\omega_r)}{dt} \end{aligned} \quad (11)$$

Substituting for  $d\bar{\omega}_r/dt$  given by (12) in (7), we get (12)

$$\frac{2H}{\omega_0} \frac{d^2\delta}{dt^2} = \bar{T}_m - \bar{T}_e \quad (13)$$

A damping torque is added by adding a term proportional to speed deviation in (13),

we get, (14)

$$\frac{2H}{\omega_0} \frac{d^2\delta}{dt^2} = \bar{T}_m - \bar{T}_e - K_D \Delta\bar{\omega}_r$$

Equation (13) represents the equation of motion of a synchronous machine. It is commonly referred to as the swing equation as it represents swings in rotor angle  $\delta$  during disturbances. Figure 2.4 shows the transfer function relating speed and torques.

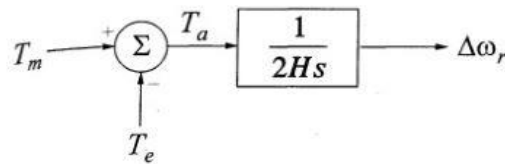


Figure 2.4. Transfer function relating speed and torque [29]

In a power system, load-frequency control is important as most loads are frequency dependent. The main goal of load-frequency control is to maintain a zero system frequency change by keeping a balance between load and generation. Hence it is preferable to express the relationship between speed and torque in terms of speed and electrical and mechanical power. This relationship can be seen in (15)

$$P = \omega_r T \quad (15)$$

Considering a small deviation (denoted by  $\Delta$ ) from initial values (denoted by 0), we get

$$P = P_0 + \Delta P$$

$$T = T_0 + \Delta T$$

$$\omega_r = \omega_0 + \Delta\omega_0$$

Substituting the above in (15), we get

$$P = P_0 + \Delta P = (\omega_0 + \Delta\omega_r)(T_0 + \Delta T) \quad (16)$$

Higher order terms are neglected hence we get (17)

$$\Delta P = \omega_0 \Delta T + \Delta\omega_r T_0 \quad (17)$$

Therefore,

$$\Delta P_m - \Delta P_e = \omega_0(\Delta T_m - \Delta T_e) + (T_{m0} - T_{e0})\Delta\omega_r \quad (18)$$

Since in steady state both electrical and mechanical torques are equal,  $T_{m0} = T_{e0}$ .

Speed is expressed in PU,  $\omega_0 = 1$ . Hence

$$\Delta P_m - \Delta P_e = \Delta T_m - \Delta T_e \quad (19)$$

Thus (19) can be expressed in terms of  $\Delta P_m$  and  $\Delta P_e$  in Figure 2.5

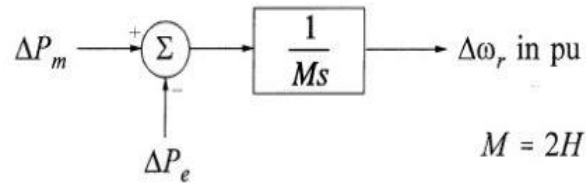


Figure 2.5. Transfer function relating speed and torque [26]

The turbine mechanical power is essentially a function of valve or gate position and independent of frequency. Thus from (19), the swing equation can be written as seen in (20)

$$\frac{2H}{\omega_0} \frac{d^2\delta}{dt^2} = P_m - P_e \quad (20)$$

Where  $2H = M$ , H is the inertial constant

Thus the swing equation helps to determine the transient stability of a power system.

### 2.2.2 Load Response to Frequency Deviation

In a power system, there are different kinds of loads for example, resistive loads such as heating loads, lighting loads etc., that are independent of any frequency change. In case of motor loads, such as fans, pumps etc., due to the changes in motor speeds, the electric power changes with frequency. Thus the electrical power is the summation of non-frequency sensitive load change and frequency sensitive load change given by the mathematical equation below [29].

$$P_e = \Delta P_L + D\Delta\omega_r \quad (21)$$

$$\Delta P_L = \text{non} - \text{frequency sensitive load change}$$

$$D\Delta\omega_r = \text{frequency sensitive load change}$$

$$D = \text{load} - \text{damping constant}$$

Damping is an influence upon a system that has the effect of reducing, restricting or preventing its oscillation [30]. It is expressed as a percent change in load for one percent change in frequency. Typical values are 1 to 2 percent which means that a value of  $D=2$  means that a 1% change in frequency would cause a 2% change in load [29]. Note that load damping constant  $D$  is included in the transfer function to represent the load effect. A block diagram is shown in Figure 2.6 to understand the effect of load damping in a system.

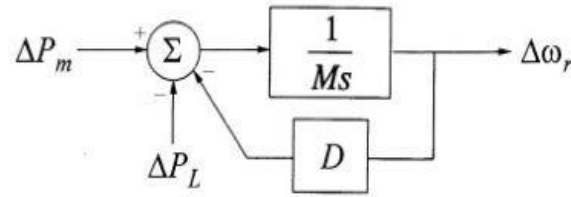


Figure 2.6. System block diagram to show the effect of load damping [29]

The reduced form can be seen in Figure 2.7

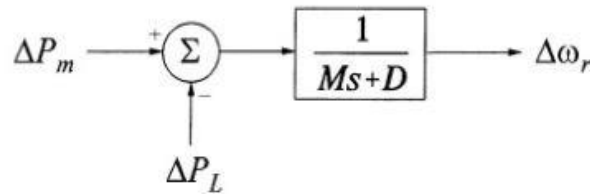


Figure 2.7. Reduced system block diagram to show the effect of load damping [29]

When there is a change in load, the system responds to the load change by the inertia constant and damping constant.

### 2.2.3 Governors with Speed-Droop Characteristic

Synchronous generators have their speed as a function of their frequency or vice versa and since they are synchronous, no generator can go faster or slower than the speed that is dictated by the frequency. Since all the synchronous generators are connected together in a grid and their rotors are locked into synchronism, the prime movers which are mechanically coupled to the generators cannot change their speeds either, as it is a function of the frequency of the generators. For a prime mover to stably control its power output while connected in parallel to other generators and prime movers in

the grid, the control systems employs a proportional control called the droop control. This is done by constantly regulating the amount of mechanical input power to the shaft of the electric generator. The degree of this modulation is called “droop” or “slope” [29]. This droop is measured as the percentage of frequency change ( $\Delta f$ ) to the percentage of power output ( $\Delta P$ ) and is usually represented by  $R$  [29].

$$R = \frac{\Delta f}{\Delta P}$$

Figure 2.8 shows ideal steady state characteristics of a governor with speed droop control.

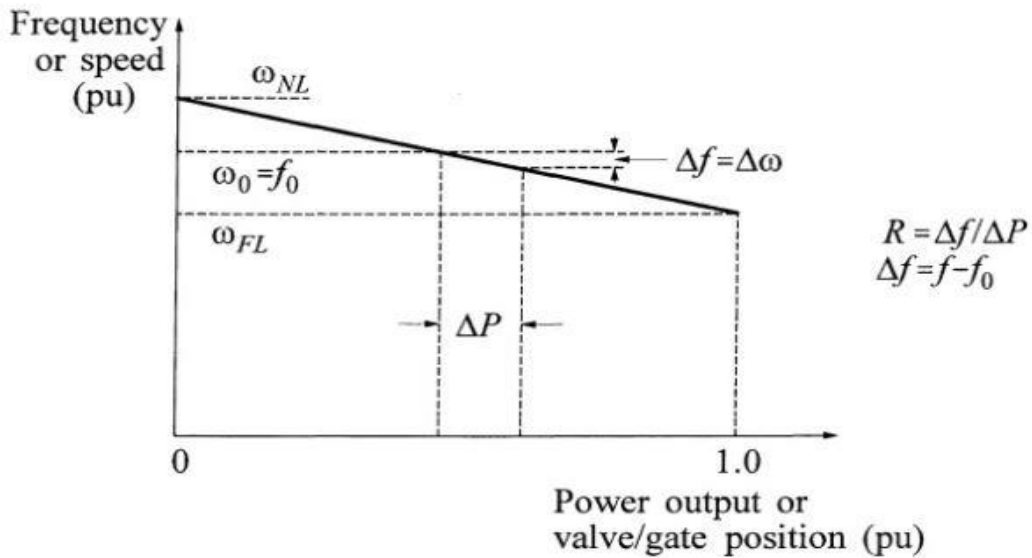


Figure 2.8. Ideal steady state characteristics of a governor with speed droop control [29]

A typical slope is 5%, which means that if the frequency error is 5% (5% of 60 Hz = 3Hz), full output of the generator would be used to counterbalance the frequency error [29]

### 2.2.4 One Area Primary Frequency Control

Figure 2.9 represents a very general or standard mechanism of a generator in a power system, where  $P^*$  is the desired power to supply the grid. A governor and a turbine represent low pass filters while modeling in Simulink.  $P$  is the actual power delivered by the turbine. Due to the presence of the low pass filters, there is some amount of time delay to get the actual power  $P$ . This is due to the governors control system which needs sometime to respond to the change in frequency in order to deliver  $P^*$ . The mechanical system (turbine) also has a time delay to respond to a change to deliver  $P^*$ . Eventually  $P=P^*$ , but during transient conditions,  $P$  does not respond instantaneously and this characteristic can be seen in Figure 2.10. There is another control function  $R$ , called the droop function that has been discussed in the above section. In Figure 2.9, if frequency is 60 Hz, it implies that  $\Delta\omega = 0$  which means everything in the grid is normal and  $P^*=P$ . If frequency is above 60 Hz, then  $\Delta\omega > 0$ , hence there is a need to back off generation, hence depending on the droop function ( $1/R$ ) a little amount of power is removed. Hence  $P^*$  still remains the same but  $P$  is a value lesser than  $P^*$  due to the droop control function. Conversely if the frequency is too low,  $\Delta\omega < 0$  and there is a need to increase generation in the system.

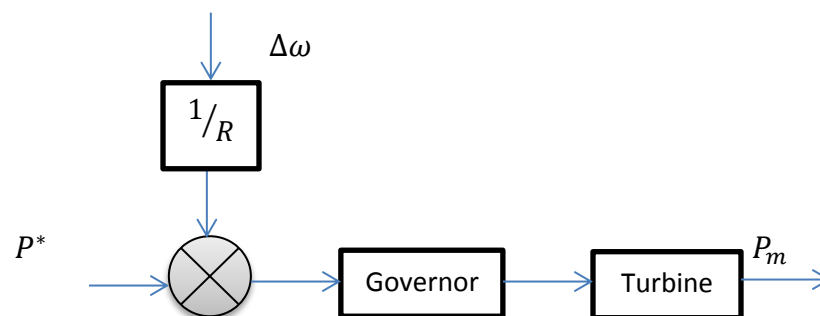


Figure 2.9. Standard generator mechanism in a power system

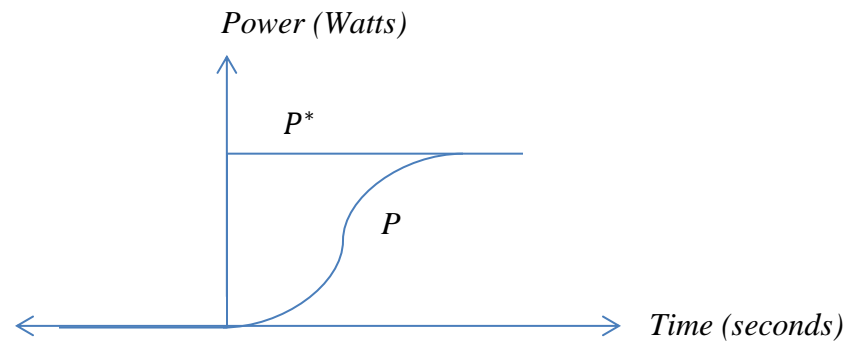


Figure 2.10. Commanded power and actual power characteristic

A single area system with primary speed control is shown below in Figure 2.11

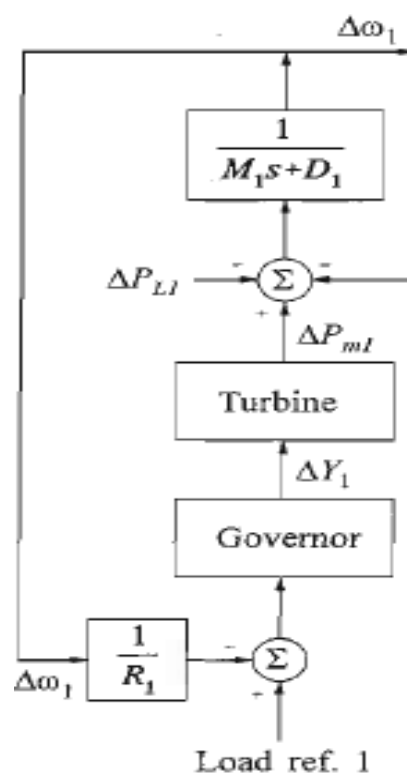


Figure 2.11. Single area system with only primary speed control [29]



The load reference seen in the above figure shows the generation required to serve the load. The inertial constants have been introduced representing the amount of inertia present in the system. The power output from the turbine is converted to electrical power and is compared with the load. Depending on if generation is positive or negative implying that generation is above 60 Hz or below 60 Hz,  $\Delta\omega$  is either positive or negative. Also the entire system shows all the parameters as a difference from their nominal values (delta values).

### 2.2.5 Aggregated Performance of All Generators in a Power System

In general, a power system has several generators running synchronously and it is interesting to study the collective performance of all the generators in the system. Thus, an assumption is made that all the coherent response generators can be represented by an equivalent generator. The equivalent generator will have an inertia constant equal to  $M_{eq}$ , which is the sum of the inertia constants of all the generating units. Similarly the effects of system loads are dumped into a single damping constant  $D$ . Figure 2.12 shows the system equivalent for load frequency control analysis where several generators are culminated to form a single large unit [29].

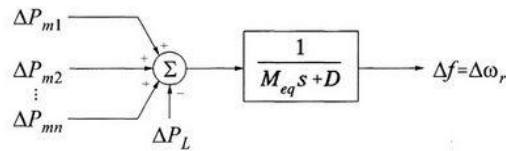


Figure 2.12. Aggregated generator system equivalent [29]

The frequency characteristics of a power system depend on the combined effect of the droops of all the governors of the generators.

Therefore,

$$R_{eq} = \frac{1}{1/R_1 + 1/R_2 + 1/R_3 + \dots + 1/R_n} \quad (22)$$

Where,

$R_1, R_2, R_3, \dots, R_n$  are the droop constants for individual generator

### 2.3 Simulation Setup and Simulation Results of the WECC Model

This section showcases the single area modeling of the WECC system in Simulink. Figure 2.11 in section 2.2.4 shows the block diagram of a one-area system with only primary speed control and its working. The basic idea of this section was to recreate the responses seen in Figure 2.1 and 2.2 so that transient analysis can be performed when wind energy and energy storage are added to the system which will be shown in the later chapters. The first step was to recreate the frequency response (call it the benchmark frequency) by taking several points of the frequency (y-axis) and its respective time (x-axis) from Figure 2.1 and interpolate it in Matlab. The next step was to model the one-area system with primary control seen in Figure 2.13 and tune various parameters of the model such as the inertia constant  $M$ , the coefficients of the transfer functions of the governor and turbine, the damping constant  $D$  and the droop speed control factor  $R$  to obtain the simulated frequency. After several sweeps the best possible result that could be achieved can be seen in Figure 2.14.

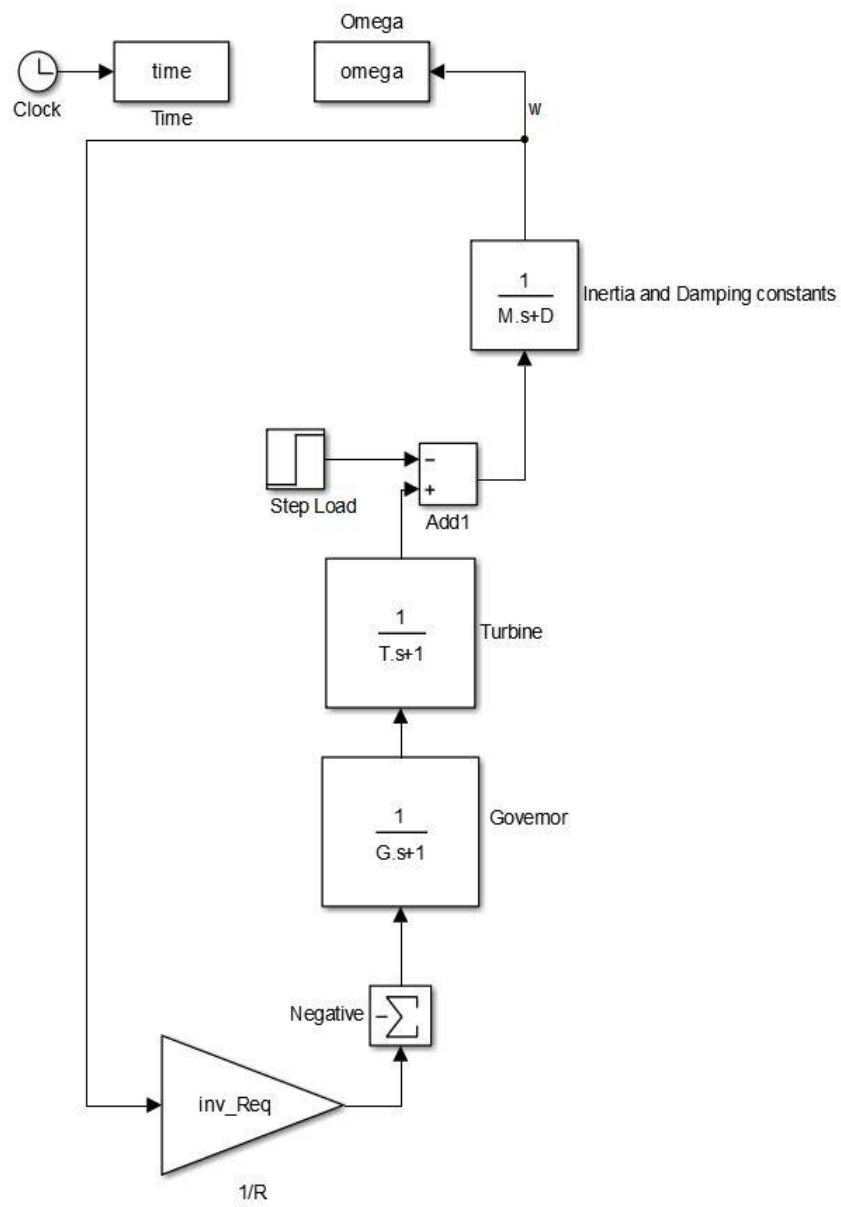


Figure 2.13. One-area system with primary speed control in Simulink

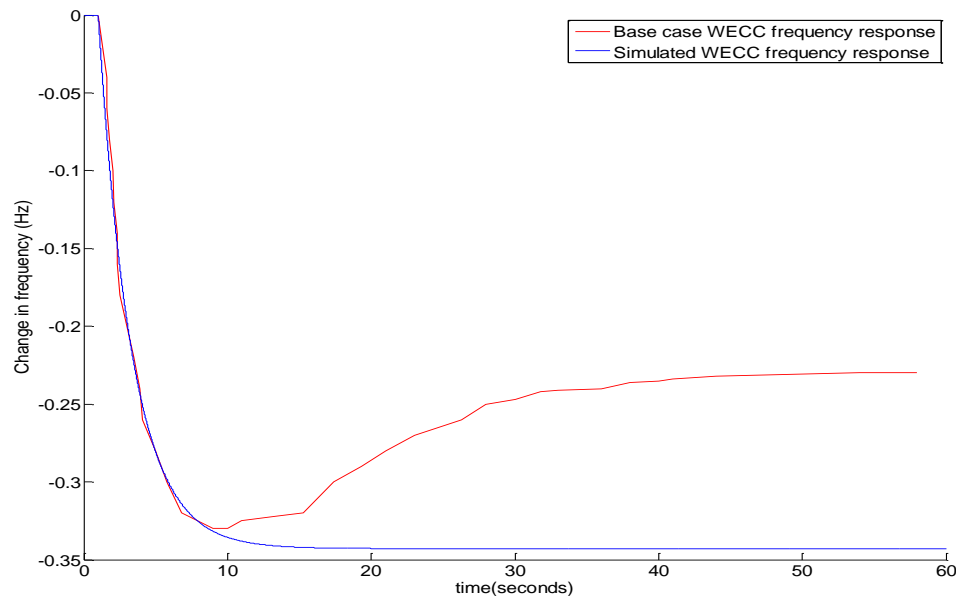


Figure 2.14. WECC base case frequency response and WECC simulated frequency response with loss of generation

From the above plot it can be seen that the benchmark WECC frequency (red) and the simulated WECC frequency (blue) follow each other only for about 9 seconds and splits apart for the rest of the time until 60 seconds. Tuning various parameters of the model did not give the desired response. This behavior concluded that the WECC model comprised of several different generators responding at different timescales, meaning that the generators had to be divided into combinations of disparate groups such as fast, medium and slow responsive generators. This conclusion was confirmed from the literature review which shows a figure describing the timing of the governor response for the case that has been used for this thesis (winter low load-high CAISO wind base case).

In Figure 2.15, each green dot represents one responsive machine, with its maximum mechanical power output in MW shown on the y-axis and time in seconds shown on the x-axis. To help understand the figure better, four time traces were shown on the right hand side representing the four bright red points. The first of these four plants rose rapidly, and produced its maximum output just before the frequency nadir. The next governor shows some overshoot (about 20%), as compared to the next unit which reached its maximum output almost as quickly, but had no overshoot. The third unit responded rapidly, but then swung back - contributing very little by 60 seconds. The final unit, which happens to be a hydro machine, exhibited characteristic transient decline on output about 1 or 2 seconds and then steadily increased output. It continued to increase its output even at the end of one minute. Its contribution to minimizing the frequency nadir appeared to be lower, but as a percent of initial output, the increase by the time of nadir (~10 seconds) is higher. In WECC, the contribution of hydro is, not surprisingly, quite important to frequency response [27].

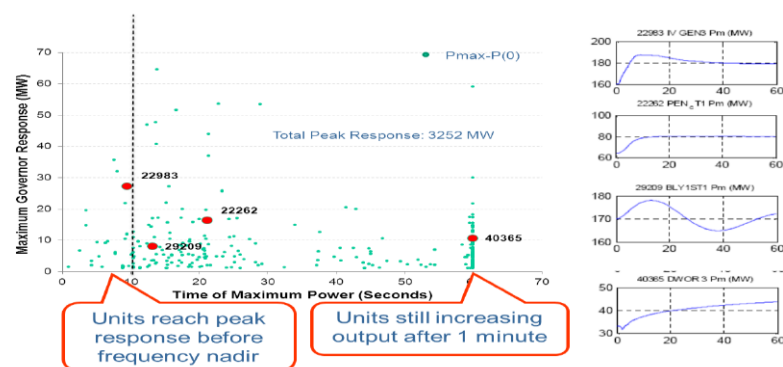


Figure 2.15. Timing of governor response for the winter low load- high CAISO wind base case

A conclusion can be drawn that there are several units present in a power system that respond at very different timescales. Few are fast responsive, few are medium responsive and few are slow or very slow responsive. The fast responsive generators thus contribute towards the frequency nadir in order to arrest the frequency from going below the under frequency load shedding point (UFLS), the medium responsive generators contribute to both frequency nadir and frequency response and the slow responsive generators contribute only towards frequency response but not frequency nadir as can be seen in the case above. Hence the model that was built in Simulink was divided into three cases to see the case would recreate the response as desired in Figure 2.1. The cases that will be shown below will show the frequency response achieved when the WECC system had all generators of a single kind with one response time (case I), fast and slow responsive generators (case II) and fast, medium and slow responsive generators (case III).

### Case I: All Generators of a Single Kind with One Response Time

Figure 2.16 shows the WECC model with one kind of generator having only one response time.

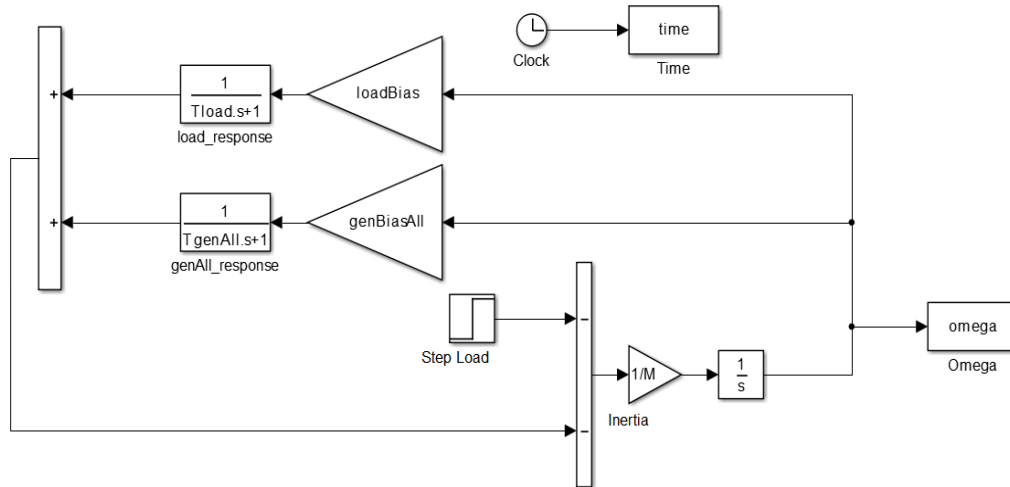


Figure 2.16. WECC model for one kind of generator having one response time

The WECC model shown above consists of an inertia constant  $M$ , bias for the generator system, and a step load to show the generation trip event. Also a response time to the load's share of primary response has been added and has been made very fast due to the reason that the load is not actively controlled and most of it should respond to the frequency as soon as the generation trip event occurs [31]. The following parameters were defined in Matlab to run several sweeps to recreate the frequency response vector in Figure 2.1.

$$P_{base} = 92 \text{ GW}$$

$$\text{Total Generation Drop} = 2.69 \text{ GW}$$

$$\text{Generation Increase} = 2.35 \text{ GW}$$

$$\text{Estimate Of Load Response} = \frac{\text{Load Drop}/P_{base}}{\Delta f/60}$$

$$\text{Load Drop} = \text{Total Genration Drop} - \text{Generation Increase}$$

$$\text{Load Bias} = \text{Estimate Of Load Response}$$

$$\text{Gen Bias All} = \text{Estimate Of Generator Response}$$

$$\text{Estimate Of Generator Response (Droop Function } 1/R) = \frac{\text{Generator Increase}/P_{base}}{\Delta f/60}$$

$$\tau_{load} = \text{Time Constant for the Load}$$

$$\tau_{genALL} = \text{Time constant for the generator}$$

Time constant ( $\tau$ ) characterizes the response to a step input of a first- order, linear time invariant system. Physically it represents the time it takes the system's step response to reach 63.2% of its final value [32].  $\Delta f$  represents the difference in frequency from the nominal value (0 Hz). Figure 2.17 shows the frequency response of the WECC system with generators responding at one timescale.



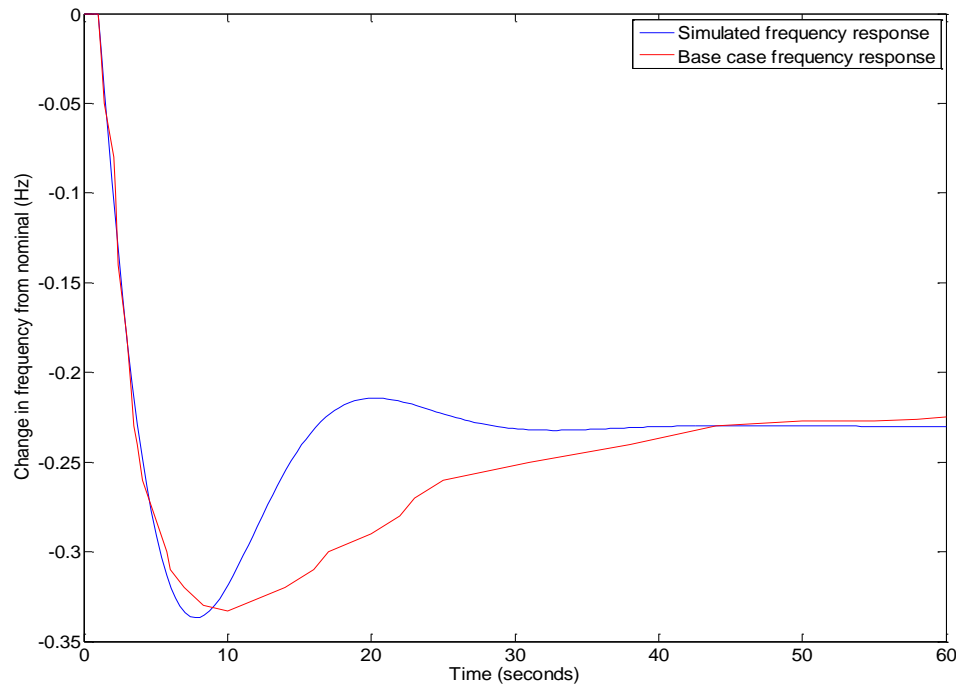


Figure 2.17. WECC's frequency response with all the generators having one response time

The above figure concludes that having just one kind of generation with one response time could not generate the benchmark frequency response (red). The next case will demonstrate the case with fast and slow generator units.

### Case II: Fast and Slow Responsive Generator Case

Figure 2.18, shows the WECC model consisting of fast and slow responsive generators. All the other parameters except 'genBiasFast' (generator bias for fast responsive generator) and 'genBiasSlow' (generator bias for slow responsive generator) from the figure below remain the same.

$$genBiasFast = frac1 * Estimate\ of\ Generator\ Response$$

$$genBiasSlow = 1 - frac1 * Estimate\ of\ Generator\ Response$$

Where,

frac1 represents the fraction of units that are fast responsive

1-frac1 represents the fraction of units that are slow responsive

Several sweeps for all the parameters were made to run in Matlab in order to attain the least Root Mean Square Error (RMSE) between the two frequency responses (benchmark frequency and simulated frequency).

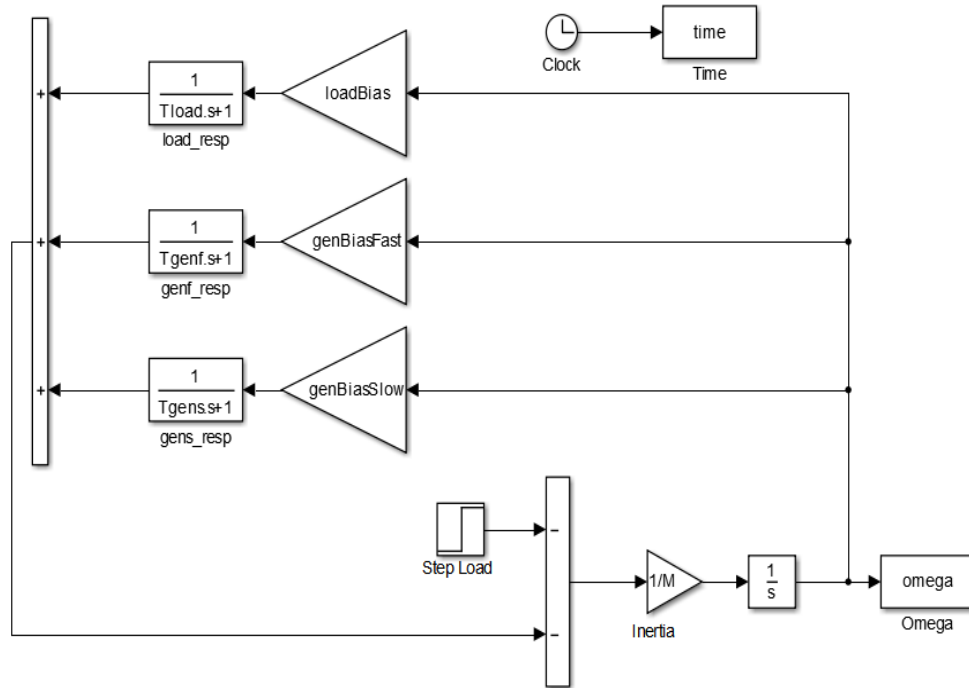


Figure 2.18. WECC model for fast and slow generator case

Figure 2.19 shows the WECC frequency response consisting of fast and slow generators for the above model.

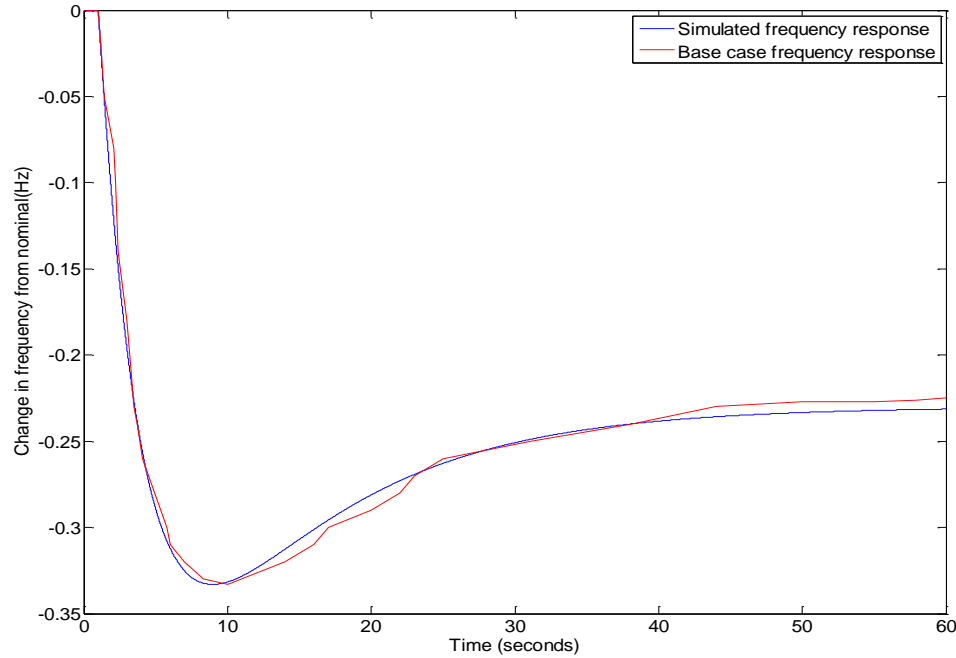


Figure 2.19. Simulated and base case frequency responses for Fast and Slow generators in the WECC system

The frequency response achieved in the above figure was the best possible response with the least RMSE. It can be seen that the by introducing generators with two responsive times gave a better frequency response as compared to Figure 2.17. This is due to the fact that certain fractions of the generators were considered as the fast responsive group while the other fraction of generators were considered as the slow responsive group in the CAISO paper.

### Case III: Fast, Medium and Slow Responsive Generator Case

In this case, three different groups of generators were considered. All the other parameters except ‘genBiasFast’ (generator bias for fast responsive generator), ‘genBiasMedium’ and ‘genBiasSlow’ (generator bias for slow responsive generator) from the figure shown below remain the same.

$$genBiasFast = frac1 * Estimate\ of\ Generator\ Response$$

$$genBiasMedium = frac2 * Estimate\ of\ Generator\ Response$$

$$genBiasslow = 1 - frac1 - frac2 * Estimate\ of\ Generator\ Response$$

frac1 represents the fraction of units that are fast responsive

frac2 represents the fraction of units that are medium responsive

1-frac1-frac2 represents the fraction of units that are slow responsive

Figure 2.20 shows the WECC system model for fast, medium and slow responsive generator case. Henceforth this model will be referred to as the FMS (Fast, Medium and Slow) base case.

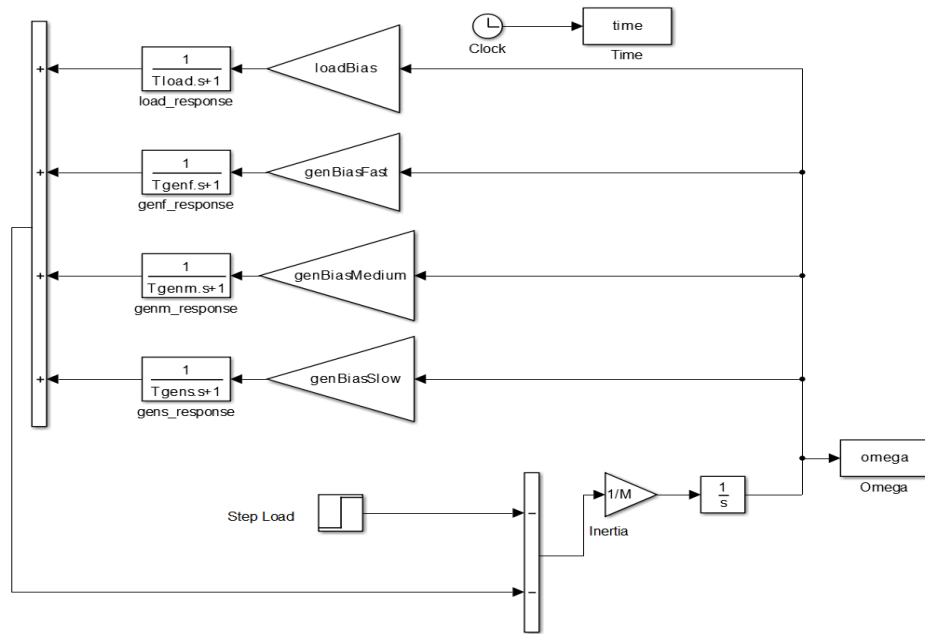


Figure 2.20 WECC system model for fast, medium and slow responsive generator case

Figure 2.21 shows the frequency response of the above model.

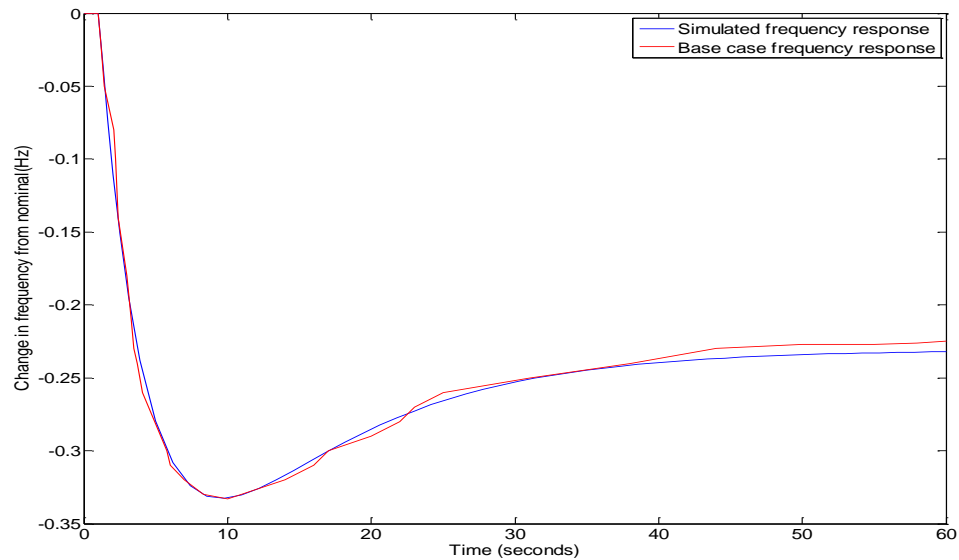


Figure 2.21. Simulated and base case frequency responses for Fast, Medium and Slow generators in the WECC system

The above plot shows the best frequency response (blue line) of the WECC system with the least RMSE after running several sweeps for the parameters seen in Table 2.3. The final value of each parameter has been listed in the table below. Hence, it can be concluded that the case with fast, medium and slow responsive generators gave the best frequency response as the benchmark frequency response and this can be accounted for the fact that different types of generators respond at different time scales. Few generators contribute towards frequency nadir (fast responsive generators) and few generators towards frequency response (medium and slow responsive generators).

Table 2.3 shows the parameters which helped achieve the WECC frequency response.

<b>Parameters for a single area primary speed control system</b>	<b>Fast, Medium and Slow Generator Case</b>
Inertia constant (M)	15
Estimate of generator response	6.6 PU/PU
Fraction of fast responsive generators(frac 1)	52%
Bias for fast generators (genBiasFast)	3.432 PU/PU
Time constant for fast generators (Tgenf)	0.4 s
Fraction of medium responsive generators(frac 2)	32%
Bias for medium generators (genBiasMedium)	2.112 PU/PU
Time constant for medium generators (Tgenm)	19 s
Fraction of slow responsive generators(1-frac 1-frac2)	16%
Bias for slow generators (genBiasSlow)	1.056 PU/PU
Time constant for slow generators (Tgens)	27 s
Estimate of load response=load bias	1.027 PU/PU

Time constant for load (Tload)	0 s
--------------------------------	-----

In Figure 2.22, we can observe the increase in generation right after primary frequency control kicks in when 2690 MW of generation was lost. It also shows the increase in generation (MW) for fast, medium and slow generators.

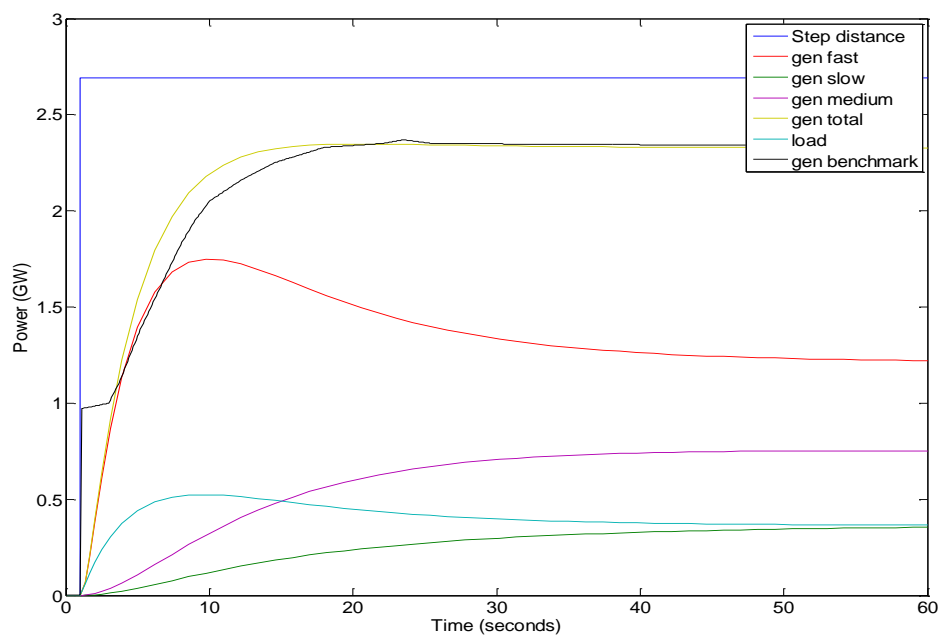


Figure 2.22. Electric power responses of generators in the WECC system for fast, medium and slow responsive generators

The plot in blue shows the step increase in load or loss in generation (2.690 GW), the red, purple and green show the increase in electrical power responses for fast, medium and slow responsive generators respectively. It can be seen that the fast responsive generators increases their generation much faster (maximum generation around 9 seconds) when compared to medium and slow responsive generators (maximum

generation at around 25 seconds and 40 seconds respectively). The load response in cyan responded fairly quickly to the trip event. The generation increase from the CAISO paper (benchmark generation) was recreated and is shown in a black plot. When simulated, the yellow plot above showcases the total generation increase of about 2,340 MW (2.34 GW), with the remaining of 350 MW (0.35 GW) responded by the load. Thus adding both the yellow (total generation increase by the generators) and cyan plot (load response to the trip event) we get the total drop in generation (2.69 GW).

## **2.4 Result Conclusion**

It can be concluded that the WECC system has different kinds of generators operating at different time scales and considering this is of primary importance for proper study of transient analysis. Thus Figure 2.23 represents the frequency response and generation increase after a sudden loss in generation and will be used for further analysis in this research.



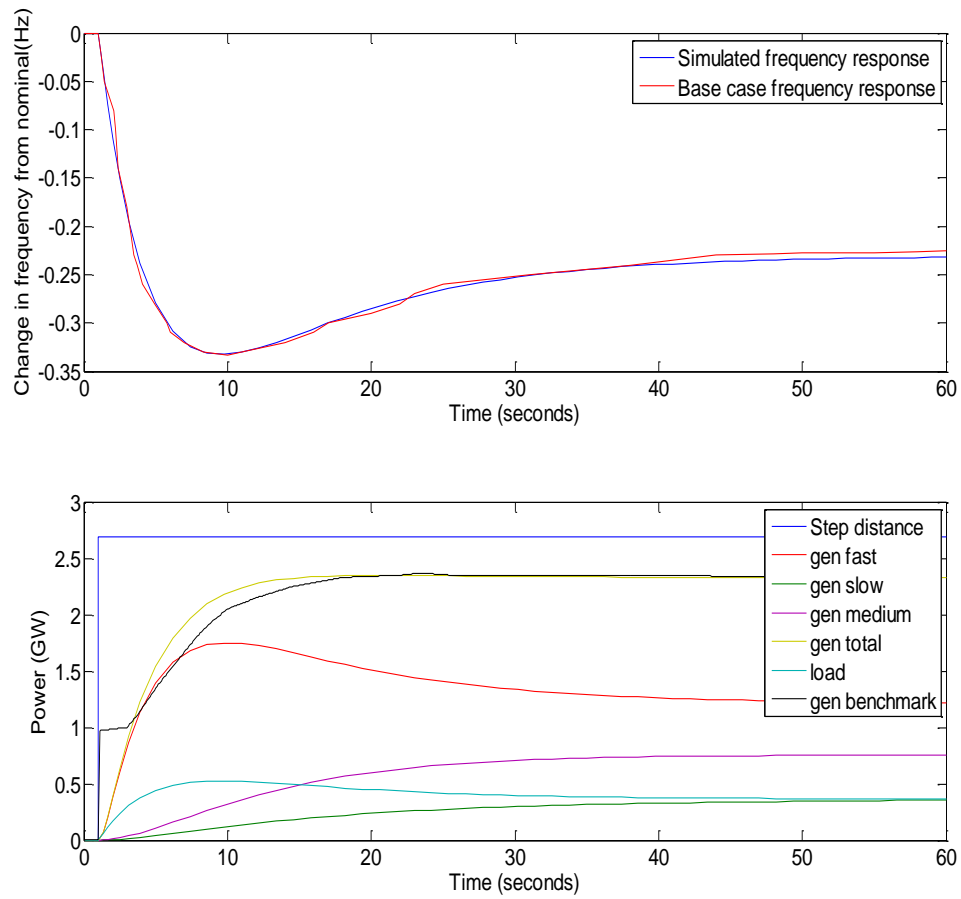


Figure 2.23. Frequency response of the WECC system including fast, medium and slow generators and the contribution of electrical power by each generator and load for the loss of 2.69 GW .

### 3 Energy Storage Modeling

In an electric power sector, electricity generated is relatively a fixed amount over short periods of time, although demand for electricity fluctuates throughout the day [33]. Therefore there is a need to develop a technology where excess energy can be stored when demand for power is low and disperse that stored energy when demand is high such that uninterruptible and flexible service can be provided. This developing technology is coined by the term “Energy Storage”, which would represent a major breakthrough in the power sector. In this section, the modeling of energy storage has been illustrated with two cases: single water heater modeling and multiple water heater modeling.

#### 3.1 Case I: Single Water Heater Modeling

Figure 3.1 shows the basic energy storage modeling for a single energy storage system.

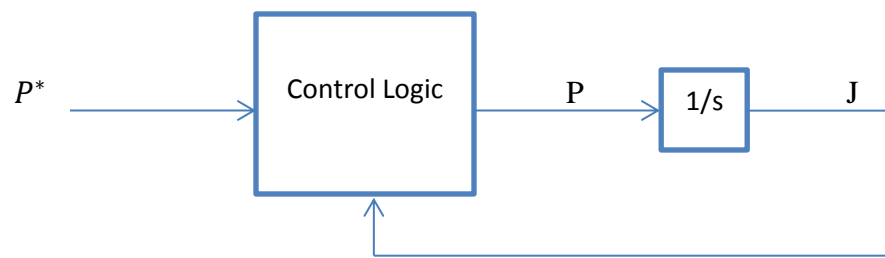


Figure 3.1. Basic energy storage modeling for a single energy storage system

$P^*$  = The power that the grid wants the energy storage to supply

$P$  = The power that the energy storage actually supplies depending on the state of charge (SOC) of the energy storage

$J$ = The energy available in the storage system.

To understand the working of Figure 3.1, let us assume that the energy storage system comprises of water heaters. 1 denotes a fully charged energy storage system and 0 denotes a fully discharged (empty) energy storage system.  $P^*$  is positive, implies that generation is more than load ( $f > 60$  Hz), thereby supplying the excess power into the energy storage system (water heaters charging) to store the energy and use it when required. On the contrary, when  $P^*$  is negative, it implies that generation is less than load ( $f < 60$  Hz), thereby a need to pump up generation to create a balance with the load, hence the water heaters start to discharge their energy, i.e., decrease load to supply to the grid until they reach a certain limit.

Modeling the limit up to which the water heaters can charge or discharge is of primary importance in order to protect the water heaters from either getting overcharged or undercharged. Therefore, when power is supplied into the water heaters or withdrawn from the water heaters to either increase or decrease their state of charge, it cannot be done indefinitely. As the maximum SOC is 1 and minimum SOC is 0, there has to be a control law which would make  $P=0$  when SOC touches 1 or 0 implying that even if  $P^*$  needs power from the water heaters to supply the grid, it will saturate at 0 and  $P$  will be equal to 0 and similarly if  $P^*$  supplies power into the water heaters to charge when there is excessive generation on the grid, it will saturate at 1 and  $P$  will be equal to 0. In all the other cases, ideally  $P^*=P$ . The above discussion sums up to say, that during overcharged and undercharge conditions one direction of power has to be shut down, but not the other, that is if the energy storage system is

fully charged, it cannot charge further, but can discharge and if the energy storage system is fully discharged, it cannot discharge further but can charge. See Table 3.1 below.

Table 3.1 Control Law for overcharge and undercharge conditions

$P^*$	$P$	SOC	Type of Protection
Positive ( $f > 60$ Hz)	0	1	Overcharge protection
Negative ( $f < 60$ Hz)	0	0	Undercharge protection

Thus, from the above discussion it shows that there are two important factors that characterize some types of energy storage systems.

1. Amount of power that the energy storage system can provide (kW) and
2. Amount of storage capacity the energy storage system has (kWh)

Let us now consider an example of having an energy storage system consisting of one water heater unit. See Figure 3.2

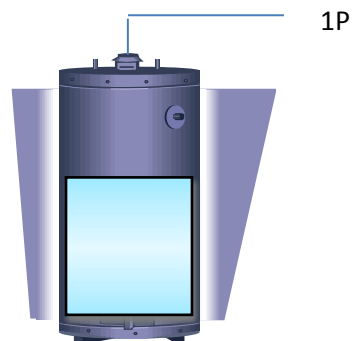


Figure 3.2. One water heater unit as the energy storage

Let us assume that a single water heater unit has a certain amount of charge present in it (represented in blue in Figure 3.2) and has a maximum power capability of  $1P$ , where  $P$  denotes power in watts. In such a case, the water heater will deliver its full power as long as there is charge present in it. Only when the water heater has an SOC of 0 or 1 will it either be able to completely sink power or completely source power as represented by red lines in Figure 3.3. The dashed black lines is when the water heater cannot source or sink power to protect from overcharged and undercharged cases. Thus charting power against SOC, it would look like the figure below.

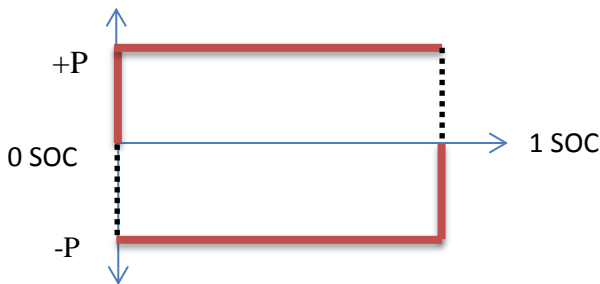


Figure 3.3. Operative region for a single water heater unit

The shaded region in beige is the operative region of the water heater as long as there is some amount of charge present in it.

Figure 3.4 shows a Simulink model implementation of a single water heater unit showcasing the above discussed concepts. Undercharge and overcharge protection has been modeled in a way such that if either of the two conditions are satisfied then the “if” block will let it through and give the actual water heater power  $P$  else it will give 0. Hence the two conditions are as follows:

- i. If  $P^*$  is positive and SOC is greater than and equal to one
- ii. If  $P^*$  is negative and SOC is less than and equal to zero

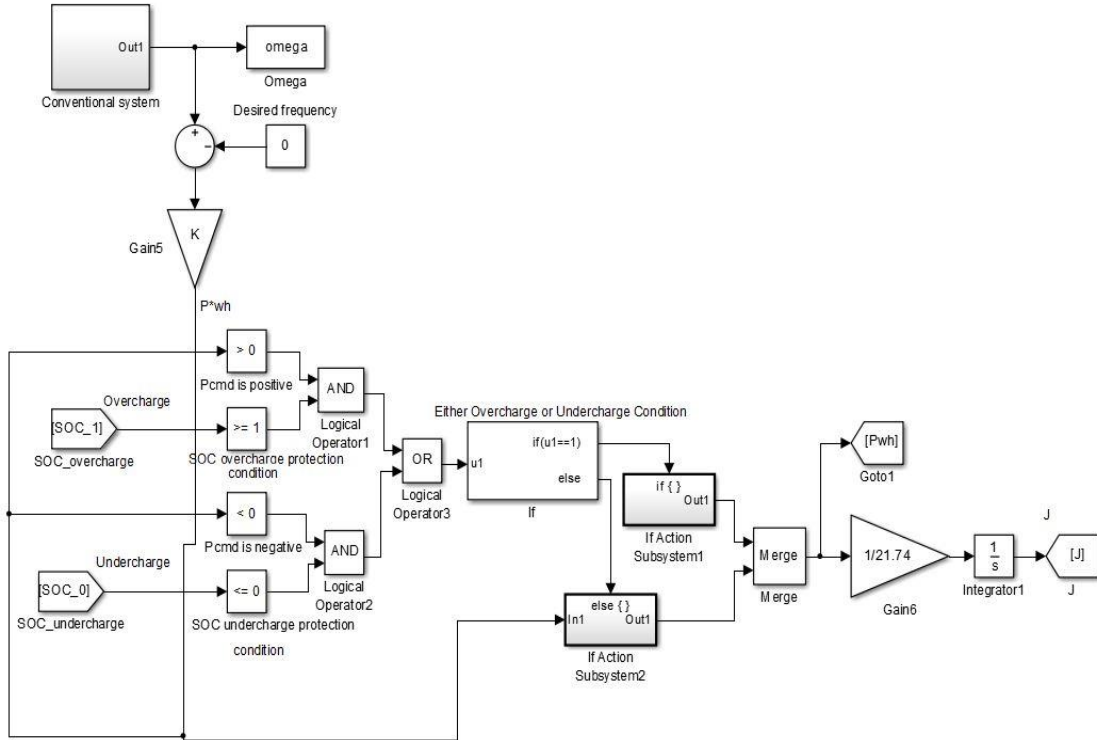


Figure 3.4. Energy storage modeling for a single water heater unit

The above model is implemented for one water heater unit, but in reality there are several thousands of water heaters available to form a large energy storage system. In such a case the above protection scheme is just a function of the model having several thousand water heaters present in it which will be seen in the Case II

### 3.2 Case II: Multiple Water Heater Modeling

Consider 3 water heaters half full; implying that the system has half state of charge.

The total power that can be supplied by the three water heaters is  $3P$ , assuming each of the water heater units has a full power capacity of  $1P$  when fully charge and  $0P$  when fully discharged, where  $P$  is power in watts. Thus  $3P$  power can be extracted until the water heaters get fully discharged, suggesting that though each of the units has only half charge in them, they can deliver full power as long as the units have some amount of charge in them. See Figure 3.5

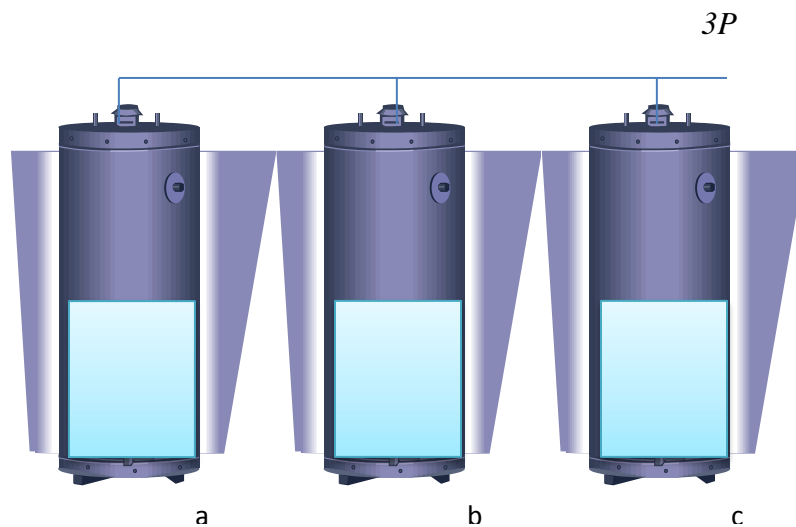


Figure 3.5. Three water heaters with half state of charge

But when the scenario is as in Figure 3.6, the power extracted is different from above and the relationship between power and state of charge changes.

Consider 3 water heaters as seen in Figure 3.6,

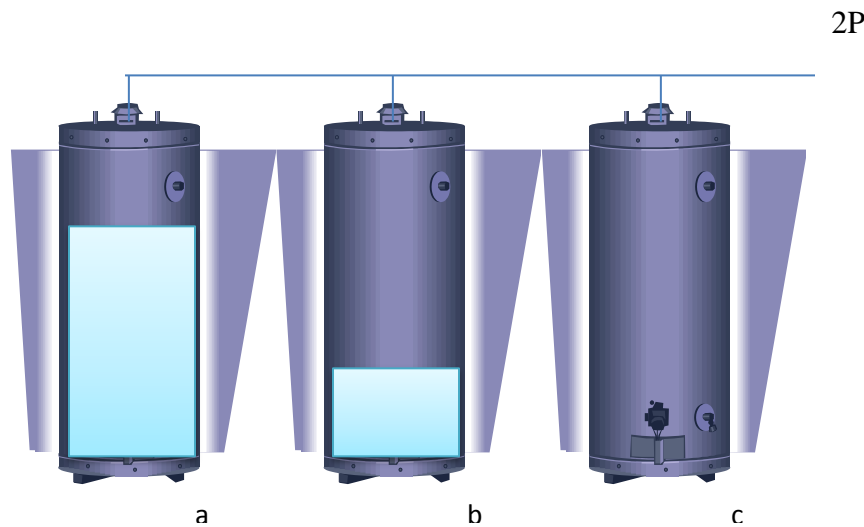


Figure 3.6. Multiple water heaters

Water heater 'a' is  $\frac{2}{3}$  full, water heater 'b' is  $\frac{1}{3}$  full and water heater 'c' is fully empty. An equivalent power of  $3P$  could be attained as there are 3 units present in the system, but only  $2P$  power can be extracted from it (as one is totally empty). After a while, the water heater having  $\frac{1}{3}$  charge will completely discharge (becomes 0) and the resultant power would be  $1P$ . This means that when all the above water heaters have a middle amount of charge in them (Figure 3.5), they are all available to give full power. But when one water heater is partially charged and the other is fully charged, full power cannot be extracted as there are lesser unit to contribute towards full power. Therefore, for several thousand water heaters present in the system, the SOC of the whole system would have some connection to the power capacity of the whole system, because some of the water heaters are at maximum temperature and some are at their minimum temperature. Therefore it can be concluded that power is a function of energy storage. The below two figures will give us an idea of the discussions held above.



Figure 3.7 shows the relationship between total SOC and the units (water heaters) available for charge.

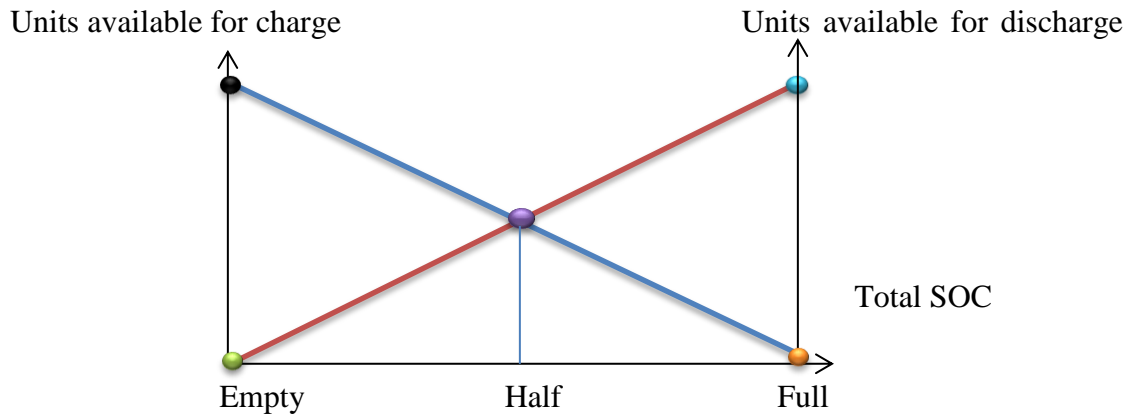


Figure 3.7. Straight line approximation

In the plot above, the total State of charge (SOC) is indicated on the x-axis, and the units available for charge and discharge on its y-axes. The blue line shows all the units available for charge, the red line shows all the units available for discharge. The black, green, cyan and orange dots give the four corners of the box (Figure 3.8). If SOC is totally empty, then all the units in the system should be available to charge (black dot) and none of the units must be available to discharge (green dot). This is due to the undercharge protection concept in chapter 3.1. Likewise, if SOC is totally full, then all the units should be available for discharge (cyan dot), and none available for charge (orange dot). This accounts for overcharged protection. When the units are half full, then half of the units are available for charge and half of the units are available for discharge (purple dot). Thus drawing two straight lines between the dots as shown above could be a way to model an energy storage system having several thousand

water heaters in it. Therefore the takeaway point from the above discussion is that, when there are several thousand water heaters present in the system and if all of them have low temperature, it implies that all of the units are available for charging, on the contrary if all the water heaters have high temperature, then all the units are available for discharging. But in reality, a large energy storage system would have several thousand water heaters with different temperatures; hence their charging and discharging capabilities are different based on the power capacity. It is not feasible to check the status of every water heater, thus a rule has to be implemented which hits the average of the energy in all the units. Figure 3.8 will show the operative region of the water heaters and the implementation of the straight line approximation.

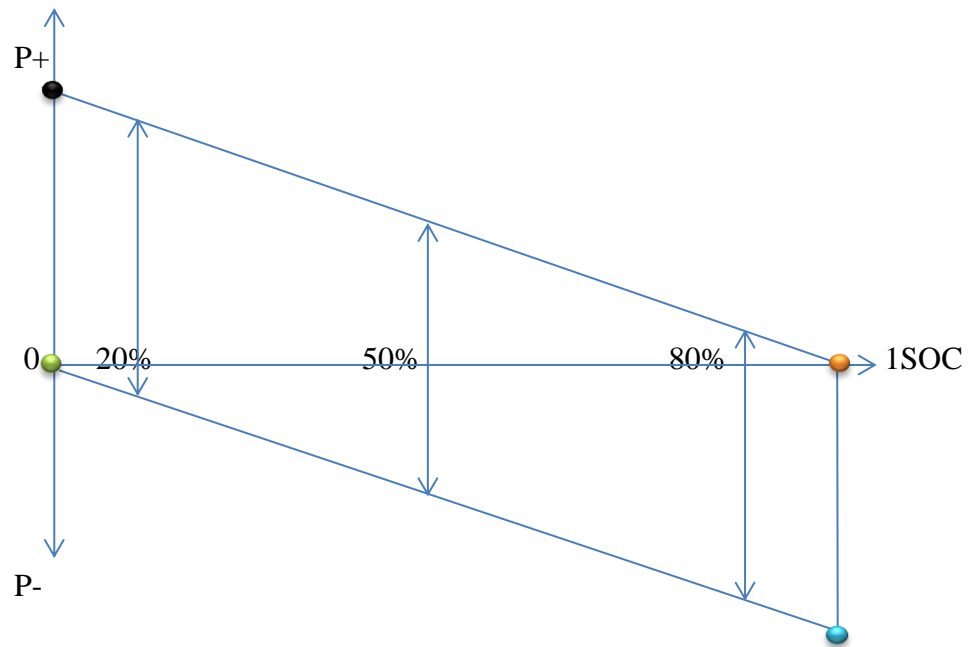


Figure 3.8. Operative regions of all the water heater units

The load power on the y-axis is the amount of power the energy storage system actually gives and takes based on its SOC. A 20% SOC means that the water heater

units can charge up to 80% of the load power and discharge 20% of the load power and will continue to do so until it either reaches fully charged or discharged state. Similarly with 80% SOC, the water heaters can charge up to 20% of the load power and discharge up to 80% of the load power. A 50% SOC implies it can sink and source 50% of the load power. The straight lines drawn between the dots are the implementation of the linear approximation concept (Figure 3.7), since the four corners of the parallelogram were definitive. All the other infinite combinations of various SOC's has to lie in between the dots, since straight lines are the easiest to implement, that was a suitable option considered in this thesis.

Thus the region within the parallelogram is the operative range of all the water heaters. As long as  $P^* = P$ , it lies within the parallelogram and for any power lying outside the parallelogram the power at the edge of the parallelogram will be given to the system due to saturation. The Simulink modeling of the saturation limits for several thousand water heaters can be seen in Figure 3.9.

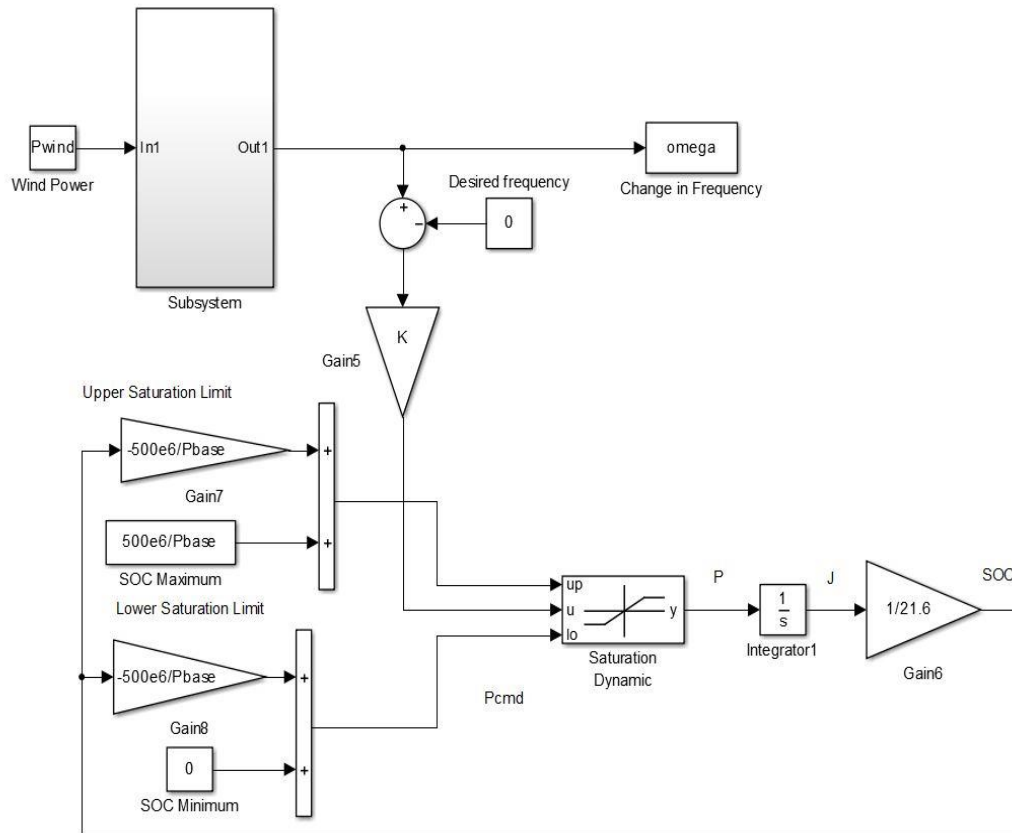


Figure 3.9. Energy storage modeling for several thousand water heaters

Figure 3.9 shows energy storage modeling 111,000 water heaters with 500 MW of load power available according of Pacific Corp Sixth power plan. This accounts for approximately 1% of estimated WECC water heater load. The number of water heaters taking part in the type of analysis that is done in this research is accounted for about 1% of water heaters in the WECC region.

The output of the conventional generation system is the change in frequency (PU) which is compared to a desired frequency. Here we consider it to be 0 as the

whole system is the deviation of frequency from its nominal value. It can be seen that the energy storage system is connected to the grid via K which is the only point of communication between the energy storage system and the conventional system. The gain value K determines the number of water heaters taking part based on the frequency deviation from nominal. Hence the output power of the energy storage system is a function of this change in frequency. Greater the value of K, implies greater the number of water heaters deployed. Once the change in frequency is set, it is given as an input to the gain factor K. The output of K is the commanded water heater power. As the commanded water heater power is a function of frequency, any change in frequency due to either wind penetration or generator loss or load loss will be detected by the energy storage unit as the frequency is the only means of communication between the energy storage system and the conventional system. The saturation block has been used to implement the concept of straight line approximation to form the parallelogram as discussed earlier. Input to the saturation block is the commanded water heater power and the output based on the SOC of the system is the actual water heater power. The actual power P is then passed through an integrator to obtain the energy (J) of the system. Once the SOC gain factor is calculated the SOC of the system can be achieved.

Some calculations have been performed to model the parallelogram with its upper and lower saturation boundaries as seen in Figure 3.8. Also the gain factor K and SOC gain factor have been calculated. The calculations have been shown below.

The slope of a line is  $y = mx + c$ . Hence, when SOC is 0, the energy storage system can accept full power, thus the upper limit will be  $\{0 * (-500 \text{ MW}/P_{base}) + (500 \text{ MW}/P_{base})\} = 500 \text{ MW}/P_{base}$ . When SOC is equal to 1, it can sink its full power, hence  $\{1 * (-500 \text{ MW}/P_{base}) + 0\} = -500 \text{ MW}/P_{base}$ . This accounts for the lower limit.

The Values of gain factor K and the scaling factor for SOC are calculated as below:

Water heater power capacity available=  $\pm 500 \text{ MW}$

Power capacity of each water heater=  $4500 \text{ W}$

Energy capacity of each water heater=  $5 \text{ kWh}$

Total number of water heaters available =  $500 \text{ MW}/4500 \text{ W} = 111,000$

Total Energy capacity of 111,000 water heaters =  $555,000 \text{ kWh}$

$P_{base} = 92 \text{ GW}$  (CAISO paper from chapter 2)

Gain  $K = \frac{\frac{500 \text{ MW}}{\Delta f/60}}{P_{base}}$ , usually  $\Delta f = 3 \text{ Hz}$  or 5% is the full output of the generator that would be used to counteract the frequency error in primary speed control. Since all units are in PU, the change in frequency has been divided by 60 Hz and the power by its base.

The SOC gain factor =  $\frac{555,000 * 10^8 \text{ } WH}{92 * 10^9 W} * \frac{3600s}{1H} = 21.6 \text{ } PU$  , which is the energy storage capacity of 111,000 water heaters each at 5kWh.

The next chapter will showcase the transient analysis of the WECC base case system with energy storage implementation.

## **4 Energy Storage for Transient Stability of Base Case - Loss of Generation**

This chapter entails the study of transient effects on the base case system (as discussed in chapter 2) in the presence of energy storage system (comprising of water heaters). The results section of this chapter will encompass the comparison of frequency responses for 3 different cases which will be discussed below. It will also showcase the power deployed by the energy storage system for two cases, hence presenting the role of energy storage system in the grid

### **4.1. Simulation Setup of Base Case System without Energy Storage**

The simulation set up for the WECC system with loss of generation (base case) without the implementation of energy storage has already been shown Figure 2.20 of chapter 2. The WECC system has been modeled in a way that it comprises of slow, medium and fast responsive generators. The frequency response of the system is shown in Figure 4.2

### **4.2. Simulation Setup of Base Case System with Energy Storage**

Figure 4.1 demonstrates the base case system in the presence of an energy storage system. This model has been used to perform transient analysis using primary control. With the addition of energy storage system into the grid, the stress on generators is reduced to a large extent in the advent of loss of generation or loss of load thereby, providing a better frequency response to stabilize the system.



### 4.3 Simulation Results

Figure 4.2 illustrates the frequency response of the base case system without the energy storage system. The starting frequency remains constant at 0 (60 Hz) until it reaches 1 second, where a generator trips and goes offline and the frequency starts to

droop until it reaches -0.3341 Hz (inertial control), which is the change in frequency from its nominal value (0 Hz), hence the actual frequency drop is about 59.6659 Hz at approximately 9.7 seconds.

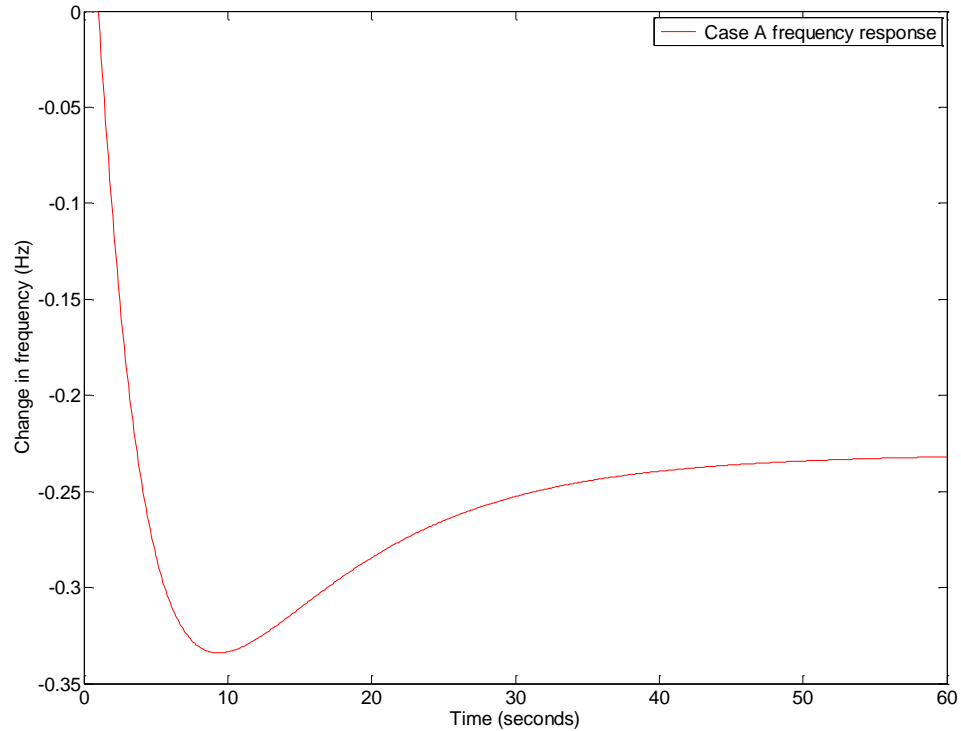


Figure 4.2. Frequency response of Case A with a frequency nadir of 59.6659 Hz and settling frequency of 59.768 Hz

The point where the frequency starts to rise is when primary frequency control kicks in. The frequency then starts to increase and settles at a point where stabilization of the system is achieved 59.768 Hz.

### 4.3.2 Case B: Response of All Water Heaters per 3 Hz

The plot in Figure 4.3 shows the frequency response of the base case in the presence of energy storage. In this case  $\Delta f$  from the gain factor K has been assigned 3 Hz as it is the standard primary response control, which means that a deviation in 3 Hz is a full response to the load. The frequency nadir was found to be 59.6723 Hz which is about -0.3277 Hz deviation from 0 Hz at about 9.7 seconds and the settling frequency is about 59.7712 Hz. An improvement in frequency profile can be observed when compared to Case A, This is attributed towards the addition of the energy storage system in the WECC base model.

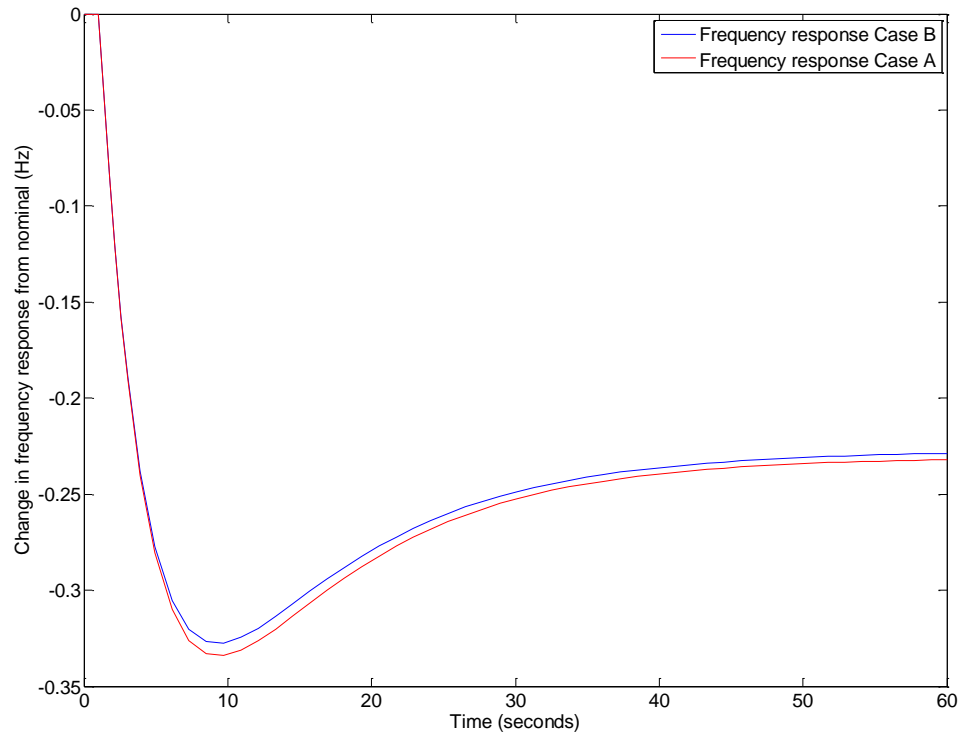


Figure 4.3. Frequency responses for Case A and Case B

The upper plot in Figure 4.4 shows the power supplied by the water heaters per 3 Hz change in frequency and the lower plot shows the deviation of frequency from its nominal value. The maximum change in power supplied by the energy storage unit is about  $-5.9364 \times 10^{-4}$  PU. This shows that not many waters have been deployed, but the frequency profile has improved due to the deployment of a few water heaters.

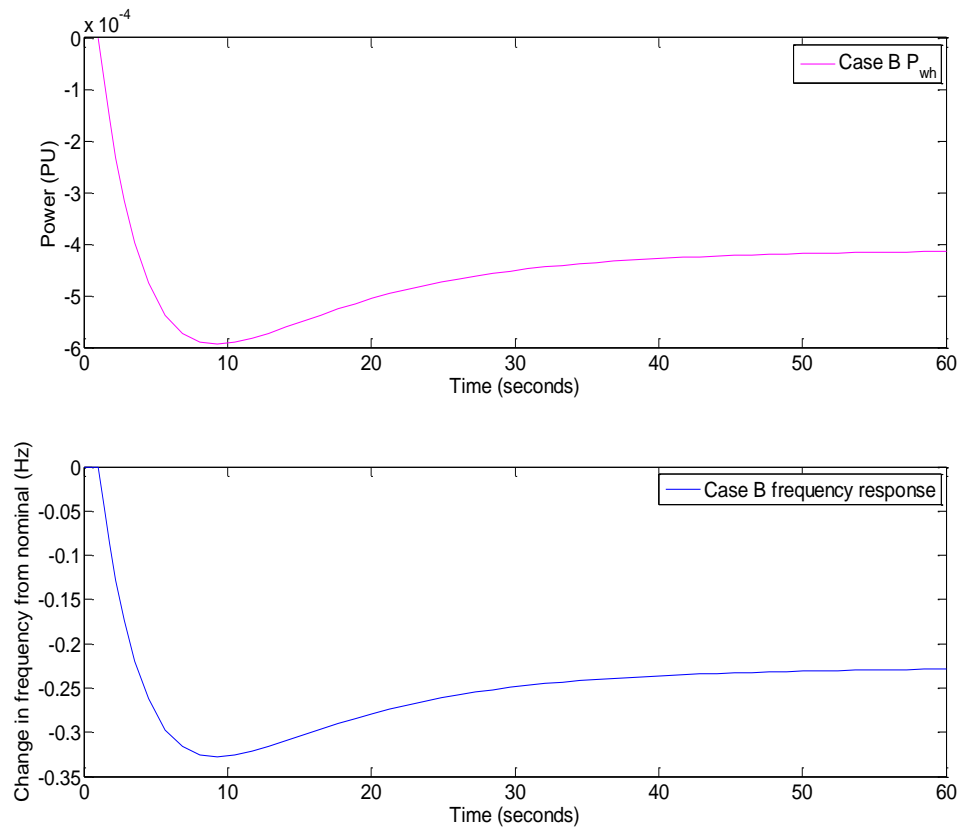


Figure 4.4. Power response of the water heaters for Case B and its corresponding frequency response

Figure 4.5 shows the commanded water heater power indicated by the blue star line ( $P_{wh}^*$ ), the actual water heater power in pink ( $P_{wh}$ ), the saturation boundaries with upper saturation limit in red and lower saturation limit in cyan, frequency of the

system in the middle plot in black and the SOC in the lower plot in green. From chapter 3,  $P_{wh}^*$  is a function of frequency, as the frequency is negative, so is  $P_{wh}^*$ , which implies that generation is lower than load and the water heaters have to discharge their energy by effectively reducing the load and temperature to enhance generation, hence the SOC can be seen declining from its initial SOC which is at 0.5 to its minimum SOC at 0.4987. As long as the commanded water heater power is equal to the actual water heater power, they lie within the saturation boundaries, which is the region of operation of all the water heater units.

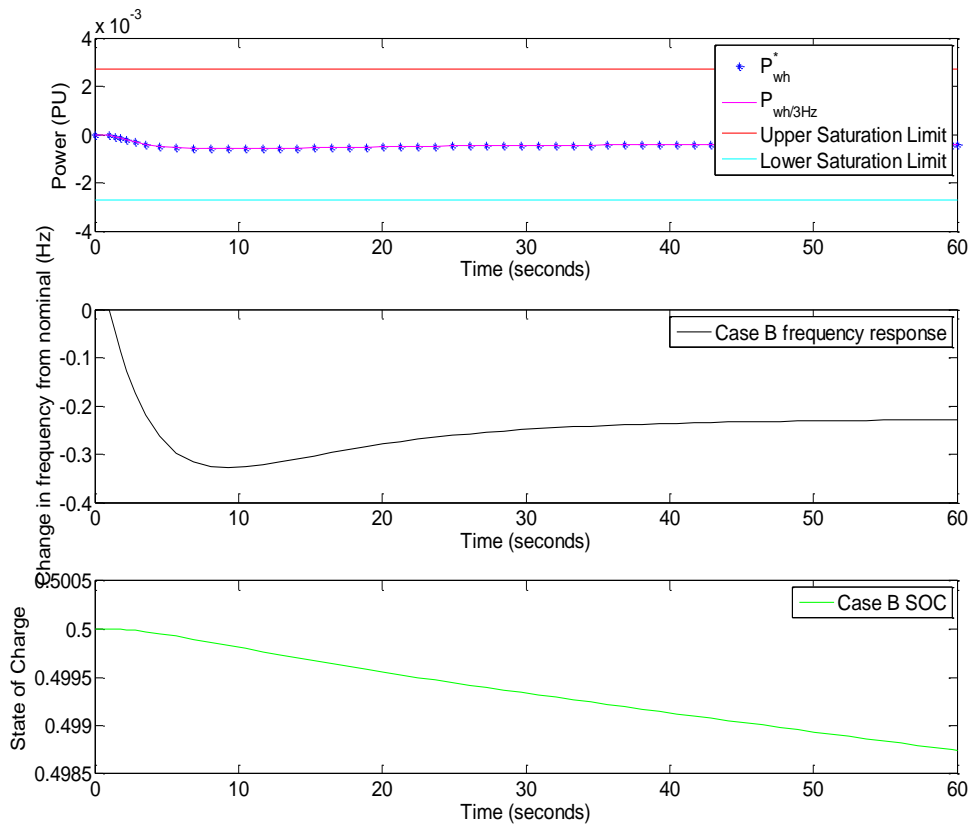


Figure 4.5 Region of operation and SOC of all the water heaters for Case B

The maximum and minimum saturation boundaries have a magnitude in the order of  $+e^{-3}$  PU and  $-e^{-3}$  PU respectively. From Figure 4.4, the actual water heater power has a magnitude of order  $e^{-4}$ , which concludes that only 10% of water heaters have been deployed. This poor response is due to the little and the involvement of energy storage, hence to increase the role of energy storage, the gain factor K has to be made larger and this is achieved by making  $\Delta f$  smaller and more aggressive, hence case C has been performed with  $\Delta f = 0.23$  Hz since 0.23 Hz is the maximum deviation of frequency from its nominal value due to the generator trip event.

### **4.3.3 Case C: Response of All Water Heaters per 0.23 Hz**

The plot in Figure 4.6 shows the frequency response of the base case in the presence of energy storage. The simulation setup and methodology is exactly the same except for the change in  $\Delta f$  value which is 0.23 Hz in this case. The frequency nadir is at 59.6972 Hz with a frequency deviation of -0.3028 Hz from nominal. The settling frequency is about 59.78 Hz.

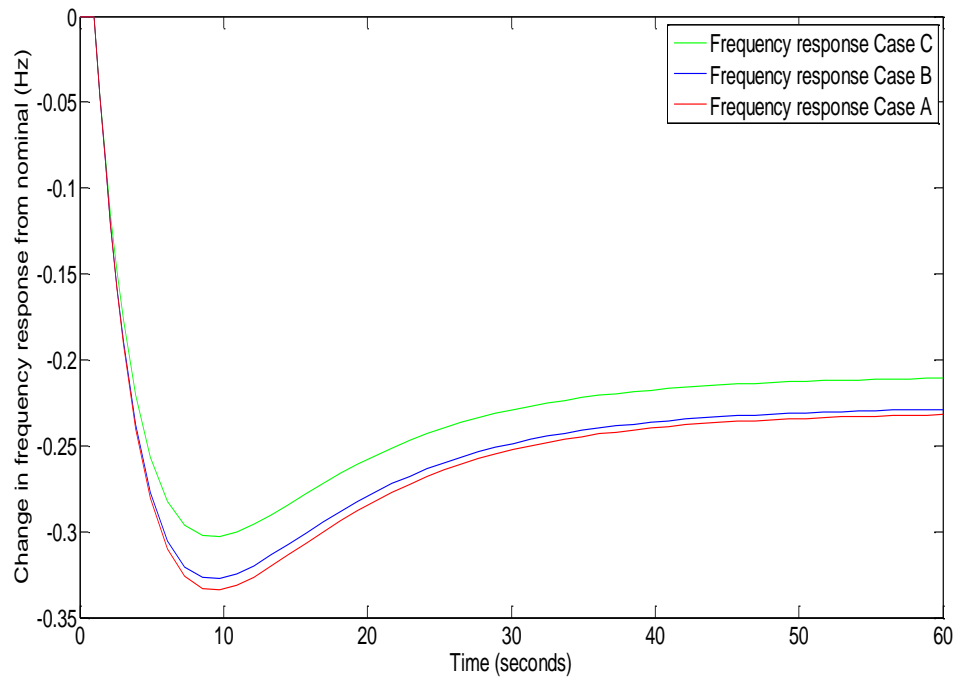


Figure 4.6 Frequency response for Case A, B and C

The upper plot in Figure 4.7 represents the power supplied by the water heaters per 0.23 Hz change in frequency and the lower plot shows the frequency response of the system. The maximum change in power supplied by the energy storage unit is about  $2.7\text{e-}3$  PU which is approximately 250 MW (taking 0.5 as SOC).

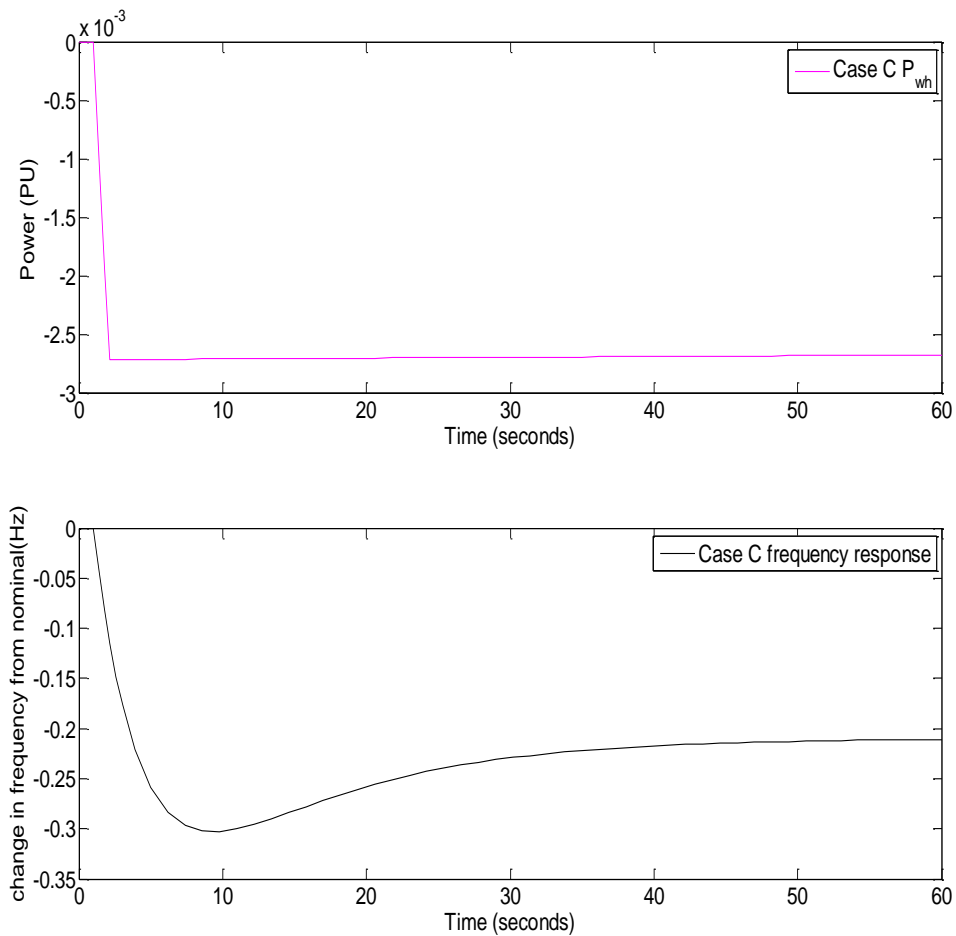


Figure 4.7. Power response of the water heaters for Case C and its corresponding frequency response

This shows that all the waters have been deployed and are saturated as it is the lower saturation limit of the operative region, and the frequency profile has improved due to the deployment of all the water heaters.

Figure 4.8 shows the commanded water heater power indicated by the blue star line ( $P_{wh}^*$ ), the actual water heater power in pink ( $P_{wh}$ ), the saturation boundaries with upper saturation limit in red and lower saturation limit in cyan, frequency of the



system in the middle plot in black and the SOC in the lower plot in green. From chapter 3,  $P_{wh}^*$  is a function of frequency and as the frequency is negative, so is  $P_{wh}^*$ , which implies that generation is lower than load and the water heaters have to discharge their energy to supply power into the grid to enhance generation, hence the SOC can be seen declining from its initial SOC which is at 0.5 to its minimum SOC at 0.4927.

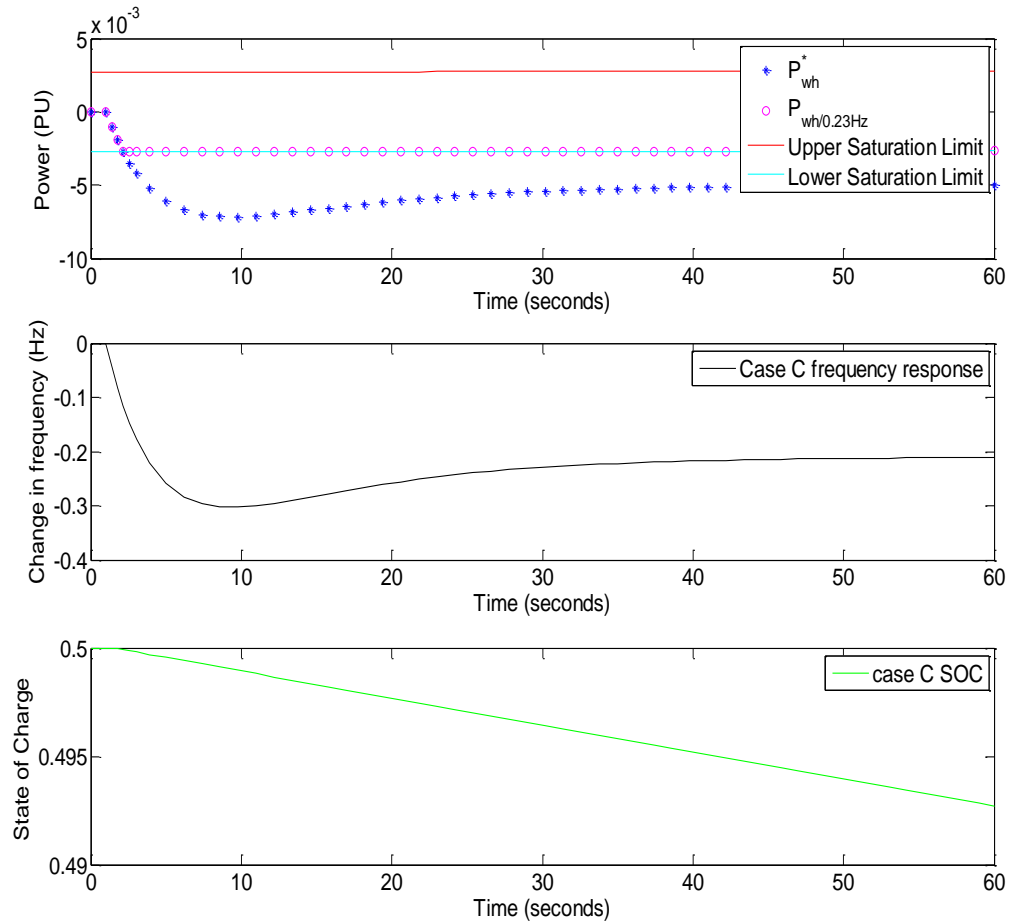


Figure 4.8. Region of operation and SOC of all the water heaters for Case

As long as the commanded water heater power is equal to the actual water heater power as seen in the first few seconds in the upper plot of the above figure, they lie within the saturation boundaries, which is the region of operation of all the water heater units. But it can be seen that the plot indicated by blue start lies outside the operative region, signifying that if  $P_{wh}^*$  is a value greater than the lower saturation limit which has been modeled in Simulink considering the overcharge and undercharge protection schemes, it will supply the power present only at the edge of the operative region, hence extreme saturation of the actual water heater power is observed in figure 4.7 (pink plot).

#### 4.4 Result Conclusion

The summary of the frequency responses for all the three cases are tabulated in 4.1.

Table 4.1 Summary of frequency responses for Case A, B and C

	Minimum change in frequency (Hz)	Frequency Nadir (Hz)	Settling Frequency (Hz)
<b>Case A</b>	-0.3341	59.6659	59.768
<b>Case B</b>	-0.3277	59.6723	59.7712
<b>Case C</b>	-0.3028	59.6972	59.78

Figure 4.8 showcases the frequency response of all the three cases. It can be concluded that by making the gain factor K more aggressive, the frequency response showed

considerable improvement both in the frequency nadir as well as the settling frequency.

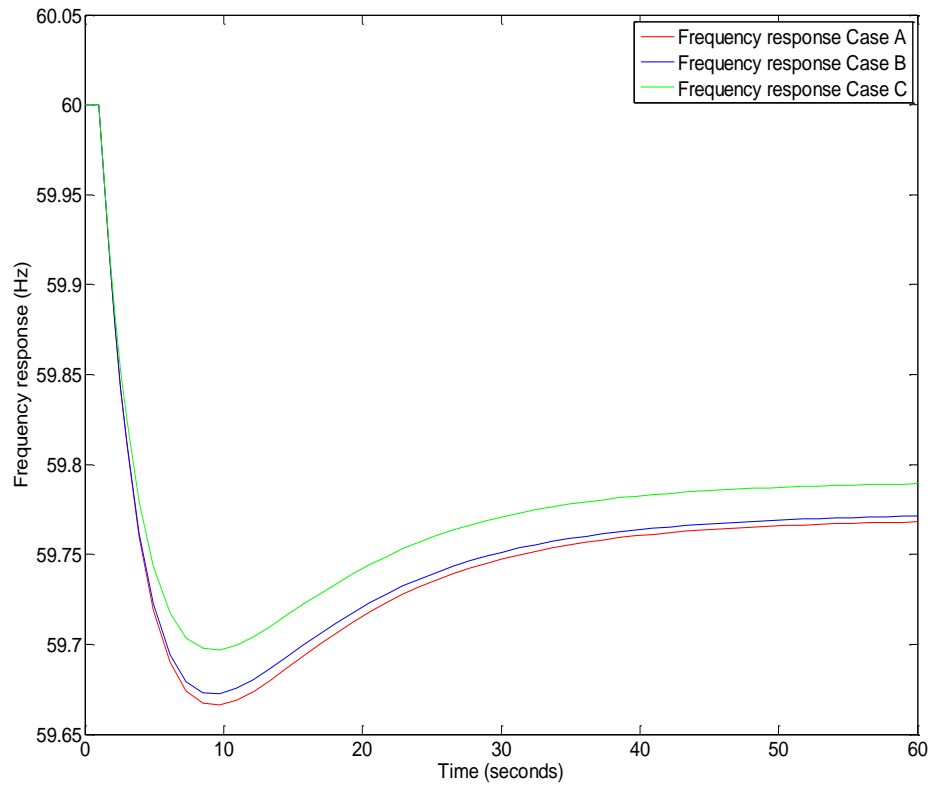


Figure 4.9. Frequency responses for Case I, II and III

Table 4.2 shows the summary of the actual water heater power responses for case II and III

Table 4.2 Summary of percentage of water heater deployed to improve the frequency profile

	Water heater power (PU)	% Water heaters deployed
<b>Case B</b>	-5.9365e-4	10%
<b>Case C</b>	-2.717e-3	100%

Figure 4.10 showcases the actual water heater power for cases B and C . It gives an estimate of the percentage of water heaters deployed in the system. A conclusion can be deduced that  $P_{wh/3\text{ Hz}}$  has only 10% deployment of water heaters whereas  $P_{wh/0.23\text{ Hz}}$  has a full deployment of water heaters. The increase in the actual water heater power responding per 0.23 Hz is due to aggressive nature of K.

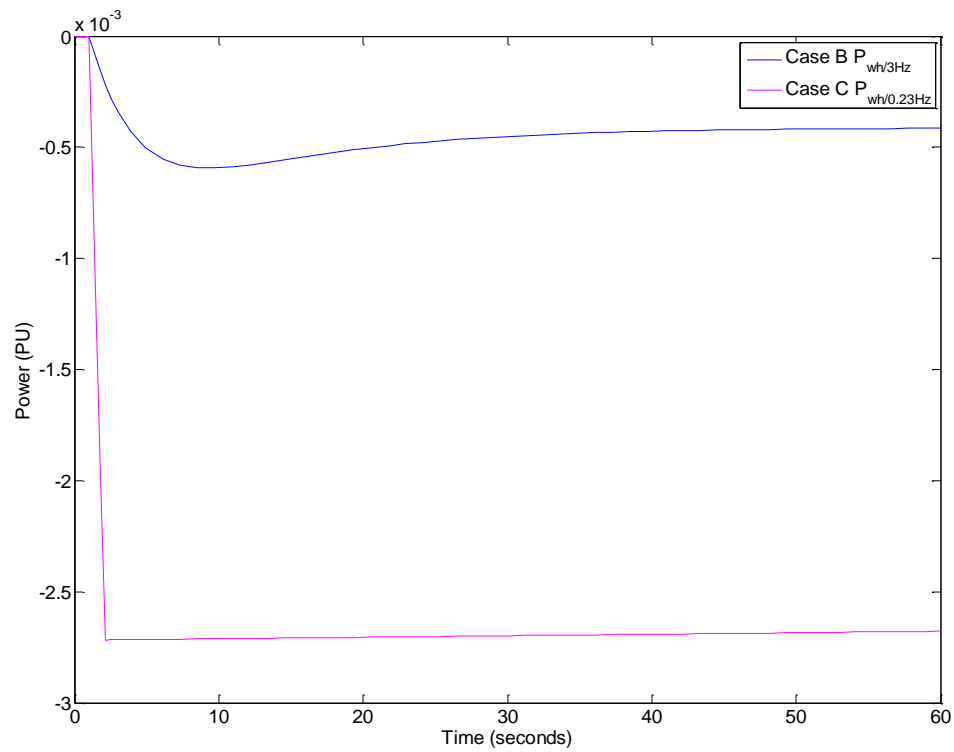


Figure 4.10. Actual water heater power for cases B and C

The next chapter will have similar analysis as chapter 4, but with wind penetration into the WECC system. Due to the sporadic nature of wind power, the frequency is never constant and is constantly changing. This change in frequency is essential for the analysis performed in Chapter 5 as the energy storage system is linked to the grid in a way that the only means of communication needed is the change in frequency from its nominal value which has already been discussed above.

## 5 Energy Storage for Wind Integration

Most wind turbines built today are known as asynchronous machines, meaning that they are decoupled from the grid, i.e. they put out maximum power all the time based on the wind speed and are not concerned to the change in frequency of the grid, hence no direct connection to the inertia of the grid at all. This is due to the presence of power electronics in between the rotating blades and the grid. Therefore, wind turbines neither take part in inertial nor primary control, implying that they do not have droop characteristics like conventional generators.

Wind power brings significant value to the energy mix today, providing clean and green energy. However, the combination of wind energy with energy storage accounts for increased substantial benefits, by helping to maximize the use of wind power available. Wind does not always blow when demand is high, thus addition of an energy storage system can be useful when demand suddenly increases by coming online to make up the difference in a very precise way. On the other hand if wind speed is high and energy demand is low, the energy storage system can store the excess energy for later, harnessing full potential of wind power [34].

The energy storage system (water heaters) itself behaves as a huge rotating mass, hence contributing towards inertial and primary frequency control. In this thesis, the energy storage system has been modeled in a way that the only means of communication needed to supply power to the grid or absorb power from the grid is the deviation in frequency from the nominal (60 Hz) which is due to the variability of wind power output. Therefore, there is no need of additional communication required

at all. Therefore, five cases have been discussed below to show the effect of energy storage system due to wind penetration. Also secondary frequency control has been implemented to compare the results for case G and case H. The significance of adding secondary control will be discussed in case H.

### 5.1 Case D: Wind Penetration to the WECC System without Energy Storage

Table 5.1 shows the wind data from Bonneville Power Administration (BPA), January 23<sup>rd</sup>, 2010 for a one hour window.

Table 5.1 BPA Wind data

<b>Date/Time</b>	<b>Total wind generation in BPA control area (MW)</b>	<b>Average wind generation in BPA control area (PU)</b>
01/23/2010 , 18:30	894	-2.2e-3
01/23/2010 , 18:35	931	-1.8e-3
01/23/2010 , 18:40	985	-1.2e-3
01/23/2010 , 18:45	1059	-0.4e-3
01/23/2010 , 18:50	1131	0.4e-3
01/23/2010 , 18:55	1203	1.2e-3
01/23/2010 , 19:00	1249	1.7e-3
01/23/2010 , 19:05	1265	1.9e-3
01/23/2010 , 19:10	1252	1.7e-3

01/23/2010 , 19:15	1183	1e-3
01/23/2010 , 19:20	1041	-0.6e-3
01/23/2010 , 19:25	1033	-0.7e-3
01/23/2010 , 19:30	996	-1.1e-3

Figure 5 shows the simulation set up with wind penetration in the WECC system.

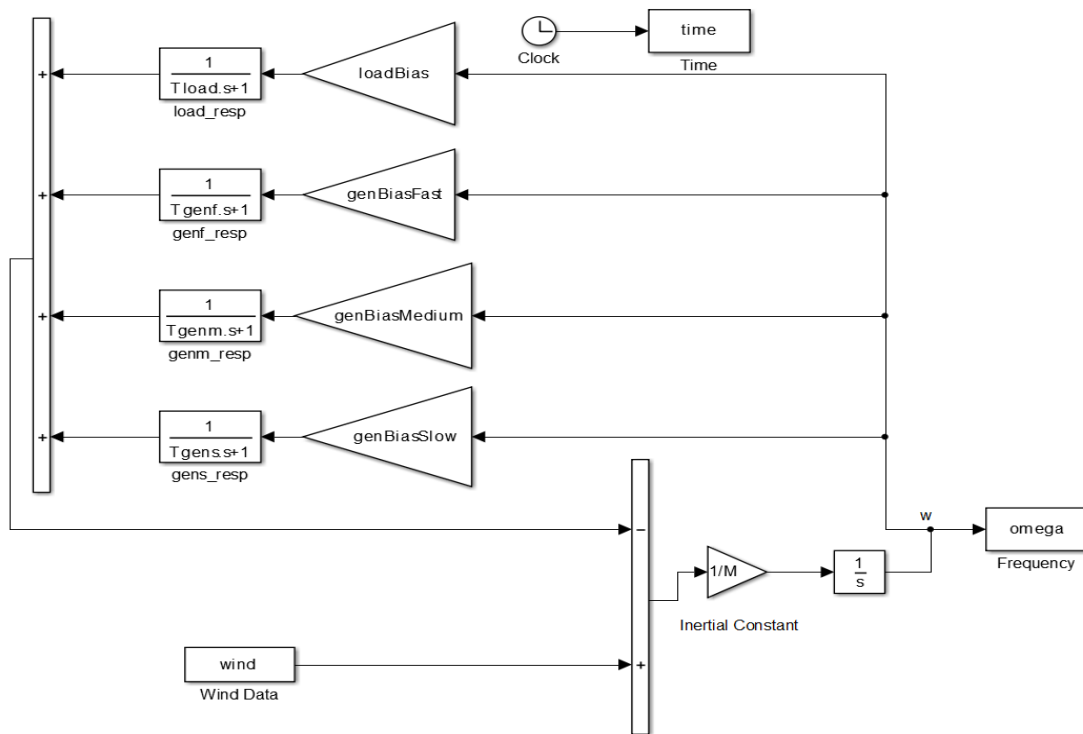


Figure 5 WECC system with wind penetration

Figure 5.1 shows the wind power and frequency response of the above system. Due to the constant change in wind power, the frequency of the system is also constantly changing. The maximum average wind power has been calculated to be approximately  $1.9\text{e-}3$  PU and the minimum average wind power is around  $-0.0022\text{e-}3$  PU (yellow



plot). The maximum and minimum frequency deviation (black plot) from 0 is 0.0146 Hz and -0.0248 Hz respectively.

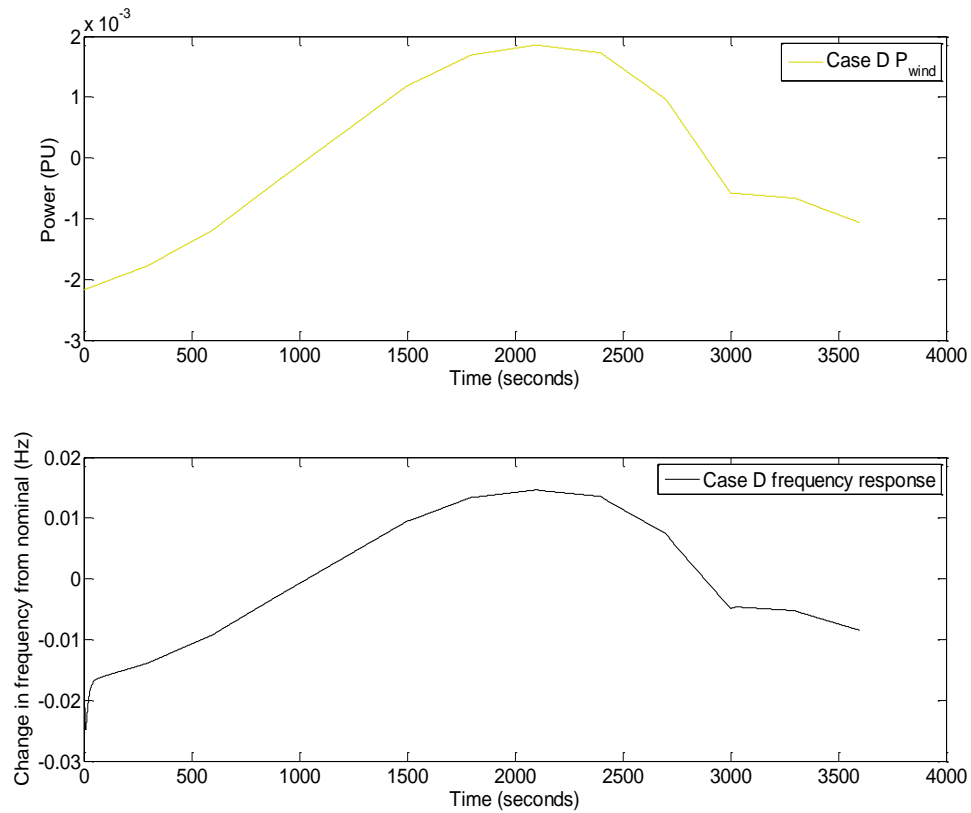


Figure 5.1 Wind power (obtained from BPA) and the frequency response of the system

When converted to actual Hz the maximum frequency is  $60 + 0.0146 = 60.0146$  Hz and the minimum frequency is  $60 - 0.0248 = 59.9752$  Hz.

## 5.2 Case E: Wind Penetration to the WECC System with Energy Storage, and Water Heaters Responding per 3Hz

This sub section focuses on the control of residential water heaters in order to provide a balancing resource for wind generation. Transient analysis were performed to see the frequency profile in the presence of the controlled load (water heaters). In order to facilitate this, as discussed in the beginning of chapter 5, the energy storage system is connected to the grid in such a way that it constantly responds to the change in frequency due to variable wind power in the system. The major factor while modelling the energy storage system which responds to the change in frequency is the gain

factor, given by,  $K = \frac{\frac{500 MW}{\Delta f / 60}}{P_{base}}$ , usually  $\Delta f = 3 Hz$  or 5% is the full output of the generator that would be used to counteract the frequency error in primary speed control. Since all units are in PU, the change in frequency has been divided by 60 Hz and the power by its base. Figure 5.2 will show the simulation set up of the WECC system with wind penetration and energy storage system.

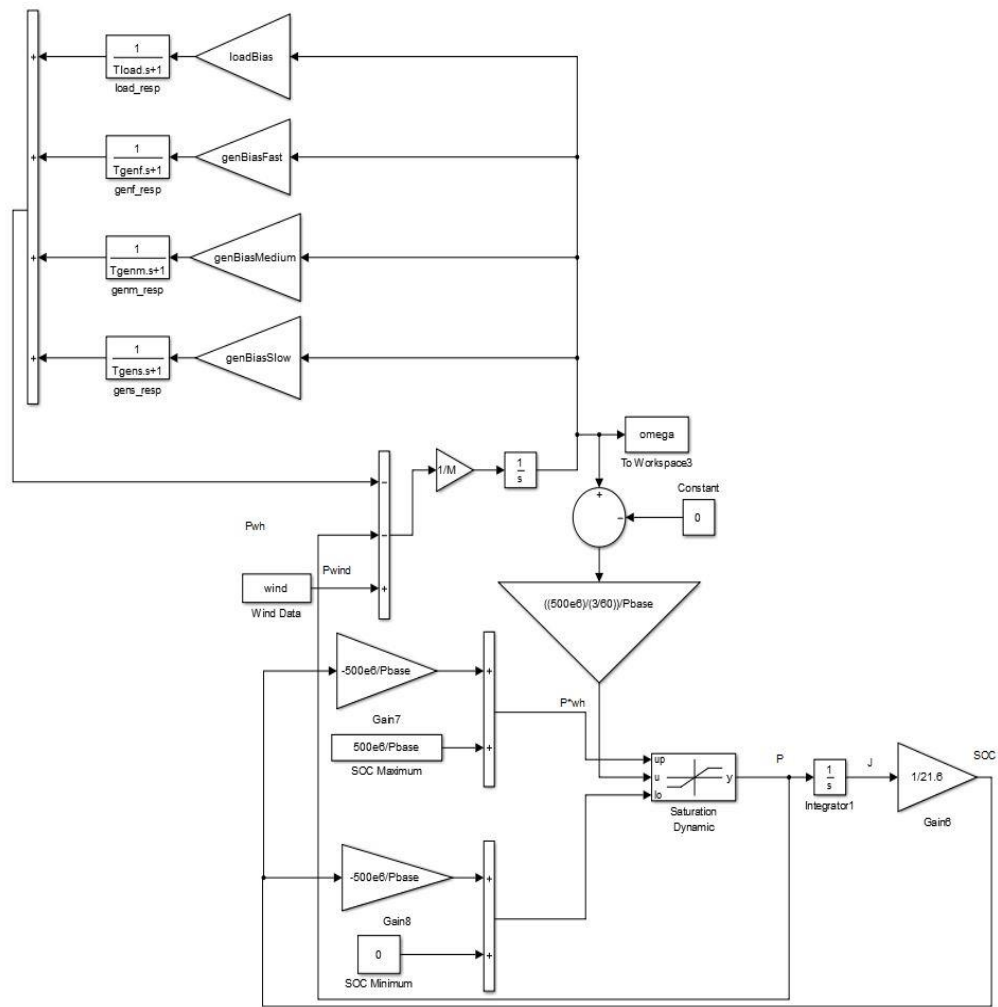


Figure 5.2 WECC system with wind penetration and energy storage system for Case E

Figure 5.3 demonstrates the positive and negative saturation limits, representing the operative region of the water heater power, the actual water heater power supplied/absorbed by the water heaters (P) and the commanded water heater power ( $P^*$ ).

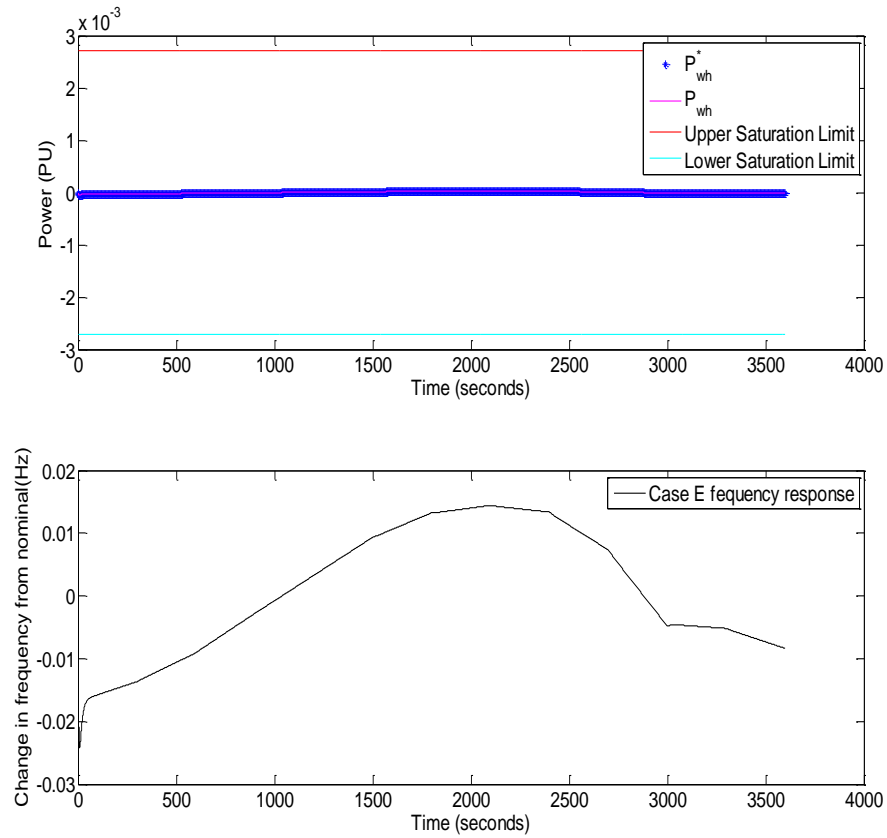


Figure 5.3 Region of operation of the water heaters and the frequency response for Case E

The first plot describes the operative region of all the water heaters. The red and cyan lines are the upper and lower saturation limits of the operative region which are around  $+2.717 \times 10^{-3}$  PU ( $+500 \text{ MW}/0.5 = +2.5 \text{ MW}$ ) and  $-2.717 \times 10^{-3}$  PU ( $-500 \text{ MW}/0.5 = -2.5 \text{ MW}$ ) respectively as the initial condition for the state of charge has been set to 0.5 to perform the simulation. The pink line within the operative region is the water heater power ( $P$ ) and the blue line is the power the grid wants the water heaters to supply ( $P^*$ ). As long as  $P = P^*$ , it lies within the operative region, thus adhering to the undercharge and overcharge protection discussed previously. The

black plot in the above figure shows the frequency deviation from nominal. A magnified portion of P and  $P^*$  will show that they are equal (same applies to the other cases). See Figure 5.4 below.

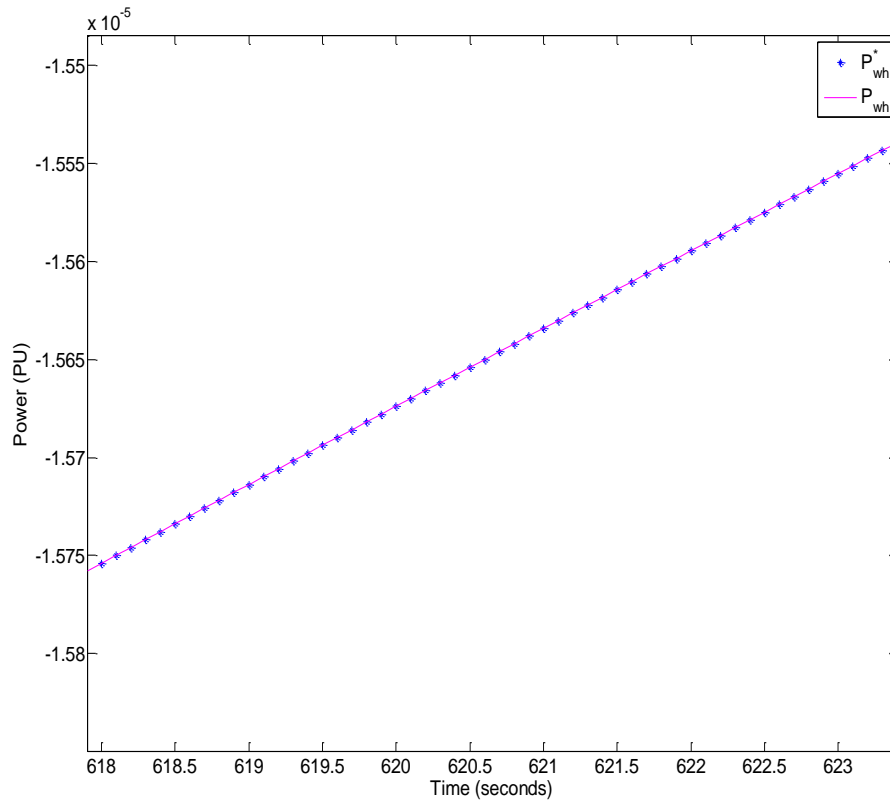


Figure 5.4 Magnified plot of commanded power and actual water heater power for Case E

For the purpose of clarity, another plot with P,  $P^*$  and frequency response have been shown in Figure 5.5. It shows that when frequency is negative,  $P^*$  is negative (since it is a function of frequency change) which implies that the grid is in need of generation to balance out the excessive load, hence the water heaters discharge to supply the deficit power into the grid, i.e., the energy storage system can effectively return power

to the grid by reducing load and temperature, which can be seen with the decrease in SOC in the green plot at the very bottom (0 s to ~1000 s).

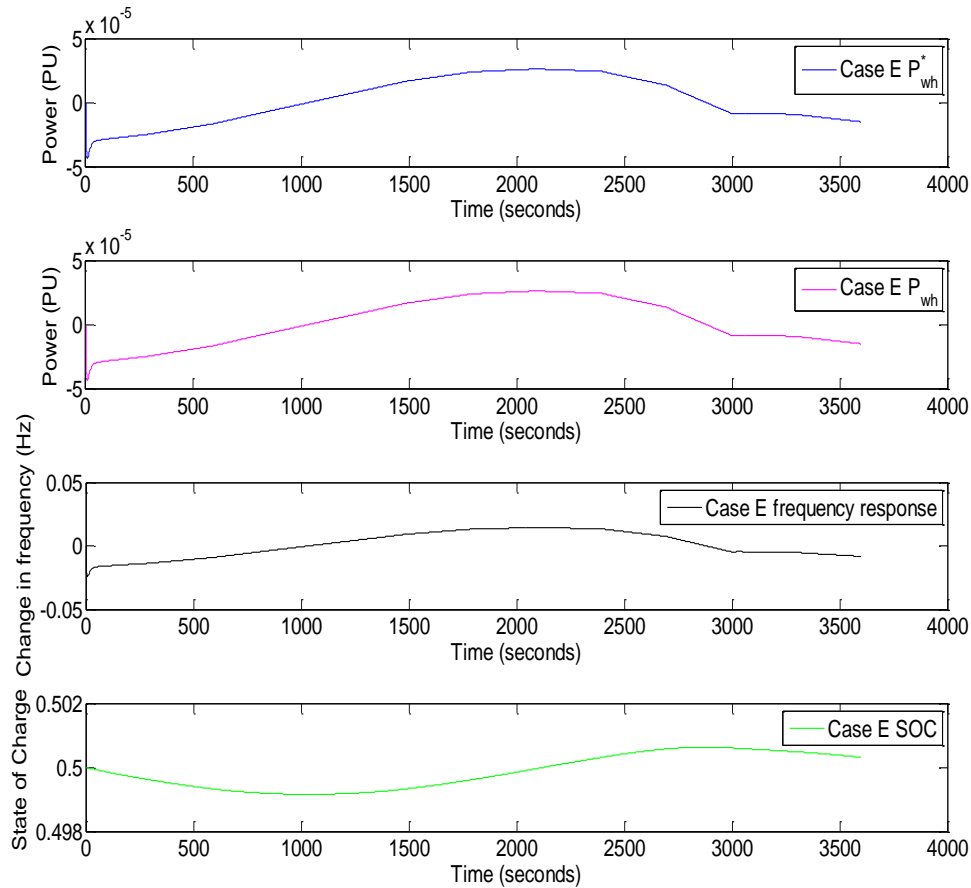


Figure 5.5 Commanded water heater power response, actual water heater power response, frequency and SOC for case E

As the frequency increases or reaches close to 0 Hz and finally becomes positive, the water heaters increase their SOC by charging (~1000 s to ~2800 s) due to excess generation in the system which can be stored and can be used later when demand response is high. From the straight line approximation that has already been discussed

in chapter 3, from Figure 3.8 (operative region of water heater power), it was clear that as the SOC of the energy storage system decreases, the upper boundary of the saturation limit increases and the lower boundary of the saturation limit decreases (forming a parallelogram). This phenomenon can be proved in Figure 5.6 by magnifying the plot.

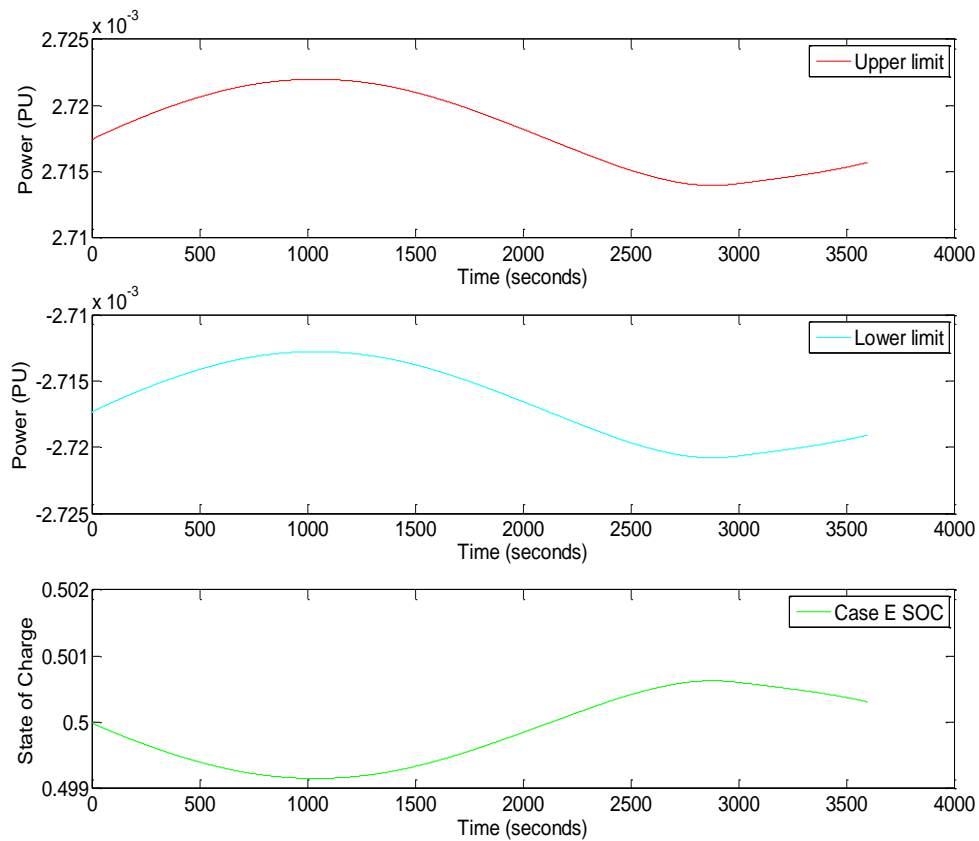


Figure 5.6 Magnified plot of upper saturation limit and SOC for case E

From the above figure it can be deduced and proved that as the SOC was decreasing, the upper and lower saturation limits of the operative region were increasing, just as approximated in chapter 3.

All the above discussions explain the working of the WECC system in the presence of energy storage and the relationship between  $P$ ,  $P^*$ , SOC and change in frequency. This change in frequency is due to constant change in wind power; hence the next few plots will focus on the control of the energy storage system to provide balancing resource for wind generation and improve the frequency profile for WECC. Figure 5.7 shows the wind power (top), the amount of water heater power per 3 Hz (middle) and the SOC of the energy storage system (bottom).

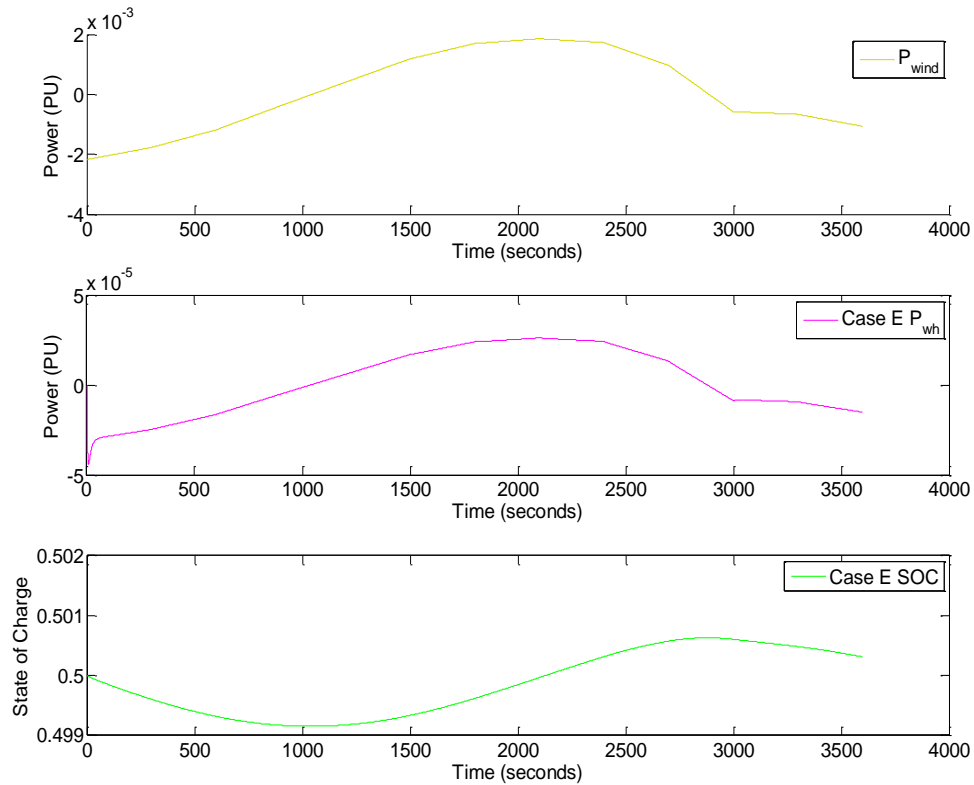


Figure 5.7 Deployment of water heaters for every 1MW of wind power and the SOC of the energy storage system for Case E



The maximum wind power from the above plot is about  $1.9\text{e-}3$  PU and the maximum water heater power is about  $2.6\text{e-}5$  PU. This shows that for every 1 MW change in wind, the number of water heaters deployed are two orders less in magnitude, thus giving two orders less of water heater power. Statistically, for every 1 MW in change of wind only 10 KW of water heater power is generated which is only 1% deployment of water heaters, which is extremely low. The maximum and minimum SOC for the system are 0.5006 and 0.4992 respectively. This shows that there is no opportunity to use the energy storage system much more aggressively. Hence to increase the role of the water heaters, and make them contribute more towards water heater power, the only factor that can be changed is K, which has been discussed in sub section 5.1. Thus introducing the next subsection in which the factor K has been made more aggressive to increase the role of water heaters.

### **5.3 Case F: Wind Penetration to the WECC System with Energy Storage, and Water Heaters Responding per 0.23Hz**

The reason for choosing 0.23 Hz to perform the simulation is because of the loss of generation case (without wind penetration), where the frequency nadir reaches 59.67 Hz, which is 0.23 Hz from the nominal. In that case, ‘all the water heaters’ were deployed with  $\Delta f = 0.23 \text{ Hz}$ . With the addition of wind in the system, the results will be as discussed below. The simulation set up is similar to Figure 5.2. The only change

would be to make  $\Delta f = 0.23 \text{ Hz}$  in  $= \frac{\frac{500 \text{ MW}}{\Delta f / 60}}{\text{Pbase}}$ .

Consider Figure 5.8, it illustrates the operative region of the actual water heater power and the commanded water heater power and its contribution to the change in frequency.

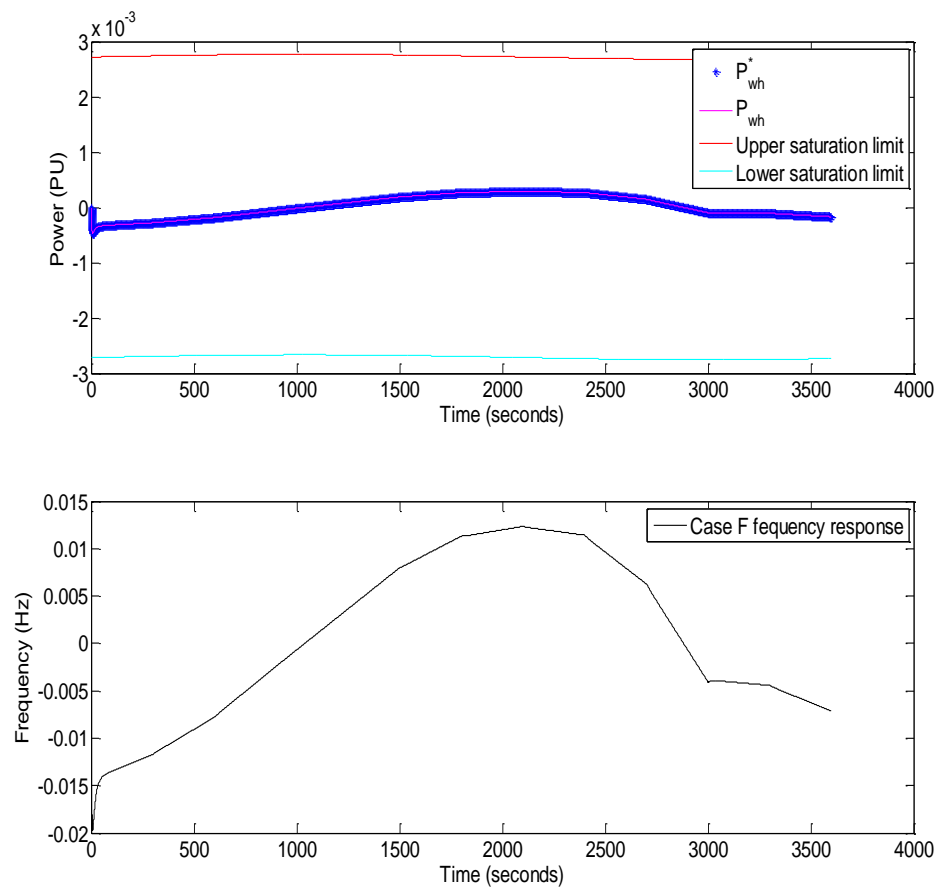


Figure 5.8 Region of operation of the water heaters and the frequency response for Case F

The red and cyan lines are the upper and lower saturation limits of the operative region. The pink and blue lines are  $P$  and  $P^*$  respectively. For better transparency, Figure 5.9 will showcase  $P$ ,  $P^*$ ,  $SOC$  and the frequency deviation from nominal.

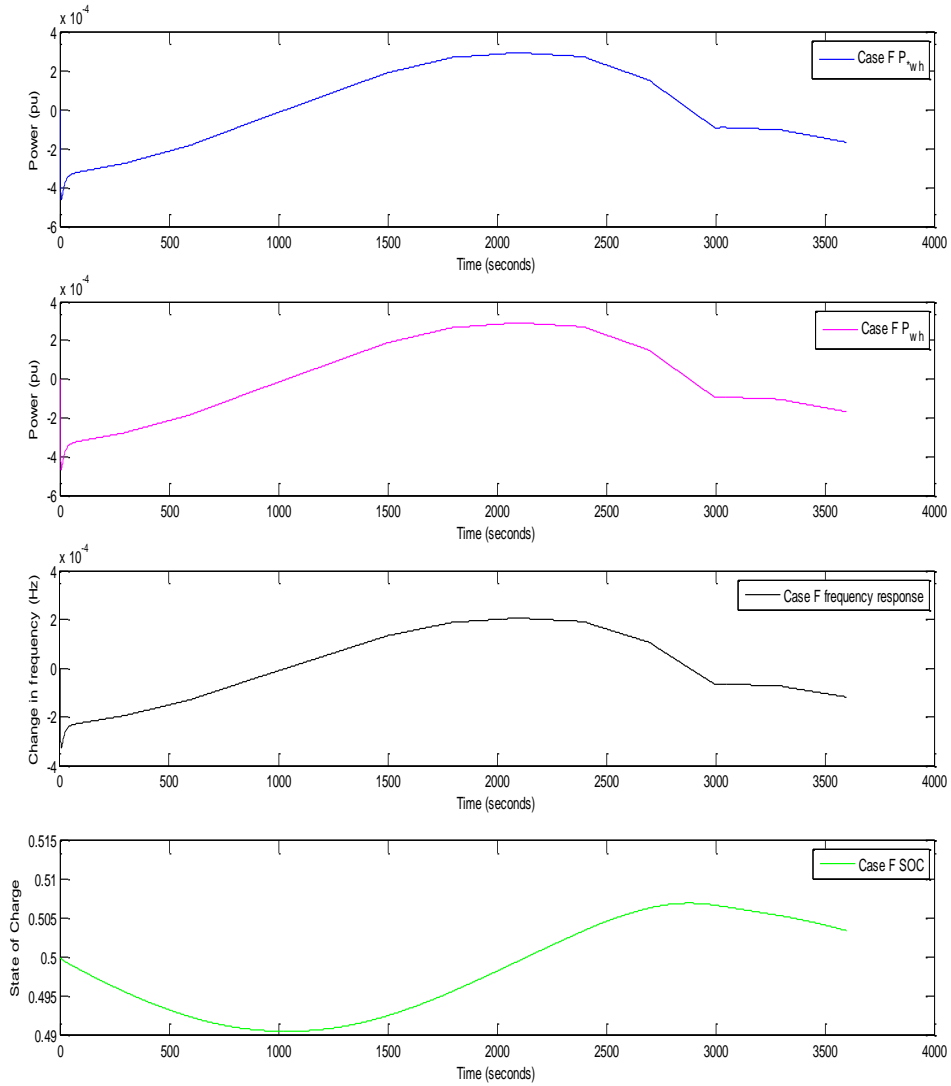


Figure 5.9 Commanded water heater power response, actual water heater power response, frequency and SOC for Case F

The theoretical explanation for the above plots is similar to Figure 5.5. The only difference seen in the above plot is in the order of magnitude of the water heater power response and SOC. Figure 5.10 shows the wind power (top), the amount of water heater power per 0.23 Hz (middle) and the SOC of the energy storage system (bottom).

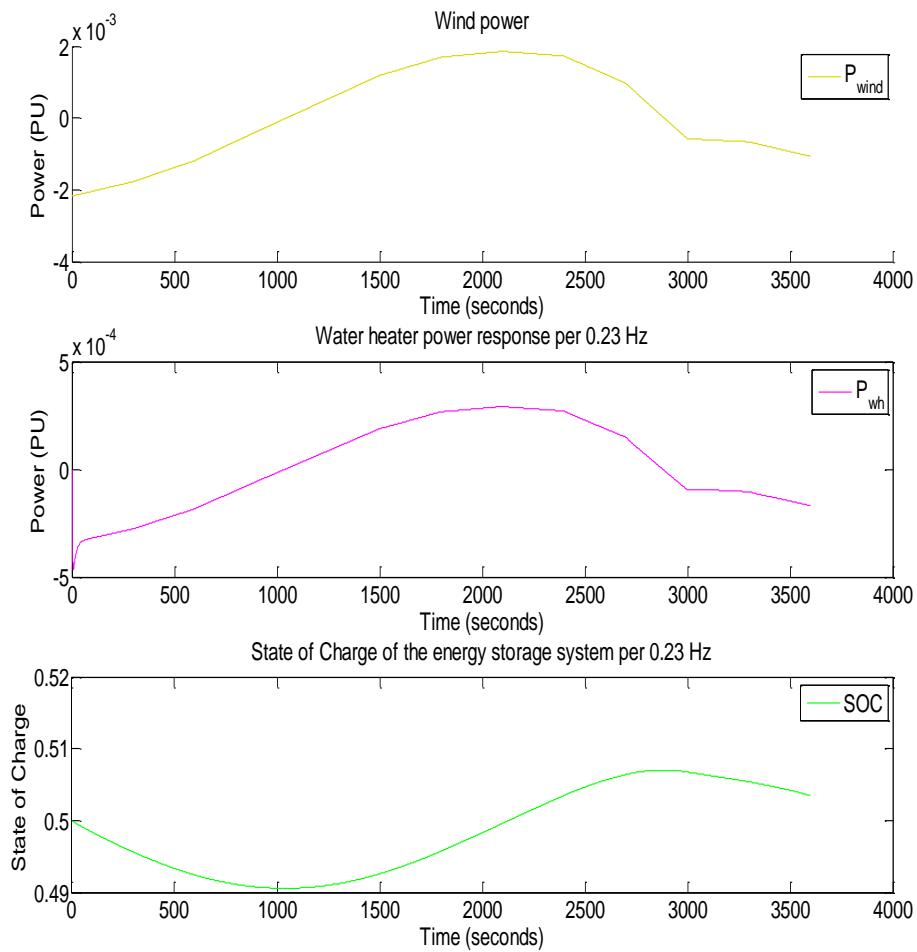


Figure 5.10 Deployment of water heaters for every 1MW of wind power and the SOC of the energy storage system for Case F

From Figure 5.10,

$$P_{wind(max)} = 1.9 * 10^{-3} pu, \quad P_{water\ heater(max)} = 2.92 * 10^{-4} pu, \quad SOC_{(max)} =$$

0.507. From the above numbers, it indicates that the maximum wind power is about 1.9e-3 PU and the maximum water heater power is about 2.92e-4 PU. This shows that for every 1 MW change in wind, the number of water heaters deployed is one order less in magnitude, thus giving one orders less of water heater power. Statistically, for every 1 MW change of wind only 100 KW of power is generated which is about 10% deployment of water heaters, which is higher than the 3Hz case, but is still considered low. The maximum and minimum SOC for the system are 0.505 and 0.4906 respectively. This shows that there is no opportunity to use the energy storage system much more aggressively. Hence to further increase the deployment of water heaters, K has to be made even more aggressive than 0.23 Hz. Hence the next case will showcase the role with water heater per 0.02 Hz.

#### **5.4 Case G: Wind Penetration to the WECC System with Energy Storage, and Water Heaters Responding per 0.02Hz**

Figure 5.11 will showcase the operative region of the commanded water heater power and the actual water heater power.

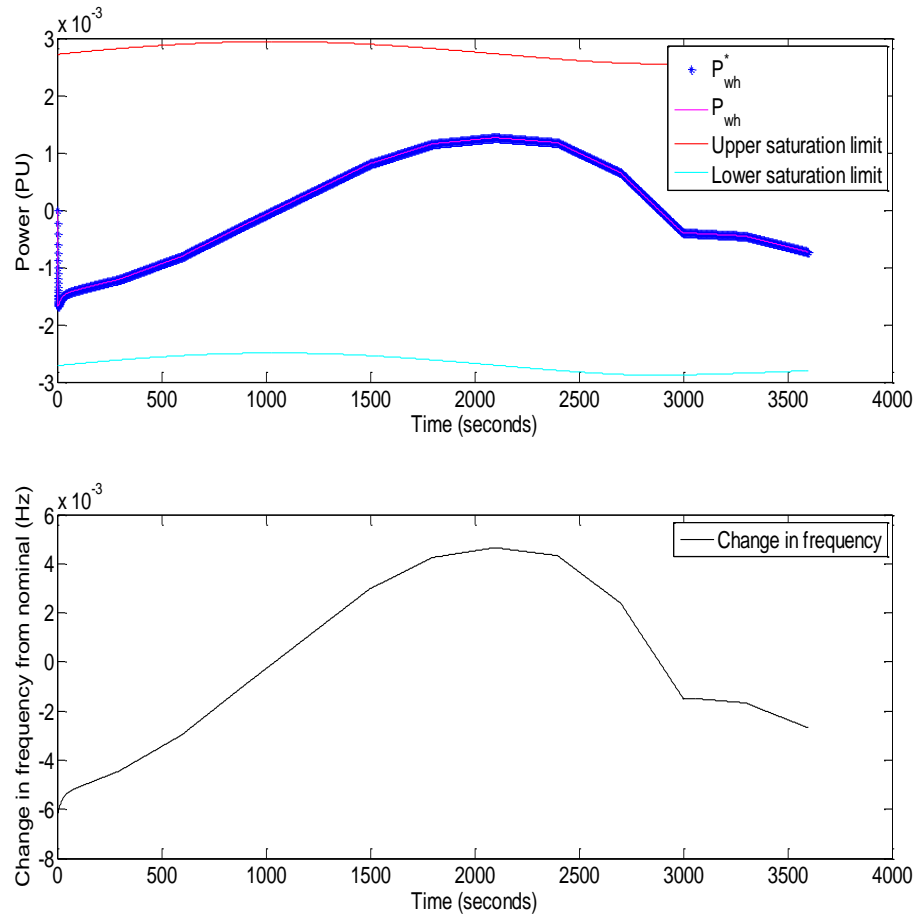


Figure 5.11 Region of operation of the water heaters and the frequency response for Case G

The above plots show that the water heater power is well within the operative region, the red and cyan lines are the saturation limits of the operative region and the blue plot is the commanded water heater power.

Figure 5.12 will demonstrate the deployment of water heater when  $\Delta f = 0.02 \text{ Hz}$  and the SOC of the system is shown in green. It can be seen from the plot

below that the order of wind power and water heater power have the same magnitude, implying that for every 1 MW change in wind power, there is 1 MW deployment of water heater power, thus concluding that all the water heaters are deployed. The maximum and minimum SOC are 0.53 and 0.459.

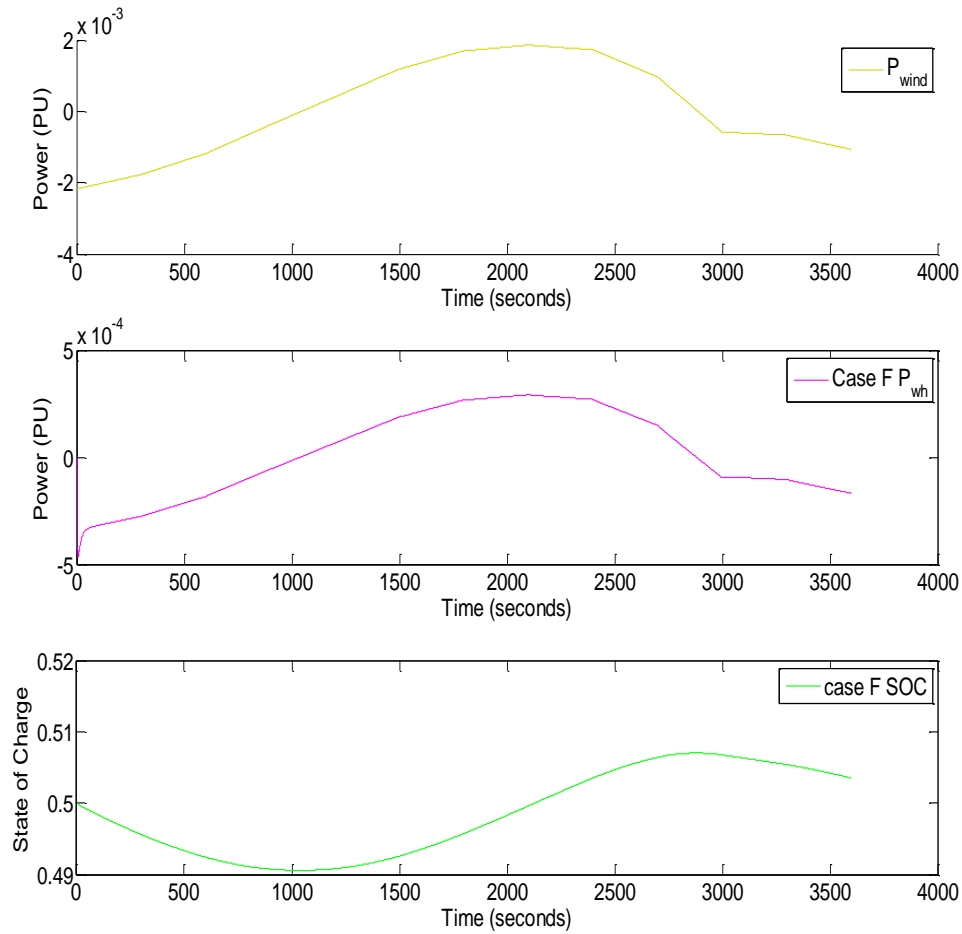


Figure 5.12 Deployment of water heaters for every 1MW of wind power and the SOC of the energy storage system for Case G

## 5.5 Case H: Energy storage for wind integration with secondary control

In an actual power system, frequency regulation is not just limited to primary control; secondary control is deployed in the “minutes” time frame. In chapter four, since simulations were performed only for 60 seconds, it was not necessary to deploy secondary control, but with wind integration to the WECC system, where simulations have been performed for 60 minutes, it is crucial to include secondary control to improve the frequency profile.

By deploying secondary control, the role of energy storage system will be reduced, due to the fact that, secondary control will drive the frequency response to 60 Hz, and the energy storage system which is communicating with the grid based on the change in frequency from its nominal, cannot detect the change in frequency as the difference in frequency will be 0 Hz. But anytime there is a change in wind, there is a window of time that the energy storage system can work and is responsive to frequency before the secondary loop tunes it out and drives the system back to 60 Hz (in this case 0 Hz as it is a delta value). However, with the implementation of the secondary control the role of the energy storage system will be reduced. Also, it would be interesting to see the number of water heaters being deployed with the addition of a secondary loop.

Figure 5.12 shows the simulation set up with the addition of a secondary loop.

If  $\Delta\omega$  is non zero, then the gain factor  $\frac{K_1}{s}$  in the secondary loop is non zero, and it is



the property of the integrator that when an integration is run on a non-zero value, it either ramps up or ramps down until it becomes zero. Hence,  $K_1$  has to be designed in a way such that, when the frequency is non zero, there is an extra generation component that keeps increasing until  $\Delta\omega$  becomes zero, once the value zero is the input to the integrator; it just holds the value it has and outputs it. The secondary loop is not as fast as the primary loop, but it eventually drives the frequency ( $\Delta\omega$ ) back to 0 Hz.  $K_1 = [1.9e - 3 * (1/300)]$  where, maximum wind power= 1.9e-3 to cancel the wind, and  $\Delta\omega = 0.01$ , this is just an assumption that has been made for the secondary loop to be implemented. 300 is the time in seconds, for the secondary control to kick in.

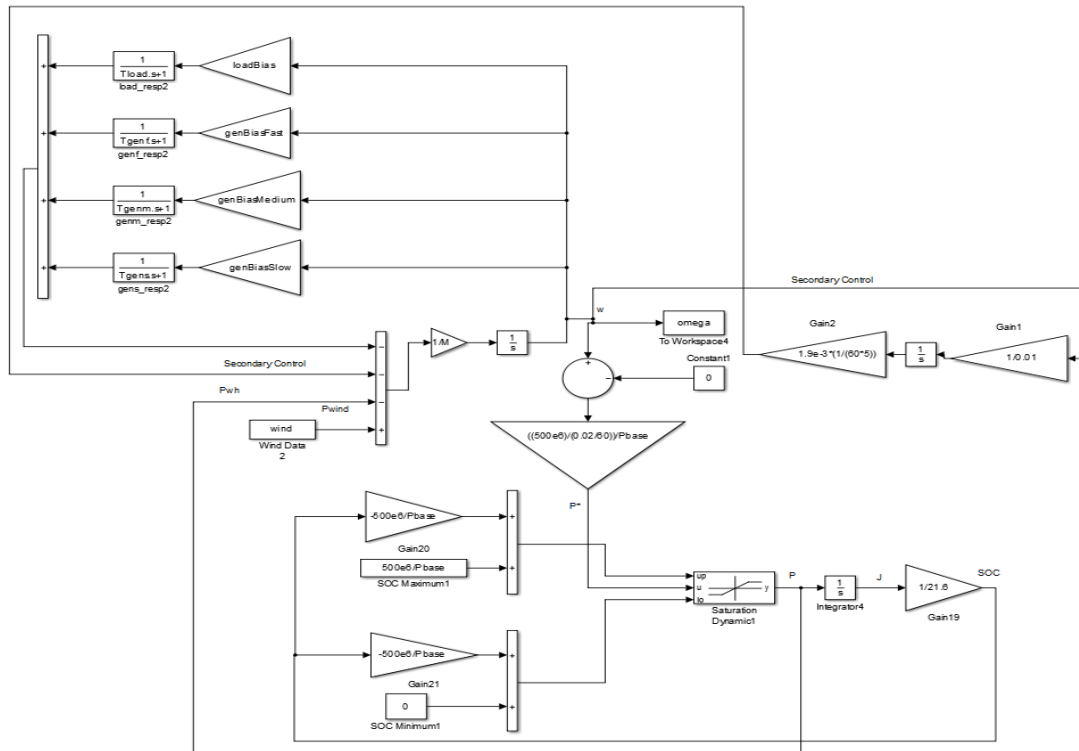


Figure 5.13. WECC model with secondary control for Case H

Figure 5.14 shows the frequency deviation from nominal, the water heater power and the SOC when secondary control was added to the WECC system in the presence of energy storage. It can be seen that the water heater power is the same when compared to the other 4 cases, as secondary control would not have an effect on the water heater power as discussed above. The frequency profile is also similar to Case G, which implies that the water heaters were still active and dominant even on the addition of the secondary loop. The reason could be that the gain factor on the secondary loop was not aggressive enough to show an effect on the energy storage system. The SOC has hardly had an effect either when compared to case G as expected.

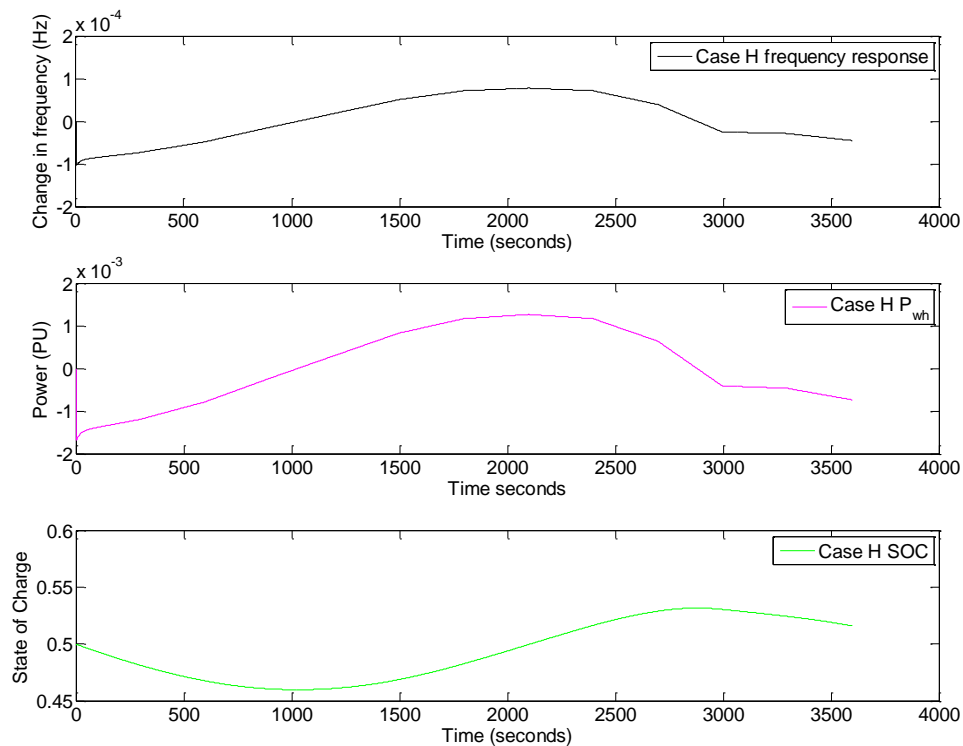


Figure 5.14. Frequency response, water heater power response and SOC with secondary control

## 5.6 Results Conclusion

The table below will conclude the results of chapter 5. It will encompass the maximum and minimum change in frequency, maximum and minimum water heater power and maximum and minimum SOC for all the 5 cases.

The results below conclude that, the frequency profile for case G (water heaters responding per 0.02 Hz) has improved when compared to the other three cases, which suggests that making the gain value K more aggressive (increasing), increased the role of water heaters in the system which contributed to the improvement of the frequency nadir. With the implementation of secondary control, the frequency nadir has improved as seen in Case H of Table 5.2

Table 5.2 Comparing the frequency response, water heater power response and state of charge for 5 different cases

	Frequency (Hz)				$P_{wh}$ (PU)		SOC	
	$Max\Delta f$	$Min\Delta f$	$Max f$	$Min f$	$Max P_{wh}$	$Min P_{wh}$	$Max SOC$	$Min SOC$
<b>Case D</b>	0.0146	-0.0248	60.0146	59.9752	—	—	—	—
<b>Case E</b>	0.0144	-0.0243	60.0144	59.9757	2.6152e-05	-4.4004e-05	0.5006	0.4992
<b>Case F</b>	0.0123	-0.0197	60.0123	59.9803	2.9165e-04	-4.6637e-04	0.5070	0.4906
<b>Case G</b>	0.0047	-0.0062	60.0047	59.9938	1.3e-03	-1.7e-03	0.5304	0.4590
<b>Case H</b>	0.0047	-0.0062	60.0047	59.9938	1.3e-03	-1.7e-03	0.5315	0.4597

Figure 5.15 shows frequency responses for all the five cases. The black plot clearly implies the involvement of secondary control as the frequency profile has improved and is closer to 60 Hz.

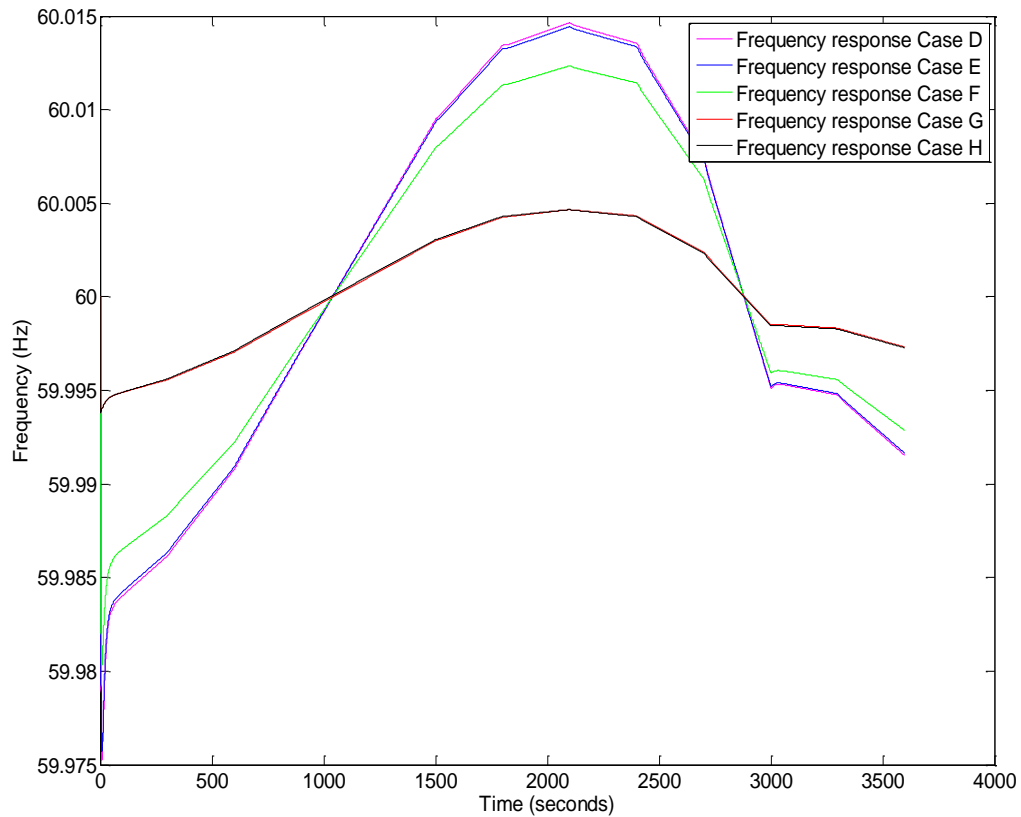


Figure 5.15 Frequency responses of Case D, E, F, G and H

Figure 5.16 showcases the contribution of water heater power for cases E, F, G and H. It can be seen from Table 5.3 above table that  $1.3\text{e-}3$  PU of water heater power was deployed which is very close to the maximum wind power generation ( $1.9\text{e-}3$  PU). Thus concentrating primarily on the order of the magnitude of both the powers, it

concludes that for the gain value of  $\frac{500 \text{ MW}}{\frac{0.02}{60} P_{base}}$  is a full deployment of the water heaters present in the system. The water heater power in the presence of secondary control is almost the same as Case G (red plot) since the role of energy storage system reduces with the implementation of secondary control. Table 5.3 gives the summary of wind power and water heater power for all the five cases.

Table 5.3 Wind power and water heaters powers for the five cases

	Minimum power (PU)	Maximum power (PU)
<b>Case D</b>	1.9e-3	-0.0022e-3

	Minimum water heater power (PU)	Maximum water heater power (PU)
<b>Case E</b>	2.6152e-05	-4.4004e-05
<b>Case F</b>	2.9165e-04	-4.6637e-04
<b>Case G</b>	1.3e-03	-1.7e-03
<b>Case H</b>	1.3e-03	-1.7e-03

From the table 5.3 only 1% of water heaters have been deployed in Case E. 10% for Case F and 100 % for Case G and Case H. The role of water heaters is unaffected for Case H due to the presence of secondary loop.

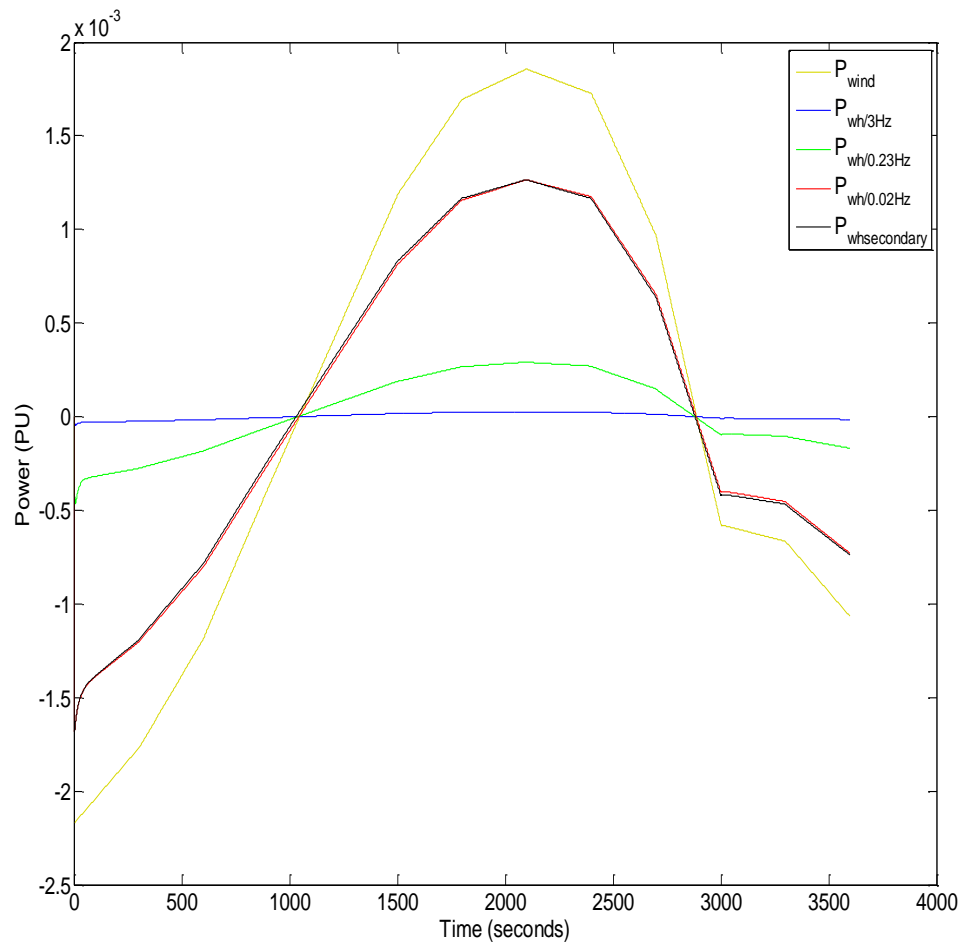


Figure 5.16 Power responses for all Cases D, E, F, G and H

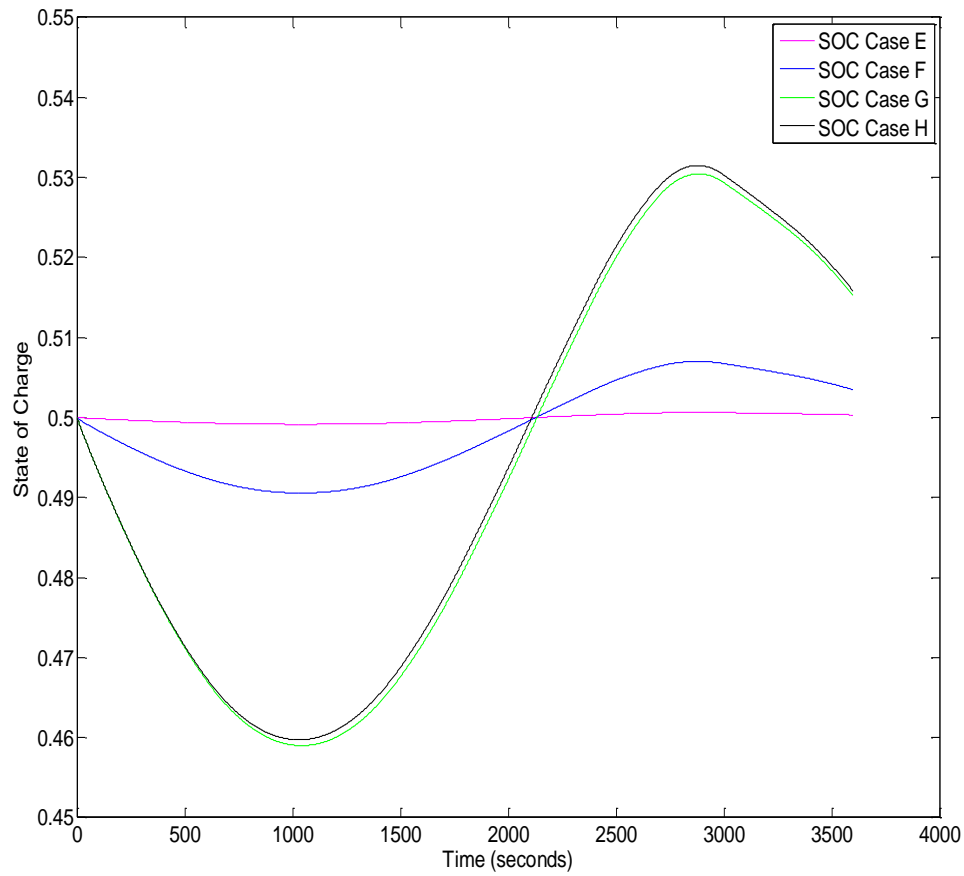


Figure 5.17 State of Charge for Case E, F, G and H

Similarly, the SOC can be compared in Figure 5.17 and it shows that for case G (green plot), maximum number of water heaters were deployed, suggesting that more aggressive the gain value  $K$ , greater is the role of water heaters to supply their power.



## 6 Conclusion

### 6.1 Discussion

This research presents its findings in two parts, the first part deals with performing transient analysis on a WECC system with sudden loss of generation of the Palo Verde unit in California (2.69 GW) with and without energy storage integration into the system and the second part of this thesis deals with transient analysis of the WECC system in the presence of energy storage and a renewable source (wind). The following conclusions are deduced from this research.

1. The WECC system consists of several different generators responding at very different time scales. The fast responsive generators actively take part in improving the frequency nadir but do not take part in improving the frequency response, i.e., settling frequency. Some generators are medium and slow responsive and they contribute less towards frequency nadir and more towards long term settling frequency. Hence a mix of various responsive generators stabilizes the frequency by adopting primary speed control.
2. Transient analysis of the WECC system with loss of generation in the presence of an energy storage system revealed that the frequency nadir improved to a certain extent when compared to the frequency nadir with no energy storage in the system. It was also observed that by making the gain factor  $K$  that improves the role of energy storage into the system more aggressive enhanced the frequency nadir by about 0.0313 Hz. The deployment of water heaters was

also improved with the change in frequency = 0.23 Hz when compared to 3 Hz.

3. Transient analysis of the WECC system in the presence of energy storage system and with high wind penetration was implemented to observe the role of energy storage with constant change of frequency, due to the variable nature of wind power which is attributed to the variable wind speeds. The energy storage system was connected to the grid in a way that the only means of communication to the grid is due to the deviation in frequency. From its operating point. Analysis showed that the frequency nadir improved as the gain factor K was made more aggressive. The difference in the frequency nadir for the case with wind penetration and no energy storage and the case with energy storage was approximately 0.0186 Hz.

4. The actual water heater power deployment gave an idea of the percentage of water heaters that actually took part and responded to the frequency change. It was found that 100% deployment of energy storage was achieved with

$$K = \frac{\frac{500 \text{ MW}}{0.02/60}}{P_{base}} .$$

5. The implementation of secondary control would effectively remove the role of the energy storage as there would not be a lot of frequency deviation from nominal. However the simulations showed that the frequency response for Case H was similar to Case G, implying that the energy storage system was still dominant even on the addition of the secondary loop, and it was not

aggressive enough to drive the frequency back to 60 Hz. If the secondary control was made more aggressive, it would have dominated the water heater power and may be driven the frequency back to 60 Hz.

## **6.2 Future Work**

While the results of this research were fruitful to study the transient behavior of a huge system like WECC, a considerable amount of investigation could still be probed into.

1. Integrate several other renewables like solar and wave with wind and observe the effect of transients in the system.
2. Increase the role of energy storage by increasing the simulation time and observe the frequency transients under the increased timeline.
3. The effect tertiary control would have on an energy storage system and transient studies if implemented.
4. Further exploration on the effect of secondary control on the energy storage system.
5. Understand the grouping of fast, medium slow generators and connect it to the results that the WECC system currently has.
6. Perform similar kind of analysis for multiple areas, apart from just the WECC region.

## 7 References

- [1] U.S Energy Information Administration  
Available: <http://www.eia.gov/tools/faqs/faq.cfm?id=427&t=3>
- [2] Website of National atlas  
Available: [http://www.nationalatlas.gov/articles/people/a\\_energy.html](http://www.nationalatlas.gov/articles/people/a_energy.html)
- [3] US Energy Information Administration, Energy, accessed 6 Nov. 2013
- [4] U.S Energy Information Administration, Monthly Energy Review, March 2012, preliminary data 2011 data  
Available: <http://www.eia.gov/totalenergy/data/monthly/pdf/sec10.pdf>
- [5] American wind power reaches major power generation milestones in 2013 March 5, 2014  
Available: <http://www.awea.org/MediaCenter/pressrelease.aspx?ItemNumber=6184>
- [6] The American Wind Energy Association (AWEA) market report of 2014,  
Available: <http://www.awea.org/generationrecords>
- [7] The American Wind Energy Association (AWEA)  
Available: <http://awea.files.cms-plus.com/FileDownloads/pdfs/oregon.pdf>  
Available: <http://awea.files.cms-plus.com/FileDownloads/pdfs/washington.pdf>
- [8] Bonnivellie Power Administration (BPA),  
Available: <http://www.bpa.gov/Projects/Initiatives/Wind/Pages/default.aspx>
- [9] Website of Solar Schools  
Available: [http://www.solarschools.net/resources/stuff/advantages\\_and\\_disadvantages.aspx](http://www.solarschools.net/resources/stuff/advantages_and_disadvantages.aspx)
- [10] BPA Balancing Authority Load and Total Wind, Hydro, and Thermal Generation, Near-Real-Time, 2014  
Available : <http://transmission.bpa.gov/business/operations/wind/baltwg.aspx>
- [11] Sharma, Sandip, Shun-Hsien Huang, and N. D. R. Sarma. "System inertial frequency response estimation and impact of renewable resources in ERCOT interconnection." *Power and Energy Society General Meeting, 2011 IEEE*. IEEE, 2011.
- [12] Eto, J. H., Undrill, J., Mackin, P., Daschmans, R., Williams, B., Haney, B., ... & LaCommare, K. H. (2010). ERNEST ORLANDO LAWRENCE BERKELEY NATIONAL LABORATORY

- [13] Balancing and frequency control, A technical document prepared by NERC Resources Subcommittee  
Available:  
<http://www.nerc.com/docs/oc/rs/NERC%20Balancing%20and%20Frequency%20Control%20040520111.pdf>
- [14] Encyclopedia Britannica  
Available: <http://www.britannica.com/EBchecked/topic/287315/inertia>
- [15] NREL fact sheet, Variable Renewable Generation Can Provide Balancing Control to the Electric Power System.  
Available: <http://www.nrel.gov/docs/fy13osti/57820.pdf>
- [16] Delille. G, Francois. B, Malarange. G,” Frequency Control Support by Energy Storage to Reduce the Impact of Wind and Solar Generation on Isolated Power System's Inertia”, Sustainable Energy, IEEE Transactions on (Volume: 3, 4), 14 August 2012
- [17] Wang- Hansen, M. ; Dept of Electr. Eng, AF Gothenburg, Gothenburg, Sweden: Josefsson. R; Mehmedovic, H, “Frequency Controlling Wind Power Modeling of Control Strategies”, Sustainable Energy, IEEE Transactions (Volume:4, Issue: 4 ), Issue Date : Oct. 2013
- [18] Arani, M.F.M. Dept. of Electr. & Comput. Eng., Univ. of Waterloo, Waterloo, ON, Canada, El-Saadany, E.F.” Implementing Virtual Inertia in DFIG-Based Wind Power Generation”, Power Systems, IEEE Transactions on (Volume:28 Issue: 2 ), 28 August 2012
- [19] Austrian Power Grid  
Available: <http://www.apg.at/en/market/balancing/control-area-imbalance>
- [20] “Grid Energy Storage”, US Department of Energy, December 2013
- [21] Available: [http://aweablog.org/blog/post/wind-power-and-energy-storage\\_1](http://aweablog.org/blog/post/wind-power-and-energy-storage_1)
- [22] PNNL  
Available: <http://www.pnnl.gov/news/release.aspx?id=1060>
- [23] V. S. K. Murthy Balijepalli, Vedanta Pradhan, S. A. Khaparde Senior Member, IEEE and R. M. Shereef, “Review of Demand Response under Smart Grid Paradigm”, 2011 IEEE PES Innovative Smart Grid Technologies – India
- [24] “Sixth northwest conservation and electric power plan,” NPCC  
Available: <http://www.nwcouncil.org/media/6284/SixthPowerPlan.pdf>

[25] Available : <http://www.greentechmedia.com/articles/read/water-heaters-for-wind-energy-storage>

[26] M Kintner-Meyer, P Balducci, W Colella, M Elizondo, C Jin, T Nguyen, V Viswanathan, Y Zhang, June 2012, National Assessment of Energy Storage for Grid Balancing and Arbitrage: Phase 1, WECC

Available:

[http://energyenvironment.pnnl.gov/pdf/PNNL21388\\_National\\_Assessment\\_Storage\\_Phase\\_1\\_final.pdf](http://energyenvironment.pnnl.gov/pdf/PNNL21388_National_Assessment_Storage_Phase_1_final.pdf)

[27] Nicholas W. Miller, Miaolei Shao and Sundar Venkataraman, 09 November 2011, Report on “California ISO, Frequency Response study”.

[28] Nicholas Miller, Clyde Loutan, Miaolei Shao and Kara Clark, Nov-Dec. 2013, “Emergency Response: U.S. System Frequency with High Wind Penetration”, Power and Energy Magazine, IEEE (volume:11, Issue:6)

[29] Prabha Kundur, (‘Power System Stability and Control’ by Prabha Kundur, Tata Mc Graw Hill Publication

[30] Power, Controlling Active, and Ol of Samuelsson. "Power System Damping." (1997).

[31] Personal Interview with Dr. Ted Brekken, Oregon State University, June 2014

[32] Bela G. Liptak (2003). Instrument Engineers’ Handbook: Process control and optimization(4 ed.). CRC Press.p. 100. ISBN 0-8493-1081-4.

[33]Website of Energy

Available: <http://energy.gov/oe/services/technology-development/energy-storage>

[34] Website of Clean Technica

Available: <http://cleantechnica.com/2014/05/02/energy-storage-greater-use-wind-power/>

